The Dissertation Committee for Taylor Ann Clark Certifies that this is the approved version of the following dissertation:

Insights into Ischemia-Induced Dendritic and Vascular Plasticity through In Vivo Imaging

Committee:

Theresa A. Jones, Supervisor

Andrew K. Dunn, Co-Supervisor

Kristen M. Harris

Boris Zemelman

Hiroshi Nishiyama

Insights into Ischemia-Induced Dendritic and Vascular Plasticity through In Vivo Imaging

by

Taylor Ann Clark

Dissertation

Presented to the Faculty of the Graduate School of

The University of Texas at Austin

in Partial Fulfillment

of the Requirements

for the Degree of

Doctor of Philosophy

The University of Texas at Austin

August 2018

Dedication

To my parents for which I owe everything

Acknowledgements

I would like to acknowledge,

My mentor Dr. Theresa Jones for shaping me into the scientist I am today and allowing me to constantly bug and nag her for scientific insight.

My co-advisor Dr. Andrew Dunn for additional guidance and support, as well as for allowing me to play with all of his high-tech imaging equipment.

My dissertation committee members Dr. Kristen Harris, Dr. Boris Zemelman, and Dr. Hiroshi Nishiyama for their time and valuable input throughout the completion of these dissertation studies.

All the undergraduates who have been involved in my projects over the years including Taliah Muhammad, Jessica Gonzales, Daniella Palmberg, RJ Franz, Sandra Kumar, Jackie Moreno, and Anh Tang

Our lab technician, Nikki Donlan for -first and foremost- keeping the lab fun even when science is stressful.

My friends and scientific counterparts, Michael Williamson, Mariana Rodriguez, Veronica Choi, Moushami Day, Evan Nudi, and Bryan Barksdale, who all know the struggles of graduate school and have been with me though the ups and downs.

My boyfriend, Adrian Fontanilla who managed to help me stay somewhat sane through this process.

My dear friend Kyra Phillips who's been with me since the start of this journey. We worked in the same lab as undergraduates at UCLA and have managed to stay the best of friends even though she is in Michigan pursuing her PhD. I don't think I could have finished this without her continued suppot and friendship.

My parents for instilling in me a strong work ethic and a passion to pursue my goals, and remining me just how much I have achieved even in the moments when I felt like a complete failure.

My (multiple pairs) of running shoes who allowed me an escape from the anxiety and stresses of graduate school even if just for several hours out of the week.

Graduate school for making me the best runner I could possibly be, and for giving me the drive (anxiety) finish my first ever marathon where I qualified for the Boston Marathon, probably my second greatest achievement outside of getting my PhD!

And finally, the many mice who devoted their lives to my scientific achievements.

Abstract

Insights into Ischemia-Induced Dendritic and Vascular Plasticity through In Vivo Imaging

Taylor Ann Clark, Ph.D.

The University of Texas at Austin, 2018

Supervisors: Theresa A. Jones & Andrew K. Dunn

Stroke remains a leading cause of long-term disability in adults, and impairments in the upper extremities are particularly common. Many post-stroke remodeling events are activity dependent and can be influenced by post-ischemic behavioral experience through similar mechanisms as experience-dependent plasticity. The overarching goal of these dissertation studies was to understand how behavioral experience, in the form of rehabilitative training (RT), after ischemia impacts neuronal and vascular structural remodeling.

This was tested using a mouse model of ischemia-induced upper-limb impairments in adult transgenic mice containing yellow or green fluorescent protein (YFP/GFP) in a subset of layer V cortical pyramidal neurons. First, I examined the impact of manual skill learning on dendritic spine dynamics *in vivo* in the trained motor cortex (MC) of intact mice (Chapter 2). We found that spine formation was significantly enhanced after 3 days of training, which was followed by an equal and opposite increase in spine elimination by day 6 and then a return to

baseline levels for the remainder of the training duration. New spines formed on day 3 were preferentially stabilized and were correlated with performance gains.

Next, I tested whether a variation of the photothrombotic stroke model that confines laser illumination to individual arteries on the cortical surface, could better reproduce aspects of the vascular penumbra, such that it would be better suited for examining how structural remodeling events are influenced by the penumbra. We monitored post-ischemic cerebral blood flow (CBF) at 6, 48, and 120 h following MC infarcts and found that artery-targeted photothrombosis created a wider, more graded penumbra. In addition, it instigated vascular structural remodeling, and caused impairments in skilled-reaching performance in mice.

Lastly, I examined the impact of RT on spine dynamics and recovery of skilled reaching performance following photothrombotic infarcts to MC. We found that ischemia instigated widespread increases in spine turnover that persisted for up to 5 weeks. RT increased the stabilization of new spines formed in weeks 2 and 3 after ischemia, which was correlated with improvements in skilled reaching, indicating that new spine maintenance could represent a structural mechanism for the recovery of reaching performance.

Table of Contents

List of Tables

List of Figures

List of Illustrations

Chapter 1: Introduction

Stroke continues to be a leading cause of long-term disability in adults (Mozaffarian et al., 2016). Disuse and dysfunction in the upper-extremities are especially prevalent, and leave stroke survivors with long-lasting impairments that impede daily functioning and negatively impact quality of life (Lai et al., 2002, Cramer et al., 2011). Rehabilitative training (RT) approaches are the main therapeutic strategies used to treat motor impairments after stroke, but are far from sufficient to normalize function. Optimization of these strategies could benefit from a more detailed understanding of the time course over which rehabilitative training promotes structural brain plasticity and improved functional outcomes.

The main goal of these dissertation studies was to understand the impact of RT on neuronal and vascular structural remodeling events over time following focal ischemia to motor cortex (MC). This goal was pursued through the following aims: (1) to understand how ischemia-induced structural remodeling events interact with structural synaptic plasticity in the intact brain (Ch. 2 and 4), (2) to improve upon an existing stroke model in order to better understand the impact that the vascular penumbra has on these events (Ch. 3), and (3) to determine how RT differentially impacts ischemia-induced structural plasticity, and how it relates to functional improvements.

The following questions were pursued using a mouse model of ischemia-induced chronic upper-limb impairments. I chose to study focal ischemia of MC because it creates impairments in skilled forelimb function in mice that are commonly seen in stroke survivors (Cramer et al., 2011). Ischemia was induced using photothrombosis because of the ease with which it can be combined with *in vivo* imaging techniques (Carmichael et al., 2008). Structural plasticity was

monitored at the level of individual dendritic spines using *in vivo* two-photon imaging in combination with transgenic mice that expressed either yellow fluorescent protein (YFP) or green fluorescent protein (GFP) in a subset of layer V cortical pyramidal neurons (Feng et al., 2000). I chose to study spine turnover because dendritic spines are the main post-synaptic site for the majority of excitatory synapses in the brain. Structural changes on spines serve as a good indicator of synaptic plasticity *in vivo*. The use of YFP and GFP lines that preferentially label layer V cortical pyramidal neurons was chosen because in MC, these neurons are the primary output to motor neurons in the spinal cord.

In Chapter 2, I used two-photon imaging to examine the impact of skilled forelimb training on dendritic spine dynamics within the superficial dendrites of layer V cortical pyramidal neurons in the trained MC of adult YFP-expressing mice. The goal of this experiment was to better understand the time course over which skilled training instigates changes in structural plasticity as a basis for understanding the effects of RT on structural plasticity after ischemia.

In Chapter 3, we developed a variation of the traditional photothrombotic approach that confines lase illumination to a pre-identified expanse of arteries on the cortical surface. The purpose of this experiment was to improve upon the main criticism of the model, that it creates a relatively small ischemic penumbra. This makes it challenging to understand the impact of events within it on mechanisms of structural plasticity in peri-infarct cortex over longer periods. An additional goal was to determine whether artery-targeted photothrombosis instigated changes in vascular structural remodeling that have been reported in other focal ischemia models.

In Chapter 4, I examined the impact of RT on dendritic spine dynamics and recovery of skilled reaching performance after focal ischemia to MC using the same approach as in Chapter 2. Additionally, we examined the impact of RT on vascular structural remodeling at later time points. The goal of this study was to advance our basic understanding of synaptic responses to RT. A better understanding the time course of RT-medtated structural plasticity is useful for identifying critical time points when RT may be maximally beneficial for driving plasticity.

The remainder of this chapter provides background information that was used to guide the formation of the current aims. The first sections describe what is currently known in the field about experience-dependent structural plasticity (with an emphasis on motor-skill training) in the adult intact brain. The following section provides an overview of animal models of chronic-upper extremity impairments, and the two most commonly used focal ischemic stroke models. The next sections describe what is known about ischemia-induced vascular and structural remodeling events in the peri-infarct cortex. The final section describes the current need, within the field, for a better understanding of how aging and sex might impact structural and functional responses to ischemia.

1.1 Experience-driven synaptic plasticity in the adult brain

Neuronal plasticity encompasses the structural and functional changes in neuronal circuits in response to experience (Fu & Zuo, 2011). Synapses represent fundamental units of neuronal circuits. Dendrites are the post-synaptic site for the majority of excitatory synapses in the brain, making them ideal for monitoring changes in synaptic connectivity. The use of transgenic mouse lines along with advanced imaging techniques has allowed us to monitor changes in synaptic

plasticity at the level of individual dendritic spines over time in the living brain. This has proven a powerful tool for understanding structural mechanisms of experience-dependent plasticity and plasticity following brain damage. Long-term, high-resolution imaging studies in adult animals have revealed that while although most dendritic spines are maintained over a large fraction of the animal's life (Grutzendler et al., 2002; Majewaska et al., 2006; Trachtenberg et al., 2002), a subpopulation appears and disappears.

Previous studies of Golgi-stained neurons in fixed tissue slices have revealed that numerous experimental manipulations including environmental enrichment (Volkmar & Greenough, 1972), motor-learning (Kolb, B., Cioe, J. & Comeau, W, 2008), stress levels (Magarinos, et al., 1996) and drugs of abuse (Robinson & Kolb, 1999) instigate structural plasticity of dendrites and spines. Electron microscopy studies have reported increased spine and synapse densities after rearing in enriched environments, and motor-learning (Greenough, Hwang & Gorman 1992; Jones et al., 1997; Kleim, Jones, & Schallert 2003; Moser et al., 1994). Recent *in vivo* studies, have found that the same experimental manipulations instigate alterations in spine turnover *in vivo* (Holtmaat et al., 2006; Majewaska et al., 2006; Trachtenberg et al., 2002; Xu et al., 2009). Furthermore, retrospective 3D EM reconstruction following *in vivo* time-lapse imaging has demonstrated that both pre-existing and persistent new spines exhibit ultrastructural hallmarks of typical synapses (Knott et al., 2006) supporting the idea that spine changes observed *in vivo* serve as a good indicator for experience-dependent structural synaptic plasticity.

In terms of motor-learning, training on a skilled forelimb reaching task, instigates increases in spine formation on the apical dendrites of layer V pyramidal neurons in the trained

MC (Xu et al., 2009). Spine formation is followed by enhanced spine elimination, resulting in no net change in spine density. However, new spines formed in response to training are preferentially stabilized, even long after training stops (Xu et al., 2009). Similar increases in spine turnover and stabilization have been observed in mice performing other motor tasks, including the rotarod task (Yang et al., 2009), and suggest that new spine maintenance could represent a structural basis for long-term memory of the acquired skills (Xu et al., 2009). It is possible that, similar to skilled training in intact animals, RT after ischemic infarcts to MC could be sufficient to promote stabilization of new spines formed after the infarct that could potentially represent a structural substrate for improvements in the recovery of skilled reaching. This hypothesis was tested in Chapter 4.

1.2 A brief overview of the organization of mouse motor cortex.

The corticospinal tract is the main descending pathway from cerebral cortex to spinal cord motoneurons, and its connecting cortical regions, including motor cortex (MC) are often injured in stroke. Therefore, focal infarcts to MC are useful for modeling motor impaiments commonly seen in stroke patients. In MC, layer V pyramidal neurons are the primary output to the spinal cord, marking this cell population as a key target for structural plasticity following brain damage (Nudo et al., 2007). The rodent motor cortex lacks a prominent layer IV, which is typically the main layer receiving afferent input from the thalamus. Therefore, the majority of thalamic input is relayed to neurons in layer II/III, which then project to layer V. Pyramidal cells within this layer have a distinct morphology. They contain large apical tufts with fanlike dendritic branches that extend all the way to the superficial layers, making them ideal targets for *in vivo* imaging. In addition these cells have oblique apical dendrites, which are extensions of the thick apical stalk,

and smaller basilar branches that terminate within layer V (Ramaswamy et al., 2015). As in layer II/III, layer V neurons contain both horizontal connections and cortico-cortical connections (Spruston, 2008). In general, the proximal dendrites receive most input from local sources where as the tuft dendrites receive input from more distant cortical regions (Spruston, 2008).

Distinct morphologies of dendritic domains within individual layer V pyramidal neurons likely contributes to variation in structural plasticity within these different dendritic subpopulations (Spruston, 2008). For example, the apical tufts have a much lower spine density compared to both oblique apical dendrites and basilar dendrites. Recent *in vivo* examinations of dendritic plasticity in response to manual skill training have shown that tuft dendrites experience spine turnover, but no net change in spine density (Xu et al., 2009). On the other hand, previous histological studies have shown that skilled training increases spine numbers in layer V of MC (Kleim et al., 1996). These results highlight that structural changes vary depending on location of the dendrite.

In rodents, the forelimb motor area (MC) consists of the caudal forelimb area (CFA), which is homologous to the primate MC, and the rostral forelimb area (RFA), which is analogous to premotor cortex. Previous studies using intracortical microstimulation (ICMS) have found that in mice, MC includes a large CFA dominated by digit and wrist representations, and a smaller RFA. The RFA was found to undergo an expansion in the cortical territory devoted to forelimb movements with RT after ischemia (Tennant et al., 2011). Furthermore, connectivity studies have shown that in rodents there is dense interconnectivity both within CFA, between CFA and RFA, and between CFA and somatosensory cortex (Donogue & Wise, 1982). Damage to the CFA has been shown to instigate large-scale cortical plasticity of these adjacent regions

that is associated with functional recovery (Tennant et al., 2011; Connor, Chiba & Tuszynski, 2005). However, cortical plasticity within the remaining CFA was the focus of these dissertation studies, given that the majority of layer V corticospinal neurons project from CFA. In the following chapters, the remaining CFA will be used synonymously with peri-infarct cortex.

1.3 Photothrombosis : strengths and weaknesses

Motor impairments of the upper-extremities are a particularly common consequence of stroke, tend to be chronic, and difficult to treat with rehabilitative therapies (Cramer et al., 2011). Rodents and nonhuman primates serve as good models for chronic upper-limb impairments. Ischemic lesions can be placed within areas of the MC known to create impairments in skilled reaching that require use wrist, and digits, and are commonly affected after stroke im humans (Adkins et al., 2004; Kleim et al., 2007; Nudo et al., 1996). Furthermore, targeting MC allows the study of the neural mechanisms associated with rehabilitative training (RT) effects on functional recovery. Rehabilitative training consists of repetitive practice (often daily) on a task requiring use of the "impaired" limb.

There are several commonly used rodent models of focal ischemia useful fore studying cellular mechanisms of recovery, each with their own set of advantages and limitations. The following sections will provide a brief overiew of two models, intraluminal suture or occlusion of the middle cerebral artery (McAO), and photothrombosis, which serve as the basis for the model proposed in Chapter 3 of the present dissertation studies.

The McAO model is commonly used for the study of neuroprotective therapies after ischemia. An advantage of the model is that progressive neuronal death in the cortex is delayed,

which is more similar to the time course of human stroke. This allows examination of cellular events in the ischemic penumbra, as well as secondary mediators of ischemic cell death including inflammation and oxidative injury, (Carmichael 2008). The main drawback of the model is that it creates damage to widespread and functionally diverse brain regions, making it challenging to study the impact of cellular recovery mechanisms in distinct brain regions on functional recovery after stroke.

On the other hand, the photothrombotic stroke model has been a popular choice for the examination of cellular mechanisms of functional recovery. It can be used to create relatively small circumscribed lesions that can be placed in anatomically precise and distinct regions of cortex (Carmichael et al., 2005). For example, photothrombosis can be used to create focal damage to MC, which is known to cause impairments in manual skill function, making it well-suited for animal models of ischemia-induced upper limb impairments (Jones & Jefferson, 2011; Kleim, Boychuk & Adkins 2007; Krakauer, Carmichael & Corbett, 2006).

During photothrombosis, following administration of a photoactive dye (Rose Bengal), illumination of a circumscribed region generates singlet oxygen, platelet activation, and damage to endothelial cells. This results in vasogenic edema, which rapidly spreads the developing lesion beyond the illuminated region, therefore compromising the development of a vascular penumbra (Dietrich et al., 1986; Watson et al., 1985). Furthermore, simultaneous and unavoidable illumination of surrounding microvasculature creates secondary ischemia, a pattern not seen in human stroke. The main criticism of this model is that it creates a relatively thin ischemic penumbra with little to no collateral flow or reperfusion. The small penumbra makes it

challenging to examine how recovery events within the penumbra relate to repair and remodeling responses that support improved functional outcomes over longer time periods.

In the following dissertation studies, we present a novel photothrombotic technique that confines laser illumination to an expanse of individual arteries on the cortical surface, the results of which are summarized in Chapter 3. The goal was to create a photothrombosis model that maintained the advantages of the original, while also increasing the size of the vascular penumbra similar to what has been observed in the McAO model, for its use in studies examining the coordination between post-ischemic vascular events in the penumbra and cellular recovery mechanisms over longer periods.

1.4 Vascular plasticity in the acute and chronic post-stroke phase

1.4.1 What is the ischemic penumbra and why is it important?

The ischemic penumbra was first defined by Astrup and colleagues (Astrup et al., 1981), by calculating CBF thresholds during the acute post-stroke phase. Astrup demonstrated that as CBF was steadily reduced to around 40% of baseline levels, electrical dysfunction was evident, at 30% electrical failure became complete, and at 10% release of potassium and subsequent cell death occurred. Importantly, however, prompt reperfusion of CBF could salvage tissue so long as flow rates did not fall below the threshold of energy and ion pump failure. Today the penumbra is more broadly defined as a region of ischemic tissue which is functionally impaired and at risk of infarction, but has the potential to be salvaged depending on the post-ischemic vascular events (Donnan and Davis, 2002). Adequate restoration of CBF to the penumbra during the acute-post stroke phase is crucial for tissue recovery, and forms the basis for current therapeutic strategies (Fisher, 1997; Gravanis 2008). Furthermore, adequate CBF reperfusion prompts active recovery

mechanisms within the penumbra that undoubtedly impact cellular recovery mechanisms over longer periods.

1.4.2 Vascular remodeling events in the acute and chronic post-stroke phase

Reductions in CBF following ischemic stroke instigate complex and heterogenous vascular remodeling events within the ischemic penumbra. However, the temporal profile of vascular changes after stroke continues to be poorly understood. Within the penumbra, there can be prolonged reductions in CBF and capillary density (Anderson et al., 1999; Mostany et al., 2010; del Zoppo et al., 2003) that may create a lasting inadequacy in the blood supply needed for activity-dependent plasticity.

Early after stroke, improvement of collateral flow plays a critical role in maintaining regional CBF to support ischemic tissue within the penumbra, a process known as arteriogenesis. This refers to the widening of existing arteries to improve CBF (Liu et al., 2014). Arteriogenesis has been linked to increases in cerebral blood volume as early as 1 day following McAO (Lin et al., 2002). In addition, induction of angiogenic genes, as well as endothelial cell proliferation, have been reported early on after ischemia, suggesting a role for neovascularization in the acute post-stroke phase (Lin et al., 2000; Marti et al., 2000, Hayashi et al., 2003). However, the magnitude and persistence of neovascularization in peri-infarct tissue at later time points, and whether it represents a population of new functional vessels is unclear. Martin and colleagues (Martin et al., 2012) found that increased vessel densities 1 week after ischemia was correlated with increased CBF, suggesting the possibility that neovascularization could support increased perfusion. However, more recent evidence from *in vivo* examinations of perfused vasculature report no evidence for increased neovascularization, indicating that increases in vascular density

might not be associated with increased CBF (Brown et al., 2007; Schrandt et al., 2014; Tennant et al., 2013; Mostany et al., 2010). It is unclear whether differences reports of neovascularization can be attributed to differences in labeling methods, the stroke model used, or both.

1.4.3 Vascular remodeling in cellular repair and recovery

Evidence from several rodent studies suggests that neovascularization plays a role in cellular repair and remodeling. New born neuroblasts in peri-infarct cortex are associated with endothelial cells in newly branching blood vessels lacking perfusion early after focal ischemia (between 1 and 2 weeks; Thored et al.2007), as well as over longer periods (16 weeks) that supported improved functional outcomes (Taguchi et al., 2004). Increased vascular density has also been tied to evidence of increased inflammation and recruitment of microglia and macrophages, highlighting a role for neovascularization in cellular mechanisms of repair (Manoonkitiwongsta et al., 2001). Administration of human cord blood-derived CD34+ cells following stroke induced revascularization in the peri-infarct cortex and increased neuroblast migration toward the damaged tissue (Taguchi et al., 2004), and transplantation of endothelial progenitor cells (EPCs) was shown to promote neovascularization and improved functional outcomes (Fan et al., 2010). Treatments that enhance neovascularization can promote neuroprotection, plasticity and improved function (Navaratna et al., 2009; Shen et al., 2006; Sun et al., 2003), but angiogenic treatments can have diverse effects. A better understanding of how vascular plasticity during the acute and chronic post-stroke phase interacts with cellular mechanisms of repair and recovery is essential for improving the efficacy of vascular-based therapies in post-stroke recovery.

1.5 Experience-driven synaptic plasticity of peri infarct cortex after stroke

Focal ischemia to cortex instigates a unique environment in the tissue surrounding the infarcted region, the peri-infarct cortex, for heightened plasticity that is extremely sensitive to behavioral experience. Animal studies have shown that many of the genes and proteins that are important for neuronal growth, synaptogenesis and the proliferation of dendritic spines early on in life are also increased following stroke (Carmichael et al., 2005; Carmichael 2006). Furthermore, many of the mechanisms that underlie functional recovery are similar to mechanisms that underlie experience-dependent plasticity in the intact brain (Murphy & Corbett, 2009).

There is strong evidence in both humans (Cramer et al., 2009; Dong et al., 2007; Liepert et al., 2003; Ward et al., 2004), and animal models (Biernaske et al., 2001; Dancause et al., 2003; Frost et al., 2005; Jones et al., 1999; Nudo et al., 1996), that behavioral experience in the form of rehabilitative training (RT) after stroke can drive functionally beneficial reorganization of MC. In rodents, training the injured limb in a skilled reaching task after ischemic infarcts to MC increases the representation of that forepaw in remaining motor cortex, as revealed using intracortical macrostimulation (ICMS) (Castro-Alamancos& Borrel, 1995; Connor, Chiba & Tuszynski, 2005; Nudo et al., 1996; Ramanthan et al., 2006). In addition to large-scale motor-map reorganization, RT has increases synaptic densities as well as dendritic complexity in remaining MC (Jones et al., 1999; Biernaske et al., 2001). Extensive cortical rewiring of axonal sprouts from this region to more distant cortical brain regions (Dancause et al., 2003; Frost et al., 2005) has also been found. However, little is known about the time course over which RT drives coincidental changes in structural plasticity that are associated with improved functional outcomes.

Recent results from *in vivo* studies have found that following photothrombosis, dendrites and spines are initially lost, but recover in a distance dependent manner from the infarct. During this period of recovery, dendritic spine turnover in the peri-infarct region remains elevated for up to 6 weeks (Brown et al., 2007, Brown et al., 2009), but is restricted mostly within the first 300 μm from the ischemic core. On the other hand, Mostany and colleagues found that early on after middle cerebral artery-occlusion, spine densities in the peri-infarct cortex both near to the ischemic core, and at distances several mm away were greatly reduced. Notably, spine turnover was increased in more distant regions even though CBF was relatively normal. However, in the more proximal regions that suffered extensive CBF deficits, the extent of spine turnover was correlated with the degree of reperfusion. These results highlight the importance of CBF in cellular recovery and plasticity at least in highly ischemic regions of peri-infarct cortex. Differences in the set of results between studies could be attributed to differences in the size of the penumbra created with both models. This possibility was tested in the present dissertation studies in Chapter 4.

Furthermore, Mostany and colleages found that while spine densities in both proximal and distant regions eventually recovered, the normalization of spine density took much longer in in proximal regions. Spine density surpassed baseline levels at further distances, but this increase in spine density was due to a transient population of spines. In fact, Mostany and colleagues found that spine stabilization was 2x greater in more proximal regions from the ischemic core compared to distant regions (Mostany et al., 2010), suggesting that spine maintenance may be more valuable for cellular recovery in peri-infarct regions that are more impacted by ischemia. However, it is possible that post-ischemic behavioral experience could have a profound impact

on the maintenance of this transient population of spines. This idea was tested in the present dissertation studies in Chapter 4.

1.6 Age and sex dependencies in functional outcomes following stroke

Age is currently the single greatest risk factor affecting recovery from stroke (Herson & Traystman, 2014). In rodents, aging is associated with increased lesion volumes (Canese et al., 1998; Canese et al., 2004). and worse functional outcomes following focal ischemia, (Anderson et al. 1999; Brown et al., 2003; Davis et al., 1995; Popa-Wagneret al., 2007; Popa-Wagner et al., 2018). Aging in normal mice is associated with a decrease in vascular density and endothelial cell function, suggesting that aging might also negatively impact vascular responses to stroke, although evidence for this is lacking. This possibility was tested in Chapter 3 of the present dissertation studies in order to examine whether middle-age, which is around the time when stroke incidence begins to rise dramatically, impacted the pattern of vascular plasticity after focal ischemia to MC.

Furthermore, over half of stroke survivors are women, who suffer worse functional outcomes after stroke compared to men (Mozaffarian et al., 2016). This emphasizes the importance for current animal models of post-stroke recovery to incorporate females into their models. To inform knowledge of sex-discrepancies in post-stroke outcomes. Female and male animals were included in Chapters 3 and 4 of the present dissertation studies, in order to interpret whether post-ischemic structural plasticity and behavioral outcomes were impacted by sex differences. However, both of these studies were underpowered to provide a comprehensive examination of of age or sex dependencies in post-stroke outcomes.

Chapter 2: Preferential stabilization of newly formed dendritic spines in motor cortex during manual skill learning predicts performance gains, but not memory endurance

[1] Reprinted from Clark, TA., Fu, M., Dunn, AK., Zuo, Y., & Jones, TA. (Copyright 2018). Preferential stabilization of newly formed dendritic spines in motor cortex during manual skill learning predicts performance gains, but not memory endurance. Neurobiology of Learning and Memory. DOI:10.1016/j.nlm.2018.05.005, with permission from Elevier. TC was responsible for experiment design, data collection, analysis, interpretation, and writing of this manuscript.

2.1 Abstract

Previous findings that skill learning is associated with the formation and preferential stabilization of new dendritic spines in cortex have raised the possibility that this preferential stabilization is a mechanism for lasting skill memory. We investigated this possibility in adult mice using *in vivo* two-photon imaging to monitor spine dynamics on superficial apical dendrites of layer V pyramidal neurons in motor cortex during manual skill learning. Spine formation increased over the first 3 days of training on a skilled reaching task, followed by increased spine elimination. A greater proportion of spines formed during the first 3 training days were lost if training stopped after 3, compared with 15 days. However, performance gains achieved in 3 training days persisted, indicating that preferential new spine stabilization was non-essential for skill retention. Consistent with a role in ongoing skill refinement, the persistence of spines formed early in training strongly predicted performance improvements. Finally, while we observed no net spine density change on superficial dendrites, the density of spines on deeper apical branches of the same neuronal population was increased regardless of training duration, suggestive of a potential role in the retention of the initial skill memory. Together, these results indicate dendritic subpopulation-dependent variation in spine structural responses to skill learning, which potentially reflect distinct contributions to the refinement and retention of newly acquired motor skills.

2.2 Introduction

While it is generally well accepted that major behavioral changes must reflect altered neural activity patterns, the nature of the synaptic changes supporting these alterations is poorly resolved (Chen et al., 2014; Gibson & Olive, 2017; Kolb & Whishaw, 1998; Makino et al., 2016). Repeatedly imaging synaptic elements over time *in vivo*, including the dendritic spines which form the majority of excitatory synapses in the brain (Bourne & Harris, 2008; Harms & Dunavesky, 2007; Yuste & Bonhoeffer, 2004; Yuste & Denk 1995) is powerful for revealing interrelationships between synaptic and behavioral change. Using transcranial two-photon imaging in transgenic mice expressing fluorescent proteins in cortical neurons, spine dynamics on superficial dendrites within the first several hundred microns of cortex can be monitored over time as an animal learns. In naive adult mouse cortex, spines are remarkably stable, with as little as 10% of spines turning over within a two-week period (Grutzlender et al., 2002). The extent of structural stability is thought to reflect the stability of synaptic connections in the mature brain. However, mice retain the ability to learn new tasks throughout their lifespan (Tennant & Jones, 2012), and this new learning presumably reflects modifications in synaptic connections. Motor skill learning, even in aged mice, results in reorganization of movement representations in motor cortex (Tennant & Jones, 2012). Similarly, in adult rats, regions in which movement representations have reorganized in response to motor skill training have been found to have increased quantities of synapses in layer V compared with untrained controls (Kleim et al., 2002).

Previous studies have examined how motor skill training affects synaptic plasticity in the motor cortex over time *in vivo* (Chen & Zuo, 2014; Fu et al., 2012; Harms et al., 2008;

Padmashiri et al., 2013; Reiner & Dunavesky, 2015; Xu et al., 2009; Yang et al., 2009). Training mice on a novel manual (skilled reaching) task promotes immediate formation followed by selective elimination of dendritic spines on the apical branches of layer V pyramidal neurons in the motor cortex contralateral to the trained forelimb (Xu et al., 2009). A similar pattern of increased spine formation followed by increased elimination has been found in mice trained on an accelerating rotorod (Yang et al., 2009; Yang et al., 2014). Continued training on either task is associated with an increase in the proportion of new spines that persist compared with new spines in untrained controls (Xu et al., 2009; Yang et al., 2009). These findings have raised the possibility that the preferential stabilization of the spines that are formed during learning is a mechanism for the long-term retention of motor skills (Xu et al., 2009; Yang et al., 2009), but this possibility had not been directly tested. The main goal of the present study was to test the hypothesis that the long-term retention of motor skills is dependent upon the preferential stabilization of apical dendritic spines that are formed during the process of acquiring those skills.

An additional goal of the present study was to investigate the possibility that patterns of spine change may vary between superficial and deeper dendrites. Numerous examinations of spine turnover on superficial dendrites in various regions of the cortex have yet to reveal net changes in spine density over time (Holtmatt et al., 2006; Trachtenberg et al., 2002; Xu et al., 2009; Yang et al., 2009). This contradicts findings of learning-related changes in spine densities on various dendritic populations of Golgi-stained pyramidal neurons in the motor cortex of rats (Greenough & Withers, 1985; Withers & Greenough, 1989; Wang et al., 2012) and nonhuman primates (Nudo et al., 1996), as well as transmission electron microscopy evidence of increases

in synapse quantities in the same species (Adkins et al., 2002; Jones et al., 1997; Keim et al., 2002; Kleim et al., 2003). Besides the species differences, a major difference between these two sets of studies has been the dendritic subpopulations examined. Most *in vivo* analyses of spine density have been restricted to the first several hundred microns of superficial cortex, which contains fanlike dendritic arbors of pyramidal neurons called apical tufts that extend into layer I of cortex. Most histological studies have focused on deeper dendrites, primarily those located within layers II/III and V. We therefore sought to clarify whether spines on different subpopulations of dendrites of the same neuronal population respond differently to manual skill learning.

2.3 Methods

2.3.1 subjects

Eighteen male C57/BL6 Yellow Fluorescent Protein (YFP)-H line transgenic mice (B6/Cg-Tg (thy-1 YFPH) 2Jrs/J) expressing YFP in a subset of layer five pyramidal neurons (Feng et al., 2000) and 5 male wild type C57/BL6 mice were used. All animals were bred at the Animal Resource Center at the University of Texas at Austin (ARC) and were between 4 and 5 months old at the time of cranial window implantation ($M \pm SE$ weight, 24.69 ± 0.64g). Mice were placed into one of three groups that underwent: (1) training for 15 consecutive days (Trained 15D, $n = 5$), (2) training that stopped after 3 days (Trained 3D, $n = 5$) or (3) no-training control procedures (Control, n=5). The timeline of experimental procedures is summarized in Figure 2.1.

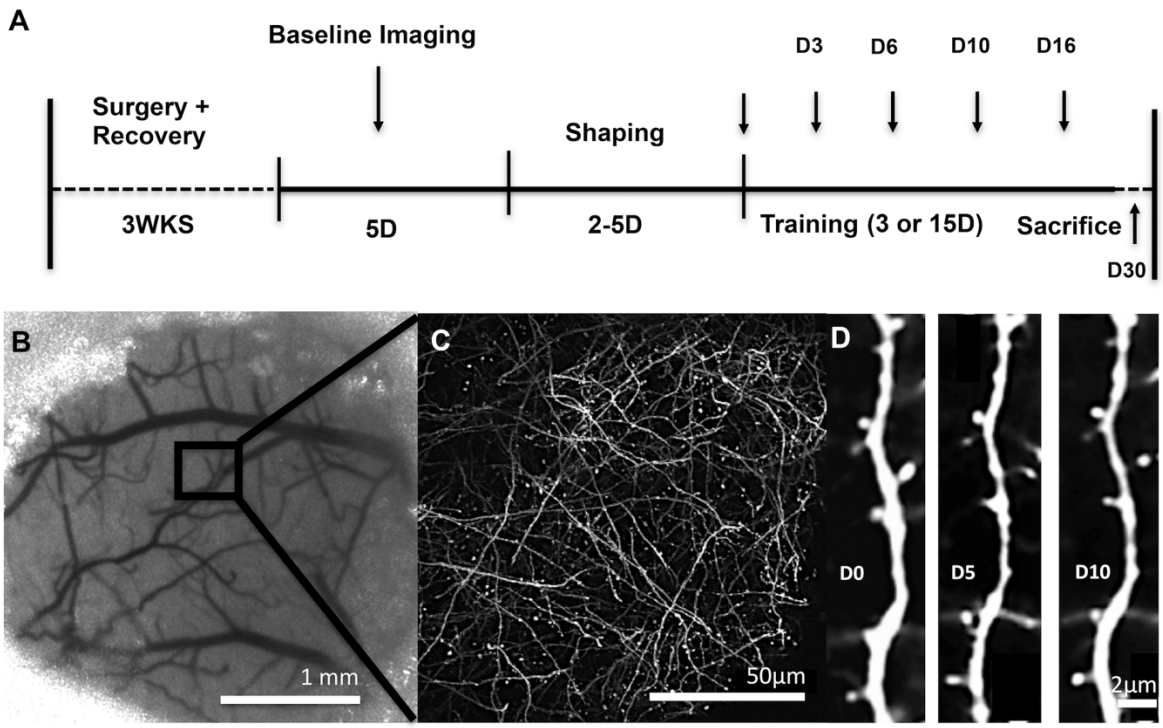

Figure 2.1 Experimental approach. (A) Experimental timeline. (B) Sample region within cranial window**.** (C) Low magnification image of YFP fluorescence. (*D*) High magnification time-lapse imaging of an individual dendritic branch within the sample region of an untrained control

Three mice with extremely dense labeling of YFP and two mice that died during early imaging sessions were omitted from the experiment. Of the remaining 15 YFP expressing mice, data from the last imaging session of 3 mice (n = 1 per group) were not available due to issues with window clarity or altered fluorescence. The wild type mice were used to corroborate the behavioral results of the Trained 3D condition. Mice were housed in groups of two to four on a 12:12 hour light/dark cycle and received food and water *ad libitum prior to behavioral testing*. Each cage had standardized supplementation including wooden toys, bedding and polyvinyl chloride pipes which were replaced weekly. During behavioral procedures, mice were placed on scheduled feeding (2.5-3g food once per day) to avoid satiation during behavioral training. Body

weights were not permitted to fall below 90% of free feeding weights (*M* ± *SE* body weight: 21.91 ± 0.49g, over the experimental time course). All animal use was in accordance with a protocol approved by the Animal Care and Use Committee of the University of Texas at Austin.

2.3.2 Cranial Window Implantation

Mice were anesthetized with ketamine (4 mg/kg, i.p.) and xylazine (3 mg/kg, i.p.). Dexamethasone (2 mg/kg, i.p.) and carprofen (2.5 mg/kg, i.p.) were administered to help minimize cortical swelling during surgical procedures. Booster injections of ketamine (50 mg/kg) were given as needed to maintain anesthetic plane. Following midline incision, a 3 mm circular region was thinned using a high-speed dental drill and a 0.5mm drill bit, and skull was removed leaving dura intact. Saline was frequently applied to protect the brain from overheating. Skull was then replaced with a thin No. 1 coverglass (Warner Instruments, #64-0720) and sealed with cyanoacrilade (3M Vetbond Tissue Adhesive, #1469) and dental cement. All windows were made over the forelimb area of the right motor cortex as defined previously from intracortical microstimulation mapping experiments (Tennant et al., 2011). Briefly, windows were placed approximately 2 mm rostral to bregma and 0.5 mm lateral to midline. Following surgery animals were given buprenorphine (3 mg/kg, s.c.) for pain management and allowed to recover in their cage for three weeks with food and water *ad libitum* prior to behavioral procedures. For the first week, animals were given daily injections of carprofen (2.5 mg/kg, i.p.) to help minimize inflammation following surgery. A three-week recovery period was chosen to ensure that spine dynamics were unaffected by any residual inflammation from surgery (Xu et al., 2007).

2.3.3 Behavioral training

Mice were trained on a skilled reaching task, the Pasta Matrix Reaching Task, as previously described (Ballermann et al., 2001; Tennant & Jones, 2012). Briefly, mice were trained to reach for and break small pieces of uncooked capellini pasta (3.2 cm in height and 1 mm diameter; DeCecco brand, Fratelli De Cecco di Filippo Fara San Martino S.p.A., Italy), arranged vertically in a matrix outside of the chamber opening (Fig. 2.2). In order to successfully retrieve a pasta piece, mice needed to reach outside of the chamber opening, grasp the pasta and break it by pulling it. Pasta pieces were not replaced once broken, such that on each successive attempt animals were required to change the reach trajectory in order to obtain the next piece of pasta.

Reaching practice was restricted to the animal's left forelimb, contralateral to cranial window implantation. For shaping, animals were given small pieces of pasta on the chamber floor, too small for pasta handling (Xu et al., 2009) and encouraged to reach towards a matrix of pasta that was placed just outside the chamber opening. To ensure that animals did not reach with their right forelimb, pasta was arranged in matrix positions on the right hand side of the chamber opening only. Given that practice in pasta handling alone can increase spine turnover in motor cortex of young animals (Xu et al., 2009), a strict criterion for the cessation of shaping was used to minimize its contribution to training effects on spine turnover. Training commenced once the animal made a total of five reach attempts or was able to break two pieces of pasta.

Training procedures lasted for either 3 (Trained 3D) or 15 days (Trained 15D). Each day, mice were placed in the chamber for either 15 minutes or until they made 100 reach attempts. Mice in the Trained 3D condition received control procedures for the remaining eleven days, followed by a final test on day 15 to probe for reaching performance. Control procedures

consisted of placing animals into reaching chambers without a pasta matrix, but with small pasta pieces (too small for pasta handling) on the chamber floor at the same time and for the same duration that a yoked mouse was being trained on the Pasta Matrix Reaching Task (Tennant & Jones, 2012).

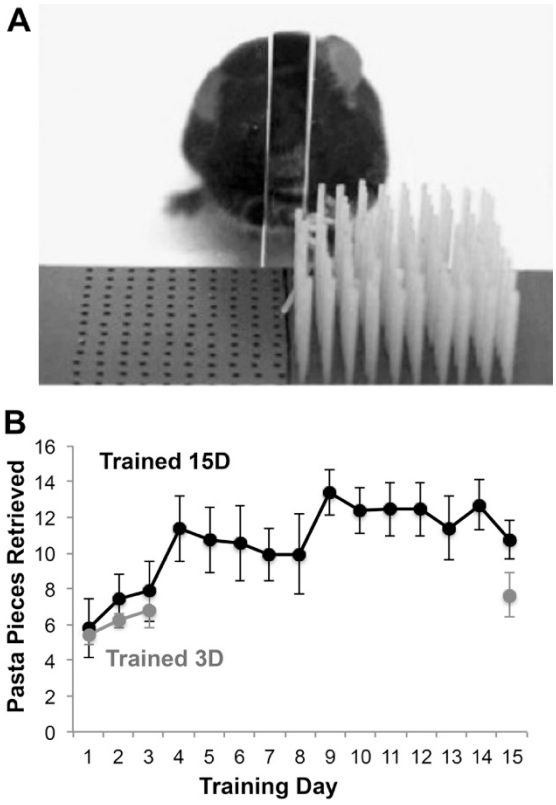

Figure 2.2 The Pasta Matrix Reaching Task. (A) Animals learned to reach for pasta arranged in a 10 x 10 matrix through an opening outside of a plexiglass chamber**.** (B) Performance on the pasta matrix task in animals trained for either 15 days (Trained 15D) or 3 days (Trained 3D). Data are *M*±*SE*. See also Supplementary Figures 1-3.

2.3.4 In vivo imaging of dendrites

Animals were anesthetized with 1.5-2.5% isoflurane and inserted into a custom made stereotaxic apparatus fitted with a headbar to minimize breathing artifact. All images were gathered within

the caudal forelimb area (CFA) of the motor cortex defined in a previous intracortical microstimulation study (Tennant & Jones, 2011). The localization of sample sites across imaging sessions was guided by superficial vascular landmarks (Fig. 2.1B). Images were acquired using a Prairie Ultima standard two-photon microscope with a Ti:Sapphire laser tuned to 920 nm (YFP) at low laser power (~30 mW) to minimize phototoxicity. Laser power was adjusted through a Pockels cell in order to obtain near identical fluorescence at each imaging location and across imaging days. High-resolution three dimensional image stacks (Fig. 2.1D) were gathered between 50 and 200 μm from the pial surface using a water immersion objective (40x, 0.8 NA, Olympus) and a digital zoom of 4X. Image stacks consisted of 150-200 optical sections spaced 0.7 μm apart covering an area of 240 μm x 240 μm (512 x 512 pixels, 0.13 μm/pixel). Four to five image stacks spaced 250 μm apart in any direction and containing at least ten dendrites with visible spines were obtained for each animal. Animals received two baseline imaging sessions spaced five days apart, with the second imaging session following the second shaping day but prior to the onset of formal behavioral training. Animals were imaged on training days 3, 6, 10 and one day following the final training session (on day 16).

2.3.5 Spine dynamics analyses

All analyses of dendritic spine turnover and spine density were performed blind to experimental condition. For analysis of *in vivo* spine dynamics a total of 8-10 dendritic segments per image stack, each at least 20 µm in length, were analyzed (~150-250 spines per animal) using ImageJ. (Rasband, 1997-2016). Spines were considered to be the same between imaging sessions based on their relative position to adjacent dendrites and spines. Only dendrites parallel to the imaging plane in both views were used for analyses to minimize possible rotational artifacts, and

dendrites containing saturated pixels were excluded. If the distance between a given spine and adjacent landmark was more than 0.7 μm from its relative position in the previous image, it was counted as different, a distance chosen based on both the resolution of the two-photon microscope (~0.7 μm) and previous reports that spines can move up to 0.3 μm in either direction due to changes in spine morphology, slight rotation of the head, or breathing artifact (Grutzlender et al., 2002). Spine turnover was measured by comparing dendritic protrusions in the image being analyzed to those in the previous imaging session. A spine was counted as stable if it appeared in both the previous imaging session and the one being analyzed, as newly formed if it was only present in the image being analyzed, and as eliminated if it was visible in the previous imaging session but not the one being analyzed. Filopodia, defined as long dendritic protrusions with no head, were rarely observed and excluded from analyses of spine turnover (Padmashri et al., 2013). The percentage of spine formation and elimination was calculated as the number of spines gained or lost divided by the total number of stable spines in the analyzed imaging session (Xu et al., 2009). Analyses were performed on raw unprocessed image stacks but for presentation purposes, images are shown as maximum intensity projections consisting of 5-10 optical sections with median and Gaussian filters applied.

2.3.6 Histological preparation and spine density analysis

Mice were overdosed with a lethal injection of sodium pentobarbital and transcardially perfused with 0.1M phosphate buffer (PB) saline and 4% paraformaldehyde two weeks following the final imaging time point. The two week delay was to ensure that any training effects on spine density could conceivably be related to skill retention. Coronal sections (50 μm) were cut using a Leica VT1000S vibratome and mounted on slides for subsequent analysis of spine density on YFP+

pyramidal neurons using confocal microscopy. Image stacks were acquired using the confocal mode on the two-photon microscope. The dichroic mirror was replaced with a lens tuned to 488nm (FITC) and image stacks containing apical dendritic branches within layer I (≤200 μm from the surface) and layer II/III (between 200-400 μm from the surface) of motor cortex were gathered using a water immersion objective (40x, 0.8 NA; Olympus). All spine density analyses were performed using Image J software. For layer II/III dendrites, a total of ten apical dendrites measuring at least 50 μm in length within cytoarchitectural motor cortex boundaries were sampled per hemisphere in each animal (Tennant et al., 2011). For layer 1 dendrites (the sample region for *in vivo* imaging) we took a slightly more liberal approach due to observed mechanical damage (presumably from sectioning) of this sampling region in several animals. Between 8-10 dendrites per hemisphere per animal measuring at least 35 μm in length were analyzed. Data from one animal in the Trained 3D group had to be omitted from spine density analyses due to tissue damage incurred at the time of extraction. Data from an additional 3 animals (n = 2 Trained 15D, n = 1 Trained 3D) had to be omitted from the layer 1 measures due to an inability to localize a sufficient sample of intact dendrites of this length. For all dendritic analyses, spines along the length of measured dendrite were manually counted, and density was calculated as total spines per length of dendrite.

2.3.7 Statistical analyses

All statistical analyses were performed using the SPSS software package. Paired and independent samples t-tests were used for within and between group examinations of behavioral performance on the pasta matrix reaching task respectively. Repeated measures analyses of

variance (ANOVAs) were used to examine group differences in spine measures over time in trained animals versus controls and between the two training durations, and the Shapiro-Wilks test was used to check for normality. When warranted by significant Group by Day interactions, post hoc group comparisons per time point were performed using Holm-Bonferroni corrected t-tests. The last imaging time point (Day 16) was omitted from the ANOVAs because of animal attrition at this time point, and instead, within-animal comparisons between Day 16 and pre-training time points were analyzed with t-tests. Day 16 was also counted as a comparison in the Bonferroni-Holm's correction when post-hoc tests per time point were warranted by ANOVA results. Pearson correlations were used to probe for relationships between behavioral and new spine survival. Paired t-tests were used to probe for within-animal differences in layer II/III spine density in trained compared to untrained motor cortices.

2.4 Results

2.4.1 Manual skill training increased dendritic spine turnover

In adult mice, spines along the superficial dendrites of YFP-labeled pyramidal neurons have been found to be remarkably stable, with only ~3% of spines forming and disappearing over a one-week period (Grutzendler et al., 2002). We found that over 3 days of training on a skilled reaching task (Fig. 2.2) spine formation in adult animals more than doubled compared to baseline (Fig. 2.3A). Prior to training, the $M \pm SE$ percentage of new-to-pre-existing spines was 3.0 ± 0.3, which increased to 7.2 ± 0.3 after 3 days of training, whereas in untrained controls there was minimal change in the percentage of new-to-pre-existing across the same time points (3.2 ± 1.3 and 3.0 ± 1.2, respectively; Fig. 2.3B). The increase in spine formation in trained animals was

followed by an equal and opposite increase in spine elimination by day 6 of training. Spine formation and elimination returned to baseline levels for the remainder of the training period, and there was no net change in spine density by either of the final two imaging sessions. Animals that received no-training control procedures showed minimal changes in spine turnover across the same imaging intervals (Fig. 2.3B). In repeated measures ANOVAs for the Trained 15D group compared with Controls, there was a main effect of time on both spine formation ($F_{(4,24)} = 11.85, p < .001$) and spine elimination ($F_{(4,24)} = 12.99, p < .001$), as well as a significant group by time interaction for both (formation: $F_{(4,24)} = 13.05$, elimination: $F_{(4,24)} = 13.05$, p's $< .001$) indicating that group differences depended on the time point.

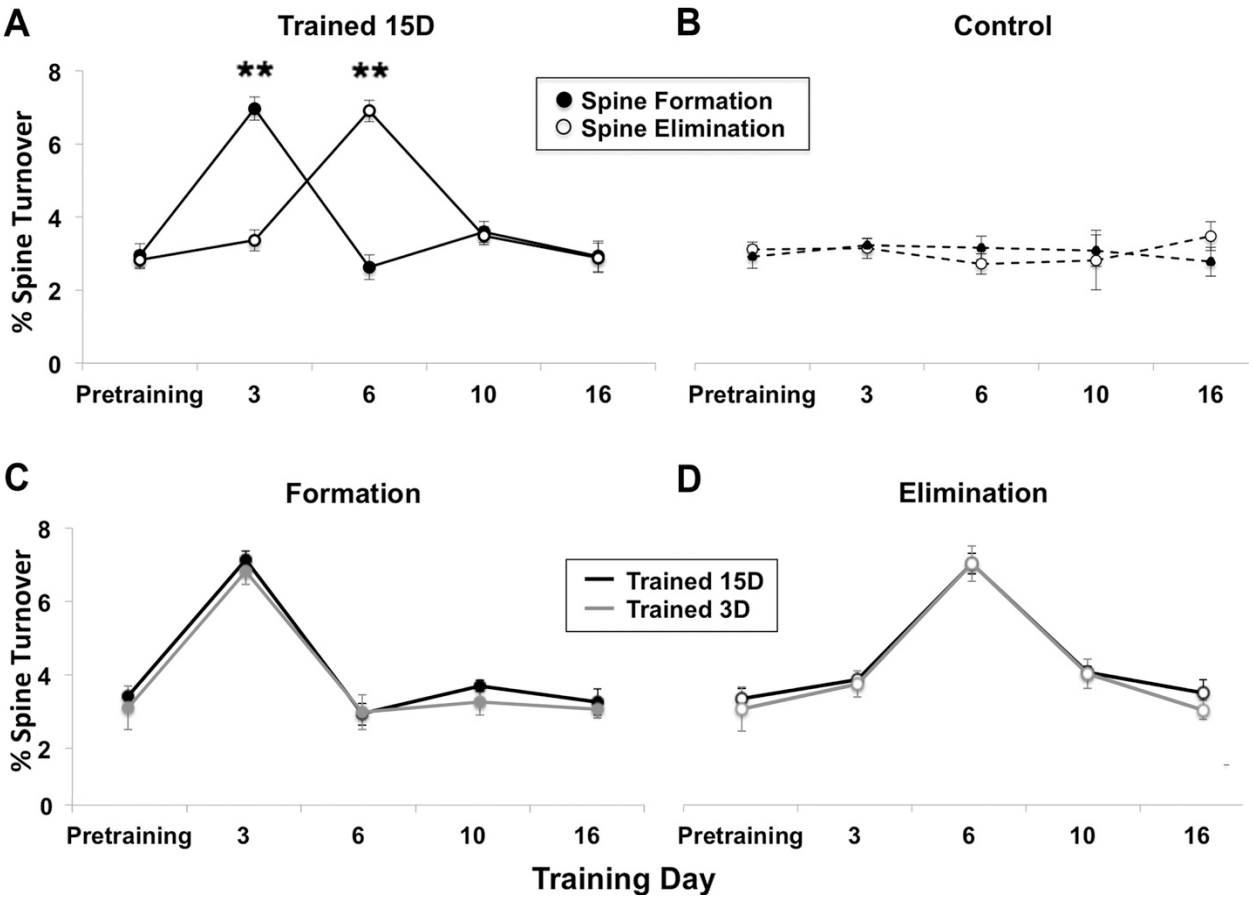

Figure 2.3 Skill training increased spine formation and subsequent elimination in trained motor cortex. (A) *M±SE* rate of spine turnover throughout the period of training on the pasta matrix task. In animals trained for 15 days (Trained 15D), spine formation increased over 3 days of training compared to baseline (**p<0.001) and was followed by an equal and opposite increase in spine elimination by day 6 (**p<0.001 versus baseline). Turnover rates returned to baseline levels by day 10. (B) There was little variation in the rate of spine turnover during the same time course in untrained controls. (C-D) The pattern and rate of spine turnover was comparable in animals that were trained for 3 days (Trained 3D) and 15 days.

Among the groups receiving either 3 or 15 days of training, behavioral performance in the first three days of training was similar (Fig. 2.2B) as were patterns of spine turnover (Fig. 2.3C and 2.3D). There was a significant main effect of time on both formation ($F_{(4,24)} = 36.39$ $p <$ .001) and elimination ($F_{(4,24)} = 51.34$, $p < .001$) but no group by time interaction (Fig 3B,

Formation: $F_{(4,24)} = 0.143$; Elimination: $F_{(4,24)} > 1.97$, p's > 0.05), indicating that both groups show similar rates of spine turnover across time points.

Similar results have been found in adolescent mice receiving training on a skilled reaching task; however the rates of spine turnover were much higher and increases were observed as quickly as one hour after the first training session (Xu et al., 2009). We imaged a subset of trained animals (n=3) after the first day of training and found no change in spine turnover compared to baseline turnover rates ($t_{(2)} = 3.00$, $p > .05$; $M \pm SE$ % turnover at baseline: 3.50 ± 0.15 formation, 2.77 ± 0.58 elimination; on training day 1: 3.27 ± 0.15 formation, 3.28 ± 0.14 elimination). Together, these results indicate that novel manual skill learning produces similar, albeit of lower magnitude and slower in time course, alterations in spine turnover on the superficial dendritic branches of layer V pyramidal neurons in the motor cortex of adults as it does in juveniles.

2.4.2 Preferential Stabilization of New Spines Depended on Continued Training

Spines formed during acquisition of a fine motor skill task in juveniles have been found to persist in much higher proportions over a period of continued training than do new spines in untrained controls, consistent with the possibility that the preferential stabilization of newly formed spines is a mechanism that contributes to retention of newly acquired skill (Xu et al., 2009). We tracked the fates of newly formed spines (Fig. 2.4A) and found that in animals with ongoing training new spines that appeared by day 3 persisted in much greater proportions at later time points than did newly formed spines in controls over the same time span (Fig. 2.4B). In contrast, spines that were present prior to the onset of training were more likely to disappear over the same time

period in trained animals than in controls (Fig. 2.4C). In both groups, new spines disappeared in greater proportions than pre-existing spines, but the relative proportion of new spines that persisted was doubled in animals with continued training (Fig. 2.4D). Repeated measures ANOVAs of the fates of new and pre-existing spines after day 3 revealed significant effects of Group (Trained 15D versus Control, F's$_{(1, 8)}$ = 13.94 and 26.03, respectively, p's < .001) but no Group by Time interactions. By day 16, the proportions of persisting new and pre-existing spines continued to be significantly greater in the Trained 15D group compared with controls (p's < .03). These results support that, as with juveniles, fine motor skill learning in adults is associated with the preferential stabilization of spines that are formed early in the process of skill acquisition on the superficial dendrites of layer V pyramidal neurons.

We next asked whether continued training was necessary for the preferential stabilization of newly formed spines. In a subset of animals, we stopped training procedures after day 3 (Trained 3D), the peak of spine formation, and followed the fates of newly formed spines over the next two weeks (Fig. 2.4A). The percentage of new spines that remained after day 3 was greatly reduced in animals that stopped training compared to those with continued training (ANOVA Trained 15D vs. Trained 3D Group effect: $F_{(1, 8)} = 70.94$, $p < .0001$). The Trained 3D group showed a similar pattern of increased spine formation followed by increased spine elimination (Fig. 2.3C and 3D), including increased elimination of pre-existing spines (Fig. 2.4C), as those trained for 15 days, but in the absence of further training, the newly formed spines were not preferentially stabilized, disappearing at very high rates similar to controls (Fig. 2.4B). These results support that the preferential stabilization of new spines that are generated early in training is dependent on continued skill practice.

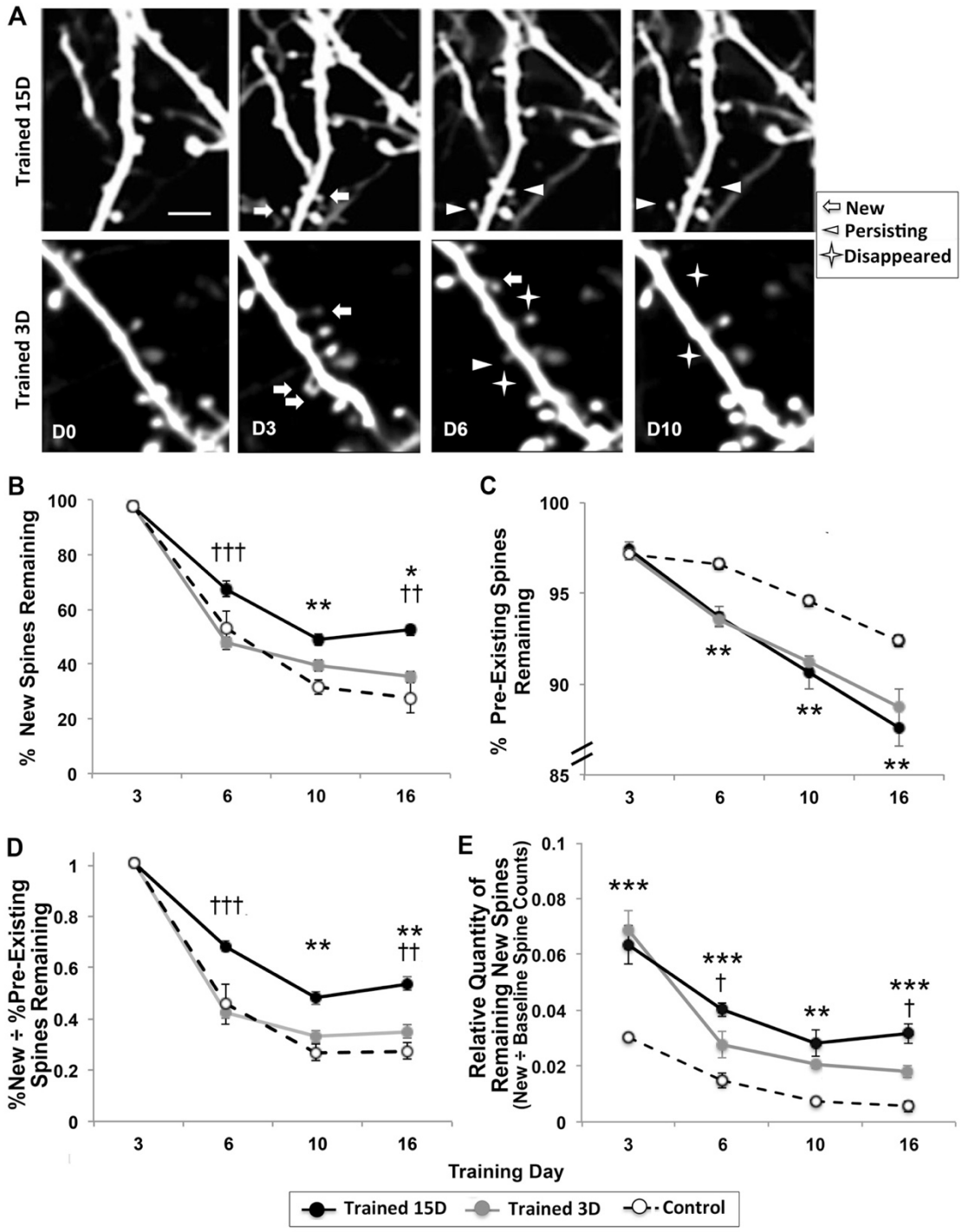

Figure 2.4 Newly formed spines were preferentially stabilized by continued training. (A) Example of spine dynamics from an animal receiving 15 days (top) and 3 days (bottom) of training. Similar rates of spine formation (arrow heads) were found across training conditions on day 3.

Figure 2.4 Cont. On subsequent days newly formed spines were more likely to remain (block arrows) in animals with ongoing training and more likely to disappear (asterisks) in animals that stopped training. Scale bar = 2um. (B) The proportion of new spines generated by the third training day that persisted to the final imaging time point was significantly greater in the Trained 15D group compared to both controls and the Trained 3D group. (C). Pre-existing spines were more likely to disappear in Trained 15D versus Control, but the two training duration groups lost pre-existing spines in similar proportions that were not significantly different. Note the difference in scales between (B) and (C). (D) The Trained 15D group showed the greatest new spine persistence in proportion to pre-existing spine persistence compared to both trained 3D animals and control animals. (E) Despite high rates of new spine elimination, the Trained 3D group had a significantly increased relative quantity of persisting new spines compared with controls on days 10 and 16 (p's≤= .017)., though these quantities were diminished relative to the Trained 15D group. *p<.017, **p<.005, ***p<.0005, Trained 15D vs. Control; †p<.017, ††p<.0005, †††p<.0005, Trained 15D vs. Trained 3D. Data are $M \pm SE$.

Unlike the stabilization of new spines, the persistence of skills learned in the early training period was not dependent on continued practice. When tested after 12 days of no-training control procedures, briefly trained mice performed as well as they did on day 3 as measured by the number of pasta pieces retrieved (Fig. 2.2B; $t_{(4)} = 2.78$, $p = .24$). Performance improvements similarly endured in a group of wild type mice that underwent the same brief training procedure (Fig. 2.5). While the difference between the two training groups at day 15 in the number of pasta pieces retrieved failed to reach significance ($t_{(8)} = 2.30$, $p = .062$), the efficiency with which mice retrieved pasta, as measured by the % retrievals per reach attempt, was significantly improved with continued training (Figs. 2.6-2.7). Nevertheless, gains in reaching efficiency that were achieved by the third training day also endured in the absence of continued training (Fig. 2.6B). These results indicate that the persistence of skill learned during the early training period did not depend on the preferential stabilization of spines that were formed during that period.

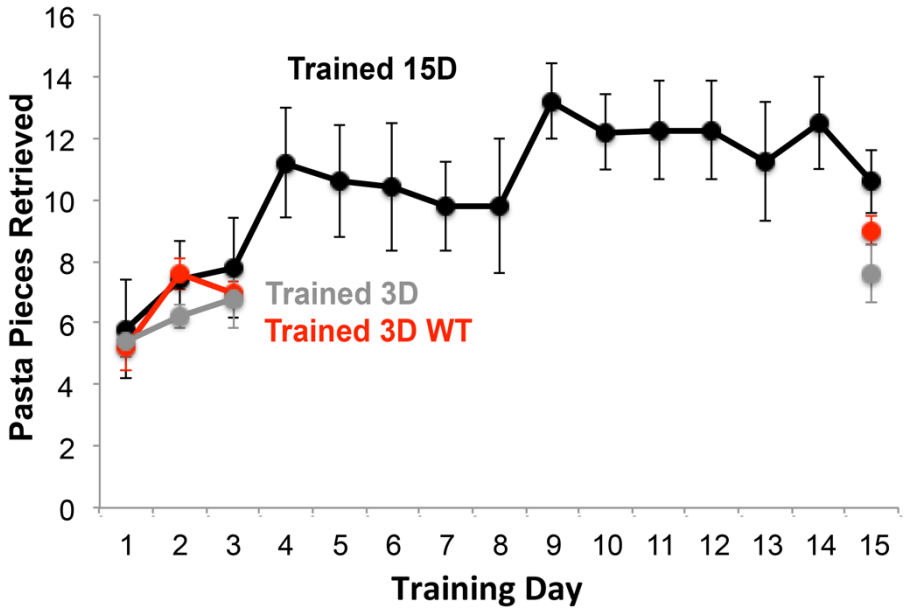

Figure 2.5 Reaching performance in YFP+ and wildtype mice. Reaching performance was very similar in YFP expressing mice that received 3 days of training compared with wild type mice (Trained 3D WT, n=5) that received the same training duration. Data from the Trained 15D and Trained 3D groups are the same as that shown in Fig. 2 of the article. Data are *M* ± *SE*.

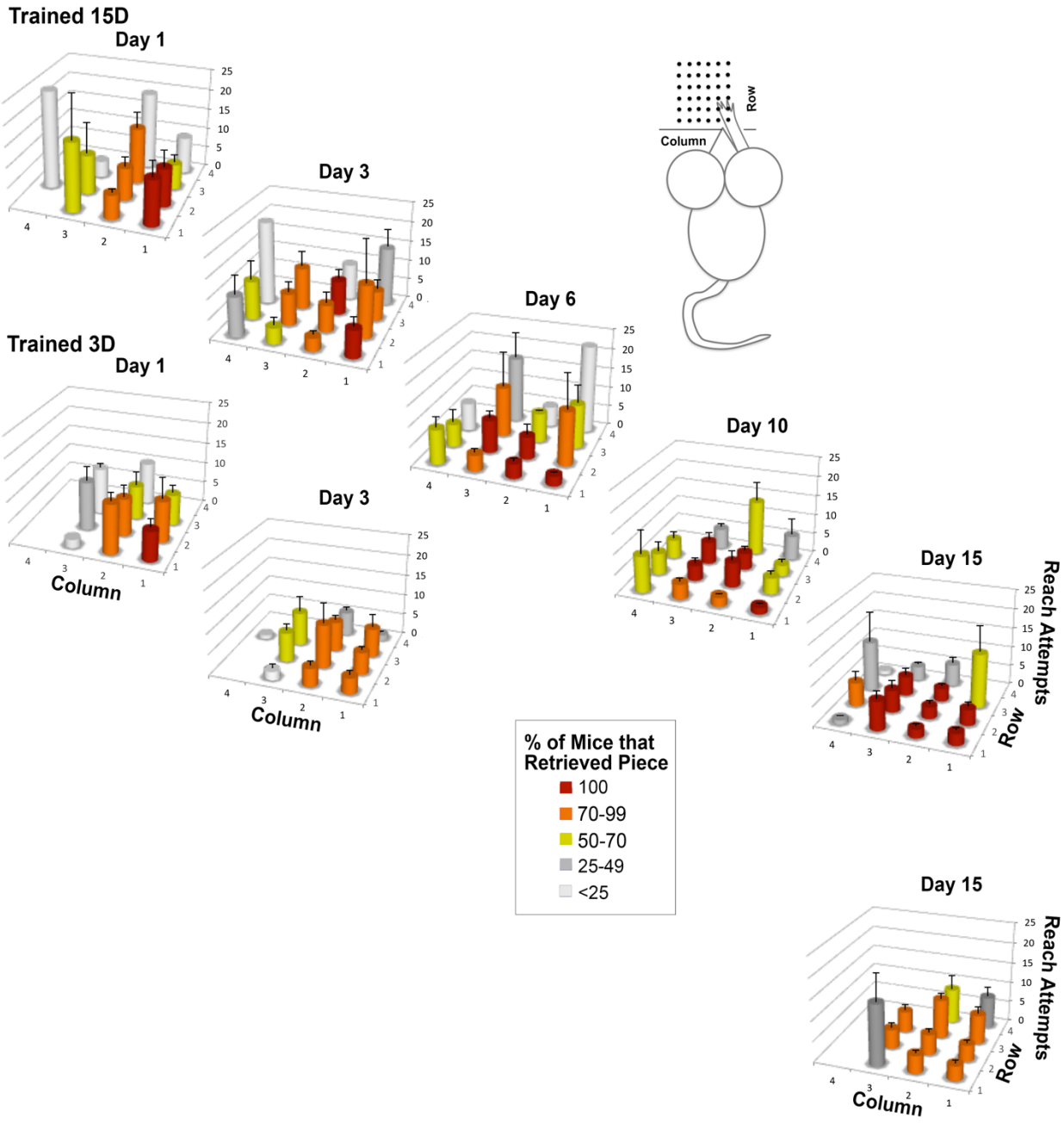

Figure 2.6 Reach attempts disaggregated by matrix position. Number of reach attempts to retrieve pasta pieces and % of mice retrieving the pieces per matrix position. The position of row 1, column 1 is closest to the reaching window. Matrix positions in which no mouse retrieved pasta are omitted from the plots. Data from YFP expressing and wildtype mice are pooled in the Trained 3D graphs. Data are $M \pm SE$.

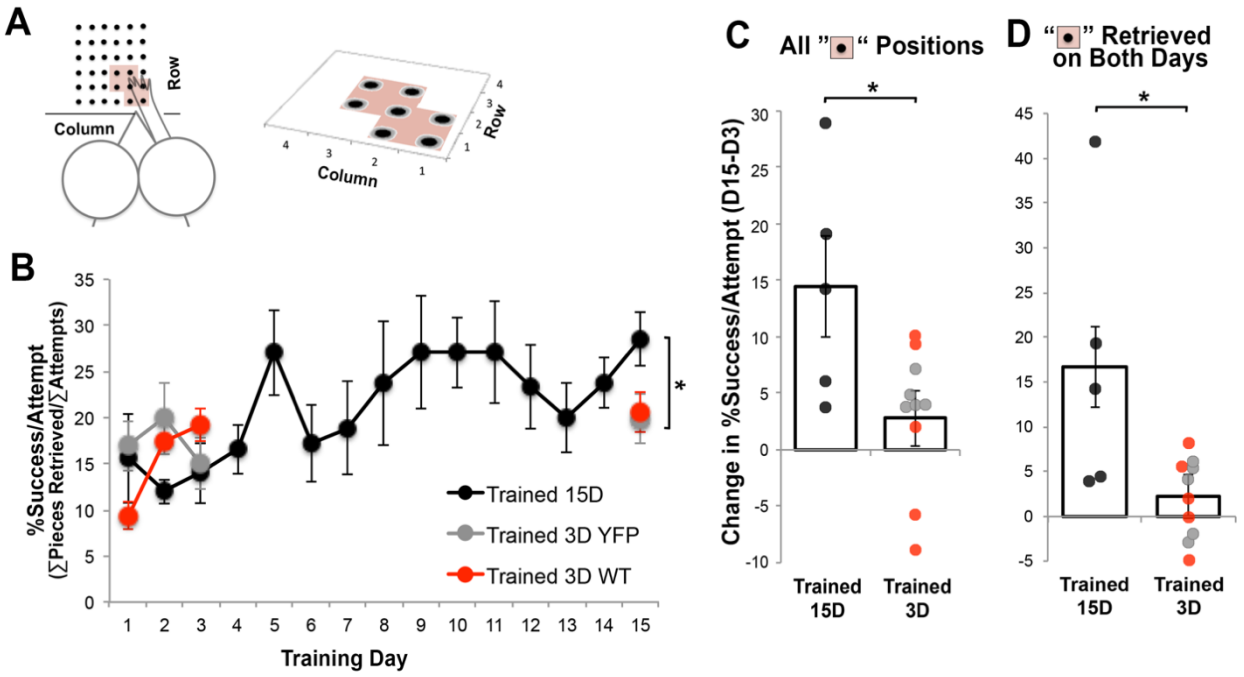

Figure 2.7 Reaching efficiency, as assessed by success per reach attempt, improved with more training. ***A***, This analysis was restricted to matrix positions (shaded) in which pasta pieces were retrieved by at least 70% of the mice of both training durations on Day 15 to minimize the contribution of increased difficulty of retrieving pieces outside of it. ***B***, On day 15, the Trained 15D group had improved success rates compared with Trained 3D (**p*=.009). ***C***, Gains in reaching success between days 3 and 15 were significantly greater in the mice with more training (**p*=.008). However, most mice in the Trained 3D condition had success rates on day 15 that were slightly improved relative to day 3. ***D***, A similar pattern of results was observed when the analysis was further restricted within mice to those shaded matrix positions from which pasta pieces were retrieved on both days 3 and 15 (**p*=.007). Note the difference in scales between ***C*** and ***D***. Data are *M* ± *SE*.

2.4.3 Training Increased the Population of Persisting New Spines Without Preferential Stabilization

The major increase in spine formation in the first three training days could be expected to increase the total population of persisting new spines relative to controls even in the absence of their preferential stabilization. We estimated new spine quantities as a relative factor of total spines counted at baseline to account for variability in the number of spines sampled between

animals (Fig. 2.4E). Mice with 3 days of training had relative quantities of persisting new spines that were intermediate between those of controls and mice with 15 days of training. In comparing mice with 3 versus 15 days of training, there was a significant effect of Group on the relative quantities of new spines that persisted on days 6 and 10 ($F_{(1,8)} = 5.51$, $p = .04$). By day 16, the relative quantities of new spines continued to be significantly increased in the Trained 15D group compared with the Trained 3D group ($p = .027$). Both training durations, however, had increased relative quantities of persisting new spines compared with controls (ANOVA Group effects, Trained 15D vs. Control: $F_{(1,8)} = 35.41$, $p < .001$, Trained 3D vs. Control: $F_{(1,8)} = 31.90$, $p < .001$). Thus, while the present results indicate that the endurance of newly learned skill cannot be attributed to *preferential* stabilization of new spines, it remains possible that the persistence, after training stopped, of a modest proportion of the new spines that were formed early in training contributed to the endurance of skills learned in the same time period.

2.4.4 Persisting New Spines Predicted Performance Gains

To probe whether preferential new spine stabilization was associated behavioral improvement, we analyzed the relationship between the proportion of persisting new spines and performance gains between days 3 and 15, as measured by the difference in pasta pieces broken. Performance gains were positively correlated with the % of new spines formed on day 3 that were still present on days 10 ($r = 0.82$, $t_{(8)} = 4.18$, $p = .015$; Fig. 2.8A) and 16 ($r = 0.87$, $t_{(6)} = 4.33$, $p = .004$), indicating that the stabilization of the spines that were formed during the first 3 days of training is associated with subsequent improvements in behavioral performance. These performance gains were similarly correlated with relative quantities of new spines remaining on day 10 ($r =$

0.84, $t(8) = 4.44$, $p = .002$; Fig. 2.8B). These results indicate that both the preferential stabilization and the persisting quantity of new spines that are formed on superficial dendrites of layer V pyramidal neurons early in the process of acquiring a new motor skill are associated with skill refinement.

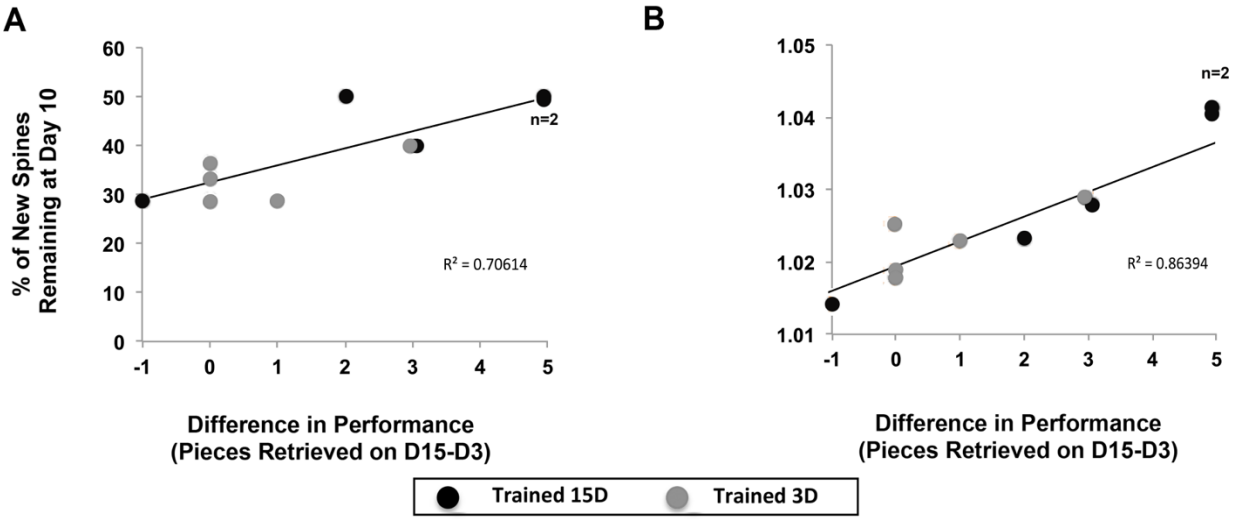

Figure 2.8 New spine stabilization predicted performance gains. (A) Performance gains, measured by the difference in pasta retrieved on day 15 versus 3, positively correlate with the percentage of new persisting spines (*p= 0.016) and (D) the relative quantities of new persisting spines (* p= 0.002) at day 10 in both training groups.

2.4.5 Skills Training Induced Subpopulation-Specific Increases in Dendritic Spine Density

While training was associated with a significant increase in spine formation and subsequent elimination on the superficial apical branches of layer V pyramidal neurons in motor cortex *in vivo*, rates of formation and elimination were nearly equal, and thus no net change in spine density was observed. The absence of net changes in spine quantities on these dendrites has been consistently reported in *in vivo* imaging studies (Grutzlendler et al., 2002; Trachtenberg et al., 2001; Zuo et al., 2005) but it contradicts reports of training induced alterations in spine density on dendrites that are deeper in the cortex (e.g., Greenough & Withers, 1985; Withers &

Greenough, 1989; Wang et al., 2012). We examined the possibility that this contradiction reflects dendritic subpopulation-dependent variation. In the same mice imaged *in vivo,* we histologically examined spine density on the apical branches of YFP expressing layer V pyramidal neurons within layers I and layer II/III of motor cortex using confocal microscopy (Fig. 2.9A and B). Consistent with the *in vivo* results, spine density in layer I was found to be similar in the trained and untrained hemispheres of both groups (Fig. 2.9C; Trained 15D, $t_{(2)} = 4.30, p = .49$; Trained 3D, $t_{(2)} = 4.30, p = .90$). In contrast, spine density in layer II/III was significantly greater in the trained compared to the untrained hemisphere in both training groups (Fig. 2.9D; Trained 15D, $t_{(4)} = 2.78, p < .01$; Trained 3D, $t_{(3)} = 2.41, p < .01$). These results suggest that there are dendritic subpopulation-specific structural responses to training, which can explain differences between *in vivo* and fixed tissue results. That spine density was similarly increased in the Trained 3D group versus Trained 15D group ($t_{(7)} = 1.93, p = .98$, Fig. 2.9D) is also generally consistent with the possibility that the net increases in spine density on this dendritic subpopulation could be a structural mechanism for long-term retention of the skill that was learned within 3 training sessions.

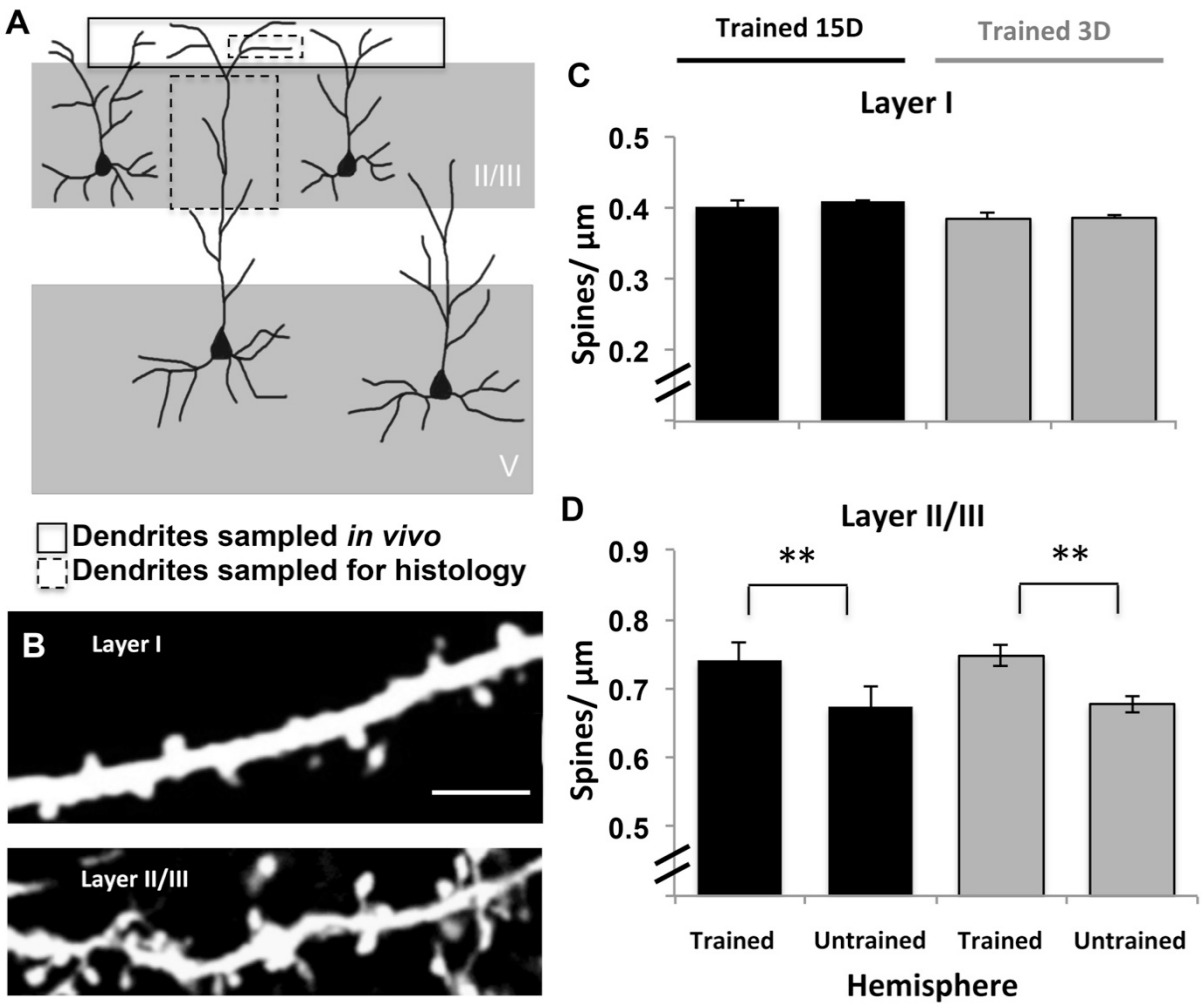

Figure 2.9 Brief and extended training increased spine densities on apical branches of layer V neurons in layer II/III but not layer 1 of trained motor cortex. (A) Illustration of apical dendritic subpopulations of layer V pyramidal neurons that were sampled *in vivo* and histologically**.** (B) Confocal images of apical dendritic branches sampled from layer I (top) and layer II/III (bottom) from histological samples. Scale bar = 10um. (C) Consistent with *in vivo* results, spine densities on layer I dendrites were similar between trained and untrained hemispheres in Trained 15D (n=3,p=0.49) and Trained 3D (n=3,p=0.90) groups. (D) Spine density on layer II/III dendrites was increased in trained versus untrained motor cortex in both the Trained 15D (n=5, **p = 0.002) as well as Trained 3D (n=4, **p= 0.002) group. Data are *M±S*

2.5 Discussion

Previous findings have raised the possibility that the preferential stabilization of new dendritic spines that are formed early in the process of learning a new motor skill in superficial motor cortex could be a mechanism contributing to lasting memory for that skill (Xu et al., 2009; Yang et al., 2009). Newly formed spines tend to be transient, disappearing in much greater proportions than do pre-existing spines (Chen et al., 2014). In mice trained in a skilled reaching task (Xu et al., 2009) or on an accelerating rotarod (Yang et al., 2009), the spines that are formed early in training during a period of increased spine turnover persist in greater proportions than do new spines in untrained controls, supporting that new spines are preferentially stabilized during motor skill learning. Whether this new population of stabilized spines was necessary for long-term retention of the newly acquired had not been determined. In the present study, by examining the maintenance of newly formed spines in mice with ongoing training compared to mice that were only briefly trained, we found that continued training is required for the preferential stabilization of spines that are formed in response to the initial training. In proportions and relative quantities, stabilized new spines were correlated with the magnitude of performance improvements between the third and final training sessions. However, the preferential stabilization of new spines could not have been essential for the retention of the new skill because mice in the briefly trained condition maintained the skill that they learned while losing new spines in proportions similar to untrained controls. A summary of these experimental results is shown in Illustration 2.1.

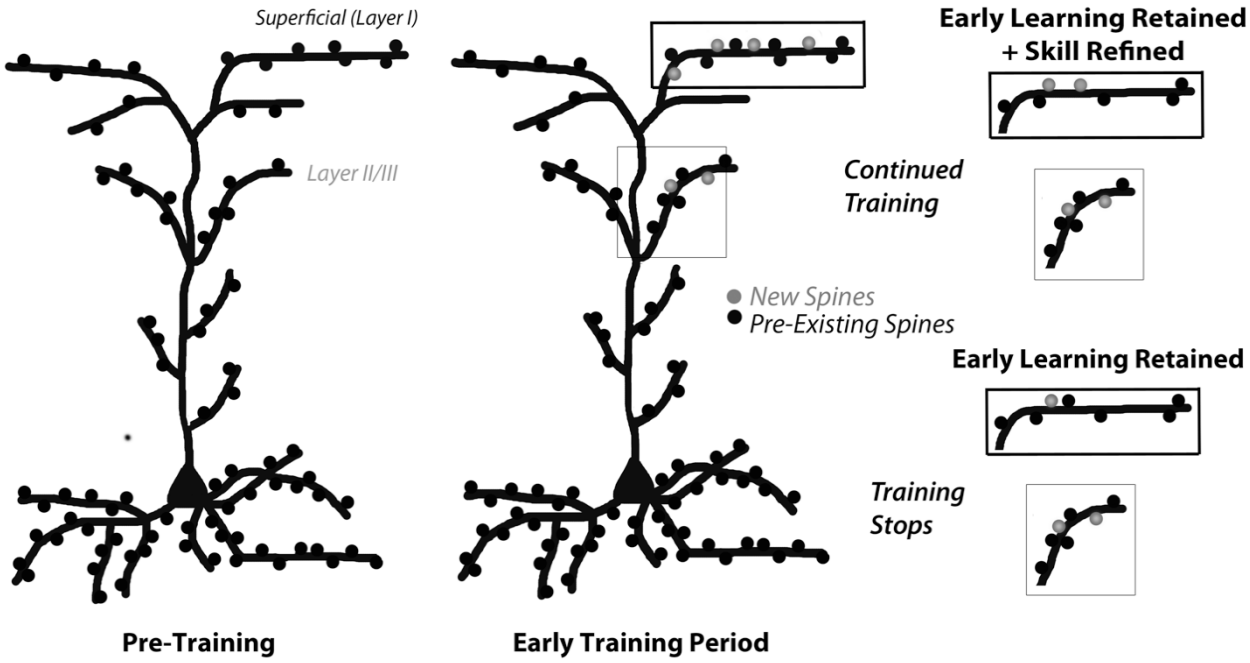

Illustration 2.1 Summary of experimental results. In adult mice, in the early phase of learning a new motor skill there are increases in spine formation on layer I apical branches in trained motor cortex. Upon continued training, the new spines are preferentially stabilized, which is predictive of performance improvements, and this occurs at the expense of pre-existing spines such that the relative spine density remains unchanged. In the absence of continued training, new spines are more likely to disappear, but the skill that was learned earlier does not. The early phase of learning also increases the density of spines on apical dendrites in layer II/III (although when that occurs is unknown) and this increase does not depend on continued training.

Motor skill learning involves the acquisition of complex movement combinations that are refined with practice and retained for long time periods (Luft & Buitrago, 2005). Across training sessions, motor skill learning curves are characterized by an early phase of rapid performance improvements followed by a period of more gradual improvements (Diedrichsen & Kornysheva, 2015; Karni et al., 1998; Kleim et al., 1996; Kleim et al., 2005; Luft & Buitrago, 2005). In the present study, the end of the brief training period was near the end of this early phase of rapid performance improvements (~ the first 4 days), which was also during the period of increased

spine formation. This was followed in both training groups by an equal amount of spine elimination. However, in mice with continued training, new spines survived this elimination process in almost twice the proportion as did the new spines of mice that had ceased training. The stabilization of new spines during motor skill learning is associated with increases in their size (Fu et al., 2012), and spine size reflects the strength of the synapse (Hofer et al., 2009; Roberts et al., 2010; Yasumatsu et al., 2008). Thus, spine stabilization can reflect synapse maturation. Since the survival and maturation of synapses is neural activity-dependent (Katz & Shatz, 1996; Marrs et al., 2001; Star et al., 2002; Wong & Ghosh, 2002; Yasumatsu et al., 2008), it seems likely that the preferential survival of nascent spines only in mice with continued training reflects that these spines were sufficiently activated to promote the maturation of their synapses as the animals practiced, and continued to subtly improve performance in the reaching task.

Given its dependency on continued training and correlation with performance improvements, the overall pattern of the present results is consistent with a greater involvement of the preferential stabilization of new spines in ongoing skill refinement than in the memory of the skill that was learned as the new spines were formed. This obviously does not rule out that the modest proportion of new spines that persisted in the absence of continued training contributed to memory for skill learned in the early training period. It also does not rule out a contribution of the preferential stabilization of this population of spines in skill memory. In the process of learning motor skills, the more subtle performance improvements that occur after the early learning phase presumably reflect the accumulation of subtle refinements in movement strategy, which depend on retention of those refinements that were established before. It may

very well be that the preferential stabilization of new spines is involved in this accumulated memory of skill refinements in the gradual learning phase.

About a third of new spines that appear during the early learning phase form in clusters, and such clusters are more likely to persist with prolonged training compared to individual spines (Fu et al., 2012). Formation of new spine clusters over 4 days depends on task practice, and successive new spines accompany strengthening of the first spine in the cluster (Fu et al., 2012). Thus, it may be the stabilization of the new spine clusters specifically, rather than newly formed spines in general, that is associated with improvements in motor performance. Consistent with this, fmr1 knockout mice (a fragile x syndrome model) have more limited performance improvements with ongoing motor training compared with wildtype mice (Padmashri et al., 2013) as well as reduced spine formation and clustering, but they do not have reductions in the proportions of new spines that are stabilized (Reiner & Dunavesky, 2015). Thus, the greater spine stabilization that was associated with performance improvements in our study was potentially mediated by repeated practice-dependent activation of newly formed spine clusters (Fu et al., 2012; Kasai et al., 2010).

We also found that spine changes varied between the superficial and deeper dendrites of layer V pyramidal neurons. Similar to previous studies (Holtmaat et al., 2006; Trachtenberg et al., 2002; Xu et al., 2009; Yang et al., 2009) we found no net change in spine density on the superficial apical dendrites of layer V pyramidal neurons imaged *in vivo*. Histological analyses of this superficial population of dendrites confirmed a lack of net change in spine densities between the trained and untrained hemispheres. In contrast, we found that spine density on deeper apical dendrites within layer II/III was increased in the trained compared with untrained

motor cortex. These results indicate variation in the structural effects of skill learning even across nearby dendritic subpopulations of the same neuronal population. Such variation is not surprising in the context of abundant fixed-tissue evidence for laminar specific (Adkins et al., 2002; Uylings et al., 1978; Wang et al., 2012) and neuron population specific (Uylings et al., 1978; Wang et al., 2012; Withers & Greenough, 1989) dendritic structural plasticity in response to various manipulations of behavioral experience in rats. Motor skill training in rats also affects the structure of different pyramidal neuron populations differently (Kleim, et al., 2002; Greenough & Withers, 1985; Withers & Greenough, 1989). Wang and colleagues (2012) have found that skilled reach training in rats induces distinct structural plasticity in different subsets of the same neuronal population (layer V apical versus basilar dendrites). The pattern of structural changes across subpopulations of pyramidal neurons and their dendrites also vary with different motor tasks (Kolb, 2008). Some differences in how spine dynamics on the superficial apical branches of layer II/III (Ma et al., 2016) versus layer V (Yang et al., 2014) pyramidal neurons of mice are affected by rotorod or treadmill training have also been reported. Thus, evidence from histological and *in vivo* studies converge to support that dendritic structural responses to skill learning vary across different dendritic subpopulations of motor cortex.

That spine densities within layer II/III were similarly increased in both training groups, as assessed two weeks after the final (Day 15) training session is generally consistent with the potential involvement of this structural change in the persistence of skill that was learned during the initial training period. However, because measurements of spine density were assessed histologically, the time course of the spine addition remains unknown, and it is also possible that there were earlier differences in spine densities between the two training groups that were

missed. However, Gloor et al. (2015) have found that the basilar and apical dendrites of layer V pyramidal neurons in rats continue to increase in length after skilled reach training stops, peaking one month after the end of training and shrinking thereafter. Therefore, it is possible that the observed increases in spine density would not have been as evident earlier and also that they may in fact return to baseline levels at later time points after the end of training.

Superficial dendrites have not been a popular choice as the focus of histological analyses, possibly due to challenges related to the high density of dendrites in superficial cortex and its tendency to accrue damage during histological tissue processing. For *in vivo* imaging, the clarity with which superficial dendrites can be visualized with two photon microscopy to enable real time assays of experience-induced synaptic plasticity is compelling of the focus on this population. Still, the exact functional relevance of the observed structural changes remains poorly understood. Here we have shown that while motor skill learning is associated with the formation and preferential stabilization of new spines on superficial dendrites of layer V pyramidal neurons, the latter is not required for the retention of the newly acquired skill. Instead, the degree to which new spines are preferentially stabilized could reflect the degree to which the process of skill mastery continues. In addition, we found strikingly different structural responses to skill learning on dendrites slightly deeper in cortex. In layers II/III, but not in layer I, spine densities on apical dendrites of layer V pyramidal neurons increased, similarly so in mice with brief or more prolonged training, indicating that spine changes even on the same dendritic population can vary greatly with dendritic location, and that net increases in spines on the deeper subpopulation is potentially a structural substrate for the long-term retention of skills acquired early in training

Motor skill learning involves the generation of complex movement patterns that are learned with repeated practice. Mastery of a motor skill is reflected in increases in efficiency and accuracy of the movements (Diedrichsen & Kornysheva, 2015). This complex learning process is likely the product of harmonized changes in the synaptic connectivity of numerous neuronal and dendritic populations occurring both within and beyond motor cortex. Ours and previous results highlight that while *in vivo* imaging is an invaluable approach for examining the structural basis of experience-dependent plasticity, spine alterations occurring on the superficial apical branches of cortical pyramidal neurons provide only a small window into training-induced structural plasticity, which undoubtedly requires coordination with synaptic changes across diverse neuronal and dendritic populations.

Chapter 3: Artery-Targeted Photothrombosis, a Variation of the Photothrombotic Stroke Model, Enlarges the Vascular Penumbra, Instigates Peri-Infarct Neovascularization and is Suitable for Modeling Upper Extremity Impairments

Currently under review for publication in The Journal of Cerebral Blood Flow and Metabolism as. 'Clark, TA., Sullender, C., Kazmi, SM., Speetles, BL., Williamson, MR., Palmberg, DM., Dunn, AK., & Jones, TA. Artery targeted photothrombosis enlarges the vascular penumbra, instigates peri-infarct neovascularization and models upper extremity impairments. CS contibted to the development of the model used for experiments. TC was responsible for experiment design, data collection, analysis, interpretation, and writing of this manuscript.

3.1 Abstract

The photothrombotic stroke model generates localized and reproducible ischemic infarcts useful for studying recovery mechanisms, but its failure to produce a substantial ischemic penumbra weakens its resemblance to human stroke. We examined whether a modification of this approach, confining photodamage to arteries on the cortical surface (artery-targeted photothrombosis), could better reproduce aspects of the penumbra. Following artery-targeted or traditional photothrombosis in mice, post-ischemic cerebral blood flow was measured using multi-exposure speckle imaging at 6, 48, and 120 h post-occlusion. Artery-targeted photothrombosis produced a more graded penumbra at 48 and 120 h. Vascular density of isolectin $B4^+$ vessels in peri-infarct cortex, was similarly increased in both groups compared to sham at 2 weeks indicating that both models instigated post-ischemic vascular structural changes. We also tested the suitability of artery-targeted photothrombosis for modeling motor impairments. In mice trained on a skilled reaching task, small motor-cortical infarcts impaired skilled-reaching performance for up to 10 days. Together, these results support that artery-targeted photothrombosis widens the penumbra while maintaining the ability to create localized infarcts useful for modeling post-stroke impairments.

3.2 Introduction

Of particular therapeutic interest in ischemic stroke, is the ischemic penumbra, the region around the ischemic core containing tissue in transition from reversible to irreversible damage, the fate of which is influenced by post-ischemic vascular events (Fisher et al., 1998; Heiss et al., 2011; Murphy & Corbett, 2009; Schaug et al., 1999). Adequate reperfusion in the penumbra early after ischemia onset limits the extent of tissue damage, and the penumbra has therefore been a focus of acute neuroprotective treatments (Fisher et al., 1998; Fisher et al., 1997; Gravanis et al., 2008; Berkhemer et al., 2015; Cronin et al., 2010; Jaffer et al., 2011). Adequate CBF also supports cellular mechanisms of repair and remodeling over longer time periods, including neuronal growth and neovascularization, which are related to improved functional outcomes (Arenillas et al., 2007; Hayward et al., 2011; Martin et al., 2012; Lin et al., 2002; Lake et al., 2017; Ohab et al., 2006; Taguchi et al., 2009; Sobrino et al., 2007; Bogoslovsky et al., 2010; Krupinski et al., 1994; Szpak et al., 1999; Cramer et al., 2011).

The photothrombotic stroke model is well suited for the study of cellular mechanisms of functional recovery following ischemia because it creates circumscribed lesions that can be placed with anatomical precision, for example, in discrete functional regions of cortex to reliably cause behavioral impairments (Carmichael et al., 2005; Dietrich et al., 1986; Watson et al., 1985). One drawback of the model is that the ischemic penumbra is narrow, making it challenging to examine how events unfolding within the penumbra relate to the repair and remodeling responses that support improved functional outcomes (Carmichael et al., 2005).

During photothrombosis, following administration of a photoactive dye (Rose Bengal), illumination of a circumscribed region generates singlet oxygen, platelet activation, and damage

to endothelial cells (Dietrich et al., 1986; Watson et al., 1985). This results in vasogenic edema, which rapidly propagates the developing lesion beyond the illuminated region, and which is thought to compromise the development of a penumbra (Carmichael et al., 2005; Dietrich et al., 1986; Watson et al., 1985). Furthermore, illumination causes non-discriminant damage to surrounding tissue, including microvasculature and veins, within the circumscribed region. The main goal of the present study was to test whether our recently established method of using a digital micromirror device (DMD) to confine illumination to a set of pre-identified arterial branches on the cortical surface (Sullender et al., 2018) thereby minimizing damage to surrounding brain tissue, could better reproduce a graded vascular penumbra compared to the traditional photothrombotic model. We additionally examined the influence of age on the development of the penumbra following artery-targeted photothrombosis.

Another goal was to determine whether there is neovascularization in the peri-infarct region after traditional and artery-targeted photothrombosis. The magnitude and persistence of neovascularization in peri-infarct tissue (Szpak, 1999) and its significance for chronic post-stroke outcomes, is unclear. In rodent models of focal ischemia (Arenillas et al., 2007; Hayward et al., 2011; Martin et al., 2012; Lin et al., 2002; Lake et al., 2017; Ohab et al., 2006; Taguchi et al., 2009) and after human stroke (Sobrino et al., 2007; Bogoslovsky et al., 2010; Krupinski et al., 1994; Szpak et al., 1999; Cramer et al., 2011), increased vascular density in the peri-infarct cortex has been associated with improved outcomes, but considerable variability in the timing and extent of neovascularization has been reported across studies. Additionally, despite ample histological evidence for neovascularization in other focal ischemia models (Arenillas et al., 2007; Hayashi et al., 2003; Hayward et al., 2011; Lin et al., 2002; Lin et al., 2008; Lake et al.,

2017; Manoonkitiwongsa et al., 2011; Martin et al., 2012; Marti et al., 2000; Ohab et al., 2006; Prakash et al., 2013; Tagushi et al., 2004; Thored et al., 2007; Wei et al., 2001; Zhang et al., 2000) evidence for it in the traditional photothrombotic model is lacking. I*n vivo* imaging studies of perfused vessels revealed no evidence for neovascularization after photothrombosis (Brown et al., 2007; Schrandt et al., 2015; Tennant et al., 2013) but this approach cannot rule out the existence of newly formed vessels that are not yet perfused. Here, we used histological measures of lectin-labeled vessels to assess neovascularization and its potential spatiotemporal variation after artery-targeted and traditional photothrombosis.

A final goal was to determine whether the new model maintains the strength of the traditional one for the study of recovery mechanisms. Sufficient damage to the caudal forelimb area of motor cortex by photothrombosis results in reliable deficits in skilled forelimb movements that have been used to model chronic post-stroke upper-extremity impairments (Nudo et al., 1999; Krakauer et al., 2006; Jones et al., 2011). Here we tested whether artery-targeted photothrombosis of the same region results in enduring impairments in skilled forelimb use in mice.

3.3 Materials and Methods

3.3.1 Subjects

A total of 45 well-handled young-adult (young-adult, 4-6mo) C57/Bl6/YFP-H line mice of both sexes were used to examine the impact of artery-targeted photothrombosis in motor cortex (MC) on CBF and vascular density (n = 22) and skilled forelimb function (n = 23). For CBF and vascular density measures, mice were placed into one of three groups: artery-targeted photothrombosis (targeted young adult; n = 5 male and n = 4 female), traditional

photothrombosis (traditional young-adult; $n = 4$ male and $n = 5$ female) or sham ($n = 2$ male and $n = 2$ female). A separate cohort of middle-aged (middle-aged, 10-12 mo) mice was included to examine the impact of age on vascular measures after targeted photothrombosis (targeted middle-aged; $n = 2$ male and $n = 4$ female). The impact of artery-targeted photothrombosis of MC on skilled forelimb function was tested in young-adults undergoing targeted-photothrombosis ($n = 7$ male, $n = 6$ female) or sham procedures ($n = 6$ male and $n = 4$ female). One male in the targeted young-adult group was included in vascular density, but not CBF, measures due to poor window clarity, and 2 males (1 traditional young-adult and 1 targeted young-adult) were included in CBF, but not vascular density, measures due to poor lectin labeling. Not included in the n's reported above were three mice in the traditional group ($n = 1$ male and $n = 2$ female) that were omitted from CBF and vascular measures due to lesions greater than 2 standard deviations above the group average, and 3 males and 1 female omitted from the behavioral measures due to lesions that were greater than 2 standard deviations below the group average. Four animals in the middle-aged group were omitted due to lesions greater than 2 standard deviations from the group average ($n = 1$ male and $n = 1$ female), issues with window clarity ($n = 1$ male), or early post-op death ($n = 1$ male).

Animals were bred at the Animal Resource Center at the University of Texas at Austin. Mice were housed in groups of two to four on a 12:12 hour light/dark cycle. Each cage had standardized supplementation including wooden toys, bedding and PVC pipes which were replaced weekly. Animals used for CBF and vascular density measures were given food and water *ad libidum*. Mice used in the behavioral study were placed on scheduled feeding (2.5-3 g food/day) for the duration of shaping, training and testing procedures. The $M \pm SE$ starting

weights were 20.97 ± 0.33 g for females and 24.69 ± 0.64 g for males. Animals were weighed daily for the first week and then once a week thereafter to ensure they did not fall below 90% of their free feeding body weight. All animal use was in accordance with a protocol approved by the Animal Care and Use Committee of the University of Texas at Austin.

3.3.2 Cranial Window Creation

Mice were anesthetized with ketamine (4 mg/kg, i.p.) and xylazine (3 mg/kg, i.p.). Dexamethasone (2 mg/kg s.c.) and carprofen (2.5 mg/kg s.c.) were administered pre-operatively to help minimize cortical swelling and inflammation during the procedures. Anesthetic plane was monitored via respiratory rate and toe pinch response throughout surgery. Booster injections of ketamine (4 mg/kg) were given as needed to maintain anesthesia. Following midline incision of the scalp, a 3 mm circular region of skull over frontoparietal cortex was thinned using a high-speed dental drill with a 0.5 mm diameter drill bit (Fine Science Tools, product #19007-05) and removed, leaving dura intact. Saline was frequently applied to protect the brain from overheating. Skull was then replaced with a 3 mm diameter No. 1 coverglass (Warner Instruments, #64-0720) and sealed with cyanoacrylate (3M Vetbond Tissue Adhesive, #1469) and dental cement. All windows were made over the forelimb area of the motor cortex as defined previously from intracortical mapping experiments (Tennant et al., 2011). Medial and anterior edges of the window were approximately 2 mm rostral to bregma and 0.5 mm lateral to midline. For animals undergoing behavioral procedures, windows were placed over the motor cortex contralateral to the preferred-for-reaching forelimb. Following surgery, animals were given buprenorphine (3 ml/kg, s.c.) for pain management and allowed to recover in their cage for 1.5-2 weeks. For the first week after surgery, animals were given daily injections of carprofen (2.5

mg/kg, i.p.) to help minimize inflammation that contributes to window clouding.

3.3.3 Artery-targeted and Traditional Photothrombosis

Mice were anesthetized with isoflurane (4% induction, 1.5-2% maintenance) in O_2 and affixed to a stereotaxic frame. Arterial oxygen saturation and heart rate from pulse oximetry (MouseOx; Starr Life Sciences Corp. Oakmont, PA, USA) were recorded and temperature was maintained at 37° C with a feedback temperature control system (FHC Bowdoin, ME, USA). For targeted photothrombosis, a green diode laser (product info for laser) was coupled to a digital micro-mirror device (DMD, LDD400-1P, Wavelength Electronics,Bozeman, MT, USA) to provide focused patterned illumination (20 mW) over arteries on the pial surface supplying the forelimb region of MC with minimal exposure to surrounding parenchyma (Fig. 3.1A). In order to account for variations in the size and caliber of the arteries targeted, a range of 1-3 branches were illuminated. The $M \pm SE$ target area was 0.15 ± 0.021 mm^2). In all animals, the main arteries targeted were distal branches of the middle cerebral artery (MCA). In animals with extensive collateralization (n = 4), 1-2 distal branches of the anterior cerebral artery (ACA) were also illuminated to control the level of collateral flow at the time of occlusion. Thirty seconds following retrooribital injection of Rose Bengal (50 µL, 15 mg/mL i.v., Sigma), target vessels were irradiated with the patterned laser. For traditional photothrombosis, following the injection of rose bengal (100 µl, 15mg/ml i.p.), a green laser fiber (532 nm, Millenia V, Spectra Physics, Santa Clara, CA, USA) coupled with a separate objective system (10x, Olympus) delivered focused laser illumination (20-24 mW) over a defined region of MC for 12-15 minutes (Fig. 3.1B). Sham animals were exposed to laser illumination after injections of sterile saline. In all animals, CBF was monitored in real time throughout and 30 min following the occlusion using

traditional laser speckle contrast imaging (Kazmi et al., 2013; Parthasarathy et al., 2010). The backscattered laser light was relayed to a CMOS camera (acA1300-60gmNIR, 1280x1024 pixels, Basler AG, Germany) with ~2x magnification and acquired at 60 frames-per-second with 5 ms exposure time using custom software.

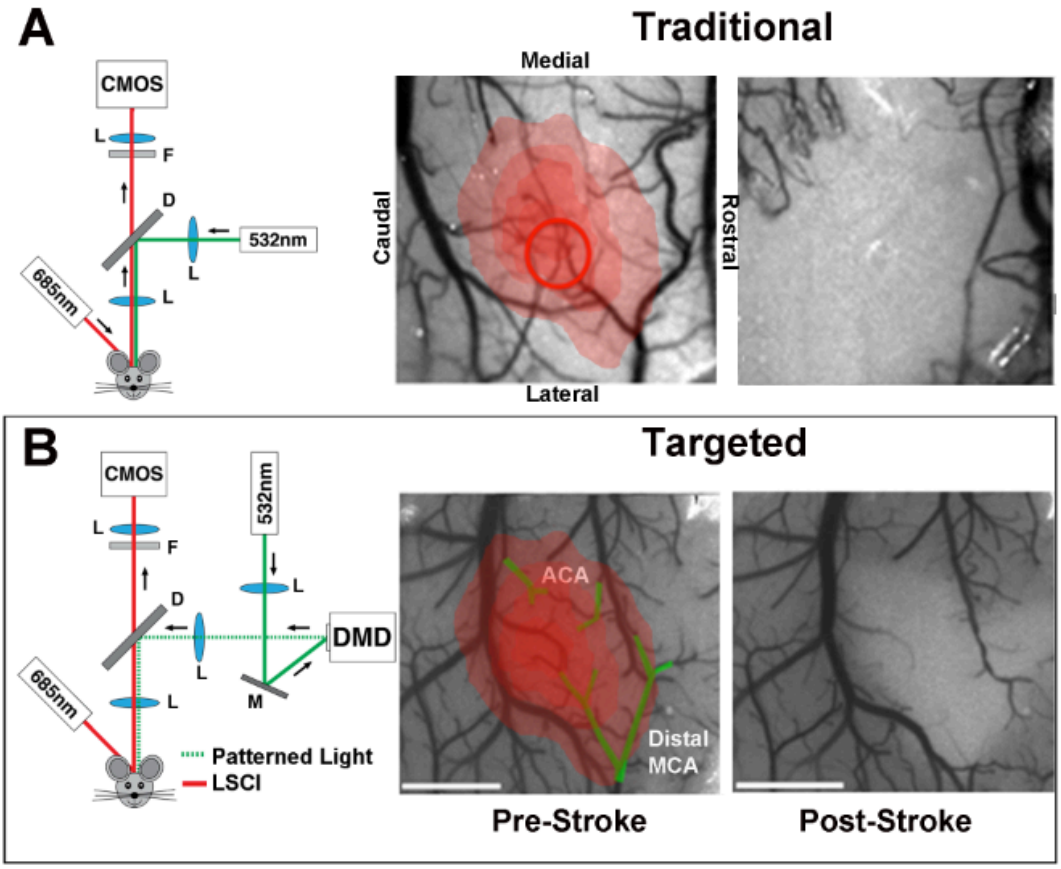

Figure 3.1 Comparison between artery-targeted and traditional photothrombotic approaches. Schematic diagrams of **(A)** traditional and **(B)** artery-targeted photothrombotic setups, and laser speckle contrast images (LSCI) depicting CBF before and 30 minutes after each (right) All images are shown in the same orientation. For traditional photothrombosis, a 532 nm laser was passed through a dichroic mirror to deliver focused photothrombosis over a cortical region (red circle). For artery-targeted photothrombosis, the 532 nm laser was coupled with the DMD (digital micromirror device) to provide patterned illumination over the cranial window (green overlay). On both setups, a separate 685 nm laser provides oblique illumination for LSCI. CMOS, complimentary metal oxide semiconductor. L, lens; M, mirror; F, filter. ACA, anterior cerebral artery; MCA, middle cerebral artery.

3.3.4 Multi-Exposure Speckle Imaging of Penumbral CBF

CBF was monitored following targeted or traditional photothrombosis using multi-exposure speckle imaging (MESI) of CBF as previously described (Kazmi et al., 2013, Parthasarathy et al., 2010). Briefly, a laser diode (660 nm, Micro Laser Systems, Garden Grove, CA, USA) illuminated the craniotomy while simultaneously triggering 15 camera (A602f; Basler Vision Technologies, Ahrensburg, Germany) exposure durations spanning 4 decades (0.05 to 80 ms). Backscattered light was collected by a 5x objective and imaged onto the camera. A 7 by 7 pixel window was used to convert the raw frames to speckle contrast images (Kazmi et al., 2013). For all MESI imaging sessions, mice were anesthetized and affixed to a stereotaxic frame, as described above. Heart rate was matched within 10% between imaging sessions within animals by controlling the depth of anesthesia and therefore regulating cardiac output. Prior to photothrombosis, two baseline measurements spaced five days apart were collected in order to account for minor differences in cardiac output that likely affected CBF measurements. Post occlusion MESI imaging sessions occurred at 6 h, 48 h and 5 d post stroke. Data from 3 animals at the 6 h time point (n = 2 targeted young-adult, n = 1 targeted middle-aged) and from 2 animals at the 5 d time point (n = 1 traditional young-adult, n = 1 targeted middle-aged) had to be excluded due to inability to sufficiently match heart rate to baseline conditions. Data from these mice were included at all other time points.

Raw images captured by the camera were converted to speckle contrast images as a ratio of the *SD* to *M* intensity of individual pixel values within a small region of the image (Kazmi et

al., 2013; Kazmi et al., 2015). The full speckle contrast image was then calculated using a 7 by 7 pixel sliding window centered at every pixel of the raw image, and was computed, displayed, and saved in real-time using an efficient processing (Kazmi et al., 2015; Parthasarathy et al., 2010). After post-processing, speckle contrast images were averaged together and converted to inverse correlation time (1/τc, ICT) images (Fig. 3.2) to provide a more quantitative measure of CBF (Schrandt et al., 2015; Kazmi et al., 2013). The ischemic core was defined at 48 h post stroke as the area of parenchyma with CBF values at or below 20% of baseline, a cutoff that was supported by comparisons between CBF reductions and histological damage, as explained below. For core measurements, ICT image sequences at the 48 h time point were thresholded against baseline ICT image sequences, vessels extracted, and matched by heart rate. Ten to twelve individual CBF measurements were then gathered from raw MESI data using a custom made middle-agedTLAB script that extracted ICT from raw speckle contrast images. Measurements were binned according to distance from the ischemic core (<100 μm, 100-300 μm, 300-500 μm and >500 μm) and then averaged. The closest distance (100 μm) was used as a border zone to account for any ambiguity between core and penumbral territory that could potentially influence penumbral measurements. The furthest distance (>500 μm) ranged between 700 μm and 1 mm between animals depending on the size and location of the core in relation to the edge of the cranial window. Results are presented as a percent decrease from baseline CBF.

3.3.5 Tissue Processing and Analysis of Lesion Volume

All animals were overdosed with sodium pentobarbital (dose, route), and transcardially perfused with 0.1 M phosphate buffer (PB) saline and 4% paraformaldehyde. For CBF and vascular density measures, animals were euthanized at either 7 days (n = 4 targeted young-adult, n = 4

traditional young-adult) or 14 days (n = 5 targeted young-adult, n = 4 traditional young-adult, n = 6 targeted middle-aged) after photothrombosis or sham procedures. For behavioral measures, all animals were euthanized 30 days after photothrombosis. Following fixative perfusion, brains were extracted and stored in 4% paraformaldehyde for no more than 48 h before being sliced into 40 µm thick coronal sections using a Leica VT1000S vibratome. The areas of eight coronal sections per animal between approximately 1.34 mm anterior to 0.58 mm posterior to bregma spaced 240 µm. Sections were viewed at a final magnification of 17x. Cortical volume was estimated with Cavalieri's method as the product of summed section areas and the distance between sections. Lesion volume was then calculated as the difference between cortical volumes of the contralesional and ipsilesional cortices (Tennant et al., 2011).

3.3.6 Comparison of MESI-estimated core sizes and histological infarct volume

MESI has been found to accurately quantify perfusion boundaries in ischemic and non-ischemic tissue regions following photothrombosis (Kazmi et al., 2015; Parthasarathy et al., 2010) and to provide reliable spatial perfusion indices that help to characterize vascular progression after ischemic stroke (Schrandt et al., 2015). Because CBF is estimated from scattered light on the surface of the cortex, MESI is most accurate at measuring CBF in superficial cortex. We therefore sought to determine the extent to which tissue loss as measured in histological coronal sections corresponded to *in vivo* estimates of core sizes, as measured by the area in which CBF deficits were ≤ 20% of baseline values at 48 h after photothrombosis. Tissue loss was mapped in 2D space based on reconstructions of lesion extents on templates of coronal sections spaced 240 µm apart. Per coronal section, lesion depth was measured as a percent of cortical depth at medial to lateral increments of 25 µm. ICT images were overlaid relative to bregma coordinates onto

images of the cortical surface taken at the time of cranial window implantation, and mean CBF was recorded in 25 × 25 μm bins. The *M* percent infarct depth of cortical regions in which CBF was between 0-20, 21-40, 41-60 and 61-100% of baseline CBF was then calculated. The targeted middle-aged group was excluded from comparisons between MESI-estimated core sizes and histological infarct extent because bregma could not be sufficiently resolved from images taken at the time of window implantation in this group due to technical issues with the surgical microscope camera.

3.3.7 Vascular labeling with isolectin B4

To visualize vasculature, one set of free-floating sections was labeled with IB4 (Griffonia simplicifolia, 1:50, Sigma-Aldrich cat no. L2140), using a protocol adapted from Walchli et al (Walchi et al., 2015). Briefly, sections were immersed in 50 mM NH_4Cl in 0.1 M phosphate-buffered saline (PBS) for 30 minutes. After several washes with PBS, sections were incubated in 50 mM glycine in 0.1 M Tris (pH 8.0) for 5 minutes at 80° C, washed in.1M PBS and then incubated in $CaCl_2$-containing buffer (0.1 mM $CaCl_2$, 0.1 mM $MgCl_2$ and 0.1 mM $MnCl_2$ diluted in 0.1 M PBS (pH 6.8), for 15 minutes at 65° C. Sections were then permeabilized in 0.1 M Tris-buffered saline and Triton X-100 (0.3% vol/vol) for 10 minutes, and incubated for 72 h with gentle shaking on an inclined table at 4° C in biotinylated IB4 diluted in $CaCl_2$-containing buffer and blocking solution (0.05% vol/vol Triton X-100 and 2% vol/vol normal goat serum in $CaCl_2$-containing buffer). Following lectin incubation and several PBS washes, sections were incubated overnight at 4° C in Cy3-conjugated strepdavidin (1:200, Jackson Laboratories, cat. no. 016-500-084) diluted in blocking solution. Sections were then thoroughly washed in PBS and mounted onto glass slides.

3.3.8 Analysis of Vascular Density

Images of IB4-labeled tissue sections were visualized using a standard light microscope with a reflected fluorescence system (Olympus America Inc; Melville, NY) and TRITC filter. Per each of 3 coronal sections per animal containing a visible lesion, eight 400 μm by 400 μm images of peri-infarct cortex were collected. Per section, one set of four images was obtained from deeper and superficial cortex within 100 μm of the medial and lateral edges of cortical infarcts, and an additional set of four was taken immediately adjacent to the first (Fig. 3.4). In a subset of the targeted young-adult group (n=3) with more laterally extending lesions, only the more proximal-to-lesion samples sites were imaged in lateral cortex to constrain the measures to anatomically defined sensorimotor cortex (Tennant et al., 2011). Samples in the contralesional cortex and in sham animals were taken homotopic to those collected in the ipsilesional cortex. Vascular density measurements were made at a final magnification of 756X in ImageJ using a custom macro that calculated the area fraction of IB4-labeled vessels in thresholded and binarized images. Vessel densities are reported as a percentage of the contralateral hemisphere. Vascular densities in the contralesional cortex were similar across, and therefore pooled across, sample positions (Suppl. Table 2).

3.3.9 Skilled Forelimb Training and Assessment

The impact of artery-targeted photothrombosis in MC on forelimb function was examined by testing a separate cohort of young-adult mice on performance of a skilled reaching task (Fig. 5). The reaching task used was a variation of the single seed retrieval task (Kleim et

al., 2007) in which mice were trained to reach for and obtain a millet seed placed on a platform outside of custom-made clear Plexiglas training chamber (20 cm tall, 15 cm deep, and 8.5 cm wide, measured from outside; 0.5 cm thick Plexiglas). There were 4 mm wide vertical openings on the left and right sides of the chamber for mice to reach through with either the left or right paw, respectively. The platform (8.5 cm long, 4 cm wide, and 1.2 cm tall) contained 3 wells at varying distances from each opening for positioning seeds. Relative to the opening edge closest to the center of the chamber, two of the wells were positioned at distances of 3 mm (position 1) and 7 mm (position 2) away from the opening and 2 mm further from the center of the chamber. A third well (position 3) was 5 mm away and 6 mm further from the center. During shaping, the preferred limb for reaching was determined by allowing mice to reach for millet seeds with either limb by placing seeds just outside of both openings. The preferred-for-reaching forelimb was defined as the first limb used to make five consecutive reach attempts. For the remainder of the shaping phase (~ 2-3 days), mice were encouraged to reach for a single seed placed in the most proximal well (position 1) outside of the chamber opening corresponding to their preferred-for-reaching forelimb. Shaping was considered to have ceased and training started once mice were able to successfully retrieve the pellet 10 times from position 1. Mice then received 11 training sessions of 30 trials each, administered once per day. Seeds were placed in one of the three positions per trial, with each position recurring ten times per training session in randomized order. Per trial, mice were allowed four reach attempts. A reach attempt was counted as a success grasped the seed and brought it inside of the chamber to its mouth. Unsuccessful reach attempts included those in which the seed was missed, displaced or dropped before eating. Mean asymptotic performance (average of last two training days) prior to infarct induction for each of

the three positions was 0.44 ± 0.02 (position 1), 0.3 ± 0.02 (position 2), and 0.2 ± 0.01 (position 3) respectively. Performance on position 3 was much lower compared to the other two positions, and therefore these trials were omitted from analyses. Data was analyzed as the percent of successful reaches per reach attempt for positions 1 and 2. Reaching performance was tested on days 3, 5, 10 and 20 following infarct induction or sham procedures.

3.3.10 Statistical Analyses

All statistical analyses were performed using the SPSS software package. Spatial differences in CBF responses to targeted and traditional photothrombosis were assessed in young adults at each post-infarct imaging time point using 2-way ANOVAs with distance from core as a within-subjects variable and group (photothrombosis method) as a between subjects variable. The effect of age (targeted young-adult vs. targeted middle-aged) by distance-from-core on CBF was assessed with separate ANOVAs per imaging time point. Each young adult group was additionally compared to the sham group in secondary analyses. When warranted by significant group-by-day interactions, post-hoc Bonferroni-Holm corrected t-tests compared groups at each distance. The same group differences as above were assessed in vascular density between 100-500μm and 500-900μm distances using independent samples t-tests. Differences between targeted and traditional young-adult groups in the relationship between MESI estimates of CBF and structural tissue damage were assessed using ANOVA with CBF as a within-subjects factor. Group differences (stroke vs. sham) in post-infarct reaching performance were examined using repeated measures ANOVAs with group as between-subjects factor, and time as a within-subjects factor. Data from males and females were combined for the primary analyses because there were no notable differences in the patterns of experimental results between them.

Supplemental materials show results disaggregated by sex. Data are reported as $M \pm SE$.

3. 4 Results

3.4.1 Artery-targeted photothrombosis produces a larger penumbra

Previous *in vivo* studies assessing CBF after cortical photothrombotic infarcts found a circumscribed area of reduced CBF around the ischemic core, outside of which CBF was relatively normal (Brown et al., 2007). We measured CBF at 6, 48, and 120 h following either targeted or traditional photothrombosis at varying distances relative to the ischemic core, defined as the region with < 20% of baseline CBF. We found a main effect of distance at each imaging time point (6 h: $F_{[3, 30]} = 44.80$, $p < 0.001$; 48 h: $F_{[3,36]} = 68.55$, $p < 0.001$; and 120 h: $F_{[3, 33]} = 17.21$, $p < 0.0001$), confirming that CBF deficits were more severe closer to the core area of ischemia (Fig. 2B, Suppl. Table 1). At 6 h, there was no significant main effect of Group (traditional vs. targeted young-adult) or Group by Distance interaction in CBF. However, at 48 h, ANOVA revealed a significant Group by Distance interaction ($F_{[3, 36]} = 13.33$, $p < 0.0001$) supporting that group differences in CBF depended on distance from the ischemic core. CBF was significantly higher in the traditional compared to targeted group at distances >500 μm from the ischemic core ($t_{[11]} = 2.2$, $p < 0.0001$, Fig. 3.2B). At 120 h, there was a significant main effect of Group ($F_{[1, 11]} = 11.25$, $p < 0.0001$, Fig. 3.2C), reflecting greater CBF in the traditional compared to targeted group, an effect which did not vary significantly with distance from the ischemic core at this time point (Group by Distance interaction: $F_{[3, 33]} = 2.88$, $p = 0.051$). Notably, in the traditional but not targeted group, CBF returned to baseline at 48 h and surpassed baseline at 120 h at distances ≥300 μm. Thus, artery-targeted photothrombosis instigated more sustained deficits in cerebral perfusion at further distances. These results are consistent with prior findings of a

sharp border between ischemic and non-ischemic territory following traditional photothrombosis (Brown et al., 2007, 2009) and provide evidence for a more graded penumbra following artery-targeted photothrombosis.

The more sustained decrease in cortical CBF in the targeted group was despite significantly higher arterial CBF compared to the traditional group (main effect of Group: $F_{[1, 7]} = 25.59$, $p < 0.0001$) an effect that varied significantly across time points (Group by Time: $F_{[2, 14]} = 8.98$, $p = 0.003$), Post-hoc t-tests indicated that arterial CBF was significantly greater in the targeted compared with traditional group at 120 h, but not earlier (Fig. 3.2C). This suggests that delayed spontaneous reperfusion was more likely after artery-targeted photothrombosis.

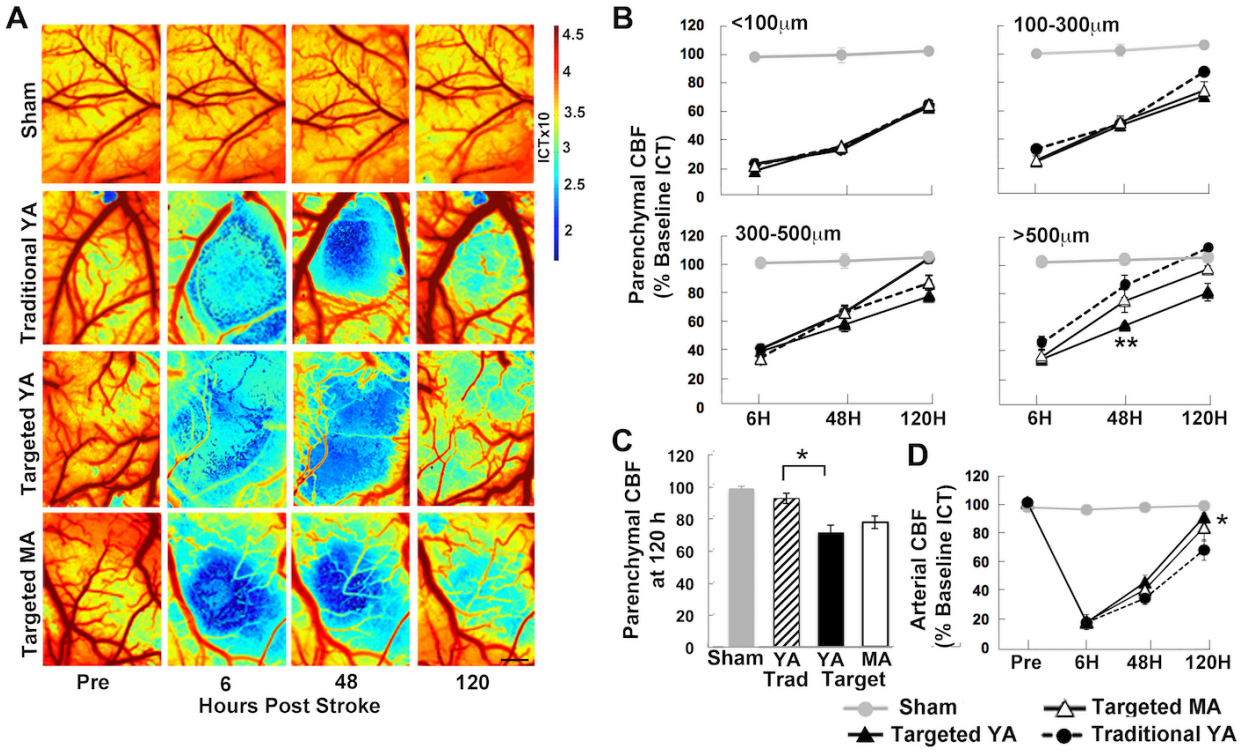

Figure 3.2 Artery-targeted photothrombosis increased the area of reduced CBF in surrounding cortical tissue (A) Representative ICT images acquired using MESI. Areas of higher CBF are represented in red, and areas of lower CBF are represented in blue. Scale bar = 500 μm. **(B)** Post-ischemic CBF deficits at each imaging time point represented as a % of baseline ICT values at different distances: <100μm, 100-300 μm, 300-500 μm, and >500 μm. At distances of > 500μm CBF was significantly increased in the traditional young adult (young-adult) group compared to targeted young-adult group at 48 h. **(C)** Parenchymal CBF pooled across distances at120 h post infarct was significantly greater in the traditional young-adult group compared to the targeted young-adult group . (**D)** CBF in occluded arteries was significantly higher at120 h in the targeted young-adult compared to traditional group. Post-stroke CBF patterns in the targeted middle-aged group (middle-aged) were not significantly different from either young-adult group. **$p < 0.001$, *$p < 0.02$ targeted young-adult versus traditional young-adult.

3.4.2 Histological damage paralleled regions of severe CBF deficits

Despite differences in post-ischemic CBF patterns, lesion volumes as estimated by intercortical volume differences were comparable between targeted young-adult and traditional young-adult groups (Fig. 3.3A; Suppl. Table 3.3). To determine whether the MESI estimated region of the ischemic core at the 48 h time point was a good indicator of the infarcted region, as assessed by the depth of structural tissue damage in Nissl stained tissue sections at 1 to 2 weeks after photothromobosis (Fig. 3.3B). Across groups, structural damage in histological tissue sections was only observed in areas where CBF was less than or equal to 40% of baseline CBF. Furthermore, areas where CBF dropped below 20% at 48 h exhibited the most severe tissue damage, supporting MESI estimates of ≤ 20% baseline CBF at 48 h as a reliable estimate of core size *in vivo*. The relationship between CBF deficits and cortical lesion depth did not differ significantly between stroke conditions (Group by CBF reduction effect on lesion depth: $F_{[1,9]} = 0.51$, $p = 0.49$).

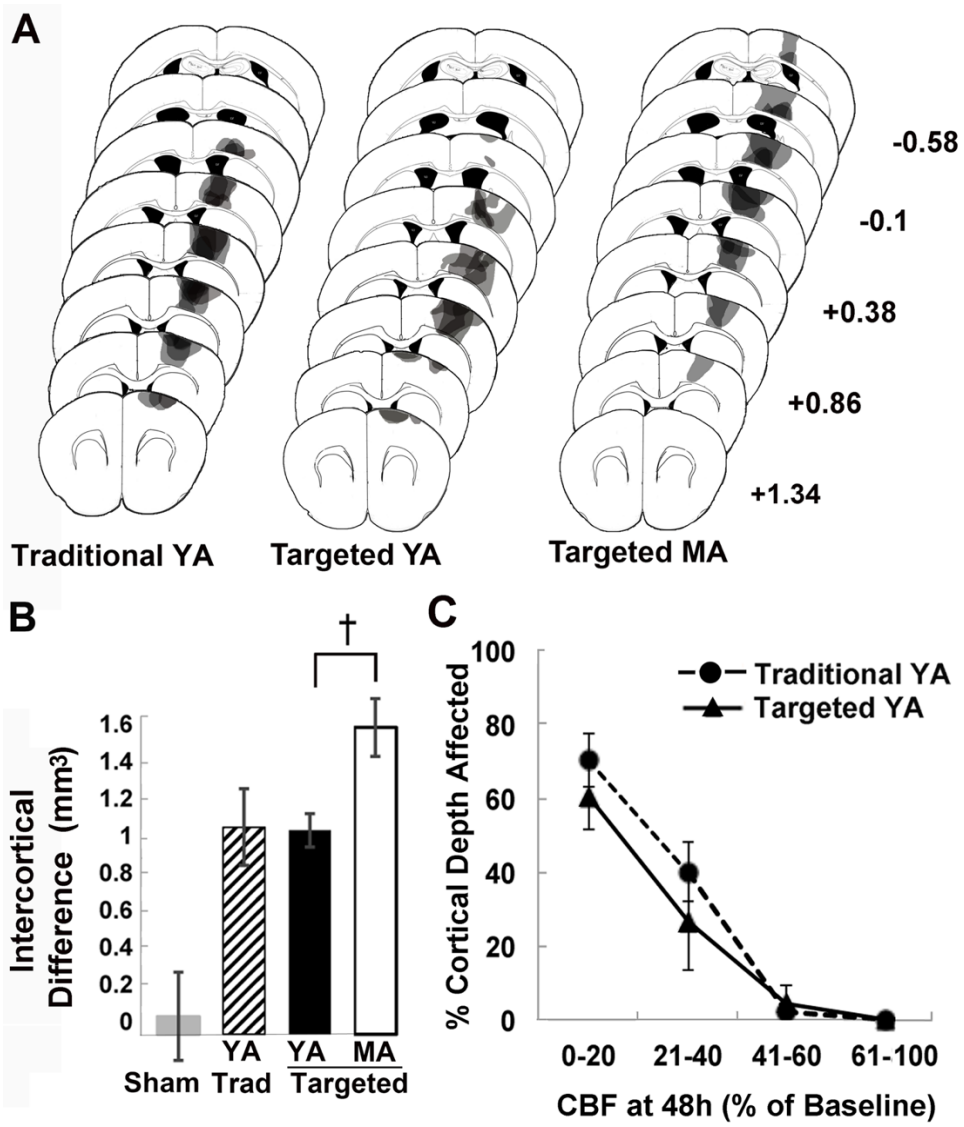

Figure 3.3 Lesion depth in histological tissue sections corresponded to cortical areas with the greatest CBF reductions following artery-targeted and traditional photothrombosis. **(A)** Representative lesion reconstructions of each infarct group overplayed on coronal templates. Numbers to the right are anterior to posterior coordinates (mm) relative to bregma. (B) Interhemispheric volume difference, the difference between intact and damaged hemisphere volumes, was used to estimate infarct size. Lesion sizes were similar between young-adult infarct groups, but the targeted middle-aged group had significantly larger lesion volumes compared to the targeted young-adult group. **(C)** Relationship between CBF deficits assessed with MESI at 48 h and structural tissue damage (cortical lesion depth). In both targeted and traditional young-adult groups, the greatest degree of tissue damage corresponded to areas where CBF fell to or below 20% of baseline CBF at 48 h. Areas where CBF was at or above 40% of baseline CBF showed little to no structural tissue damage in histological sections.

3.4.3 Vascular density was increased proximal to the ischemic core after traditional compared to targeted photothrombosis

Previous *in vivo* imaging studies of filled vessels have not found evidence for neovascularization in cortex near photothrombotic infarcts (Brown et al., 2007; Schrandt et al., 2015; Tennant et al., 2013), but some studies have found histological evidence for increased vascular density in other models of focal ischemia (Arenillas et al., 2007; Hayward et al., 2011; Martin et al., 2012; Lin et al., 2002; Lake et al., 2017; Ohab et al., 2006; Tagushi et al., 2009) and after human stroke (Sobrino et al., 2007; Bogoslovsky et al., 2010; Krupinski et al., 1994; Szpak et al., 1999; Cramer et al., 2011). In the present study, we probed for neovascularization in peri-infarct cortex using histological measures of vascular density. The density of IB4-labeled blood vessels did not vary notably between 7 and 14-day time points in either the targeted or traditional groups (M ± SE % area fraction combined for 100-500 and 500-900 μm; targeted young-adult at 7 d: 10.0 ± 0.5, at 14d: 11.0 ± 0.5; traditional young-adult at 7 d: 10.6 ± 1.2, 14d: 11.3 ± 1.4), and therefore the data were combined across these time points. As shown in Fig. 3.4, vascular density in samples between 100-500 μm from the infarct border was significantly greater after both types of photothrombosis compared to sham animals (targeted young-adult $t_{[10]} = 2.23$, $p = 0.01$; traditional young-adult: $t_{[10]} = 2.23$, $p = 0.003$). Between 500-900 μm from the infarct border, vascular density was significantly greater in the targeted young-adult group, but not traditional young-adult group, compared to sham (targeted young-adult: $t_{[11]} = 2.23$, $p = 0.002$; traditional young-adult $t_{[10]} = 2.23$, $p = 0.12$), but mean vascular densities in the photothrombotic groups were quite similar to, and not significantly different from, one another. Vascular density was not

significantly different between groups in the contralesional cortex, Although there was a nonsignificant tendency for it to be greater in photothrombotic groups relative to sham operates (targeted young-adult vs sham: $t_{[10]} = 2.20$, $p = 0.06$; traditional young-adult vs sham: $t_{[10]} = 2.20$, $p = 0.12$) In both photothrombotic groups, peri-infarct vascular density was significantly greater than that of contralesional cortex (targeted young-adult: 100-500 µm $t_{[7]} = 2.36$, $p = 0.0002$; 500-900 µm $t_{[7]} = 2.36$, $p = 0.0007$; traditional young-adult: 100-500 µm $t_{[7]} = 2.36$, $p = 0.001$; 500-900 µm $t_{[7]} = 2.36$, $p = 0.02$) These data suggest a similar magnitude of neovascularization in peri-infarct cortex 1-2 weeks after both types of photothrombosis.

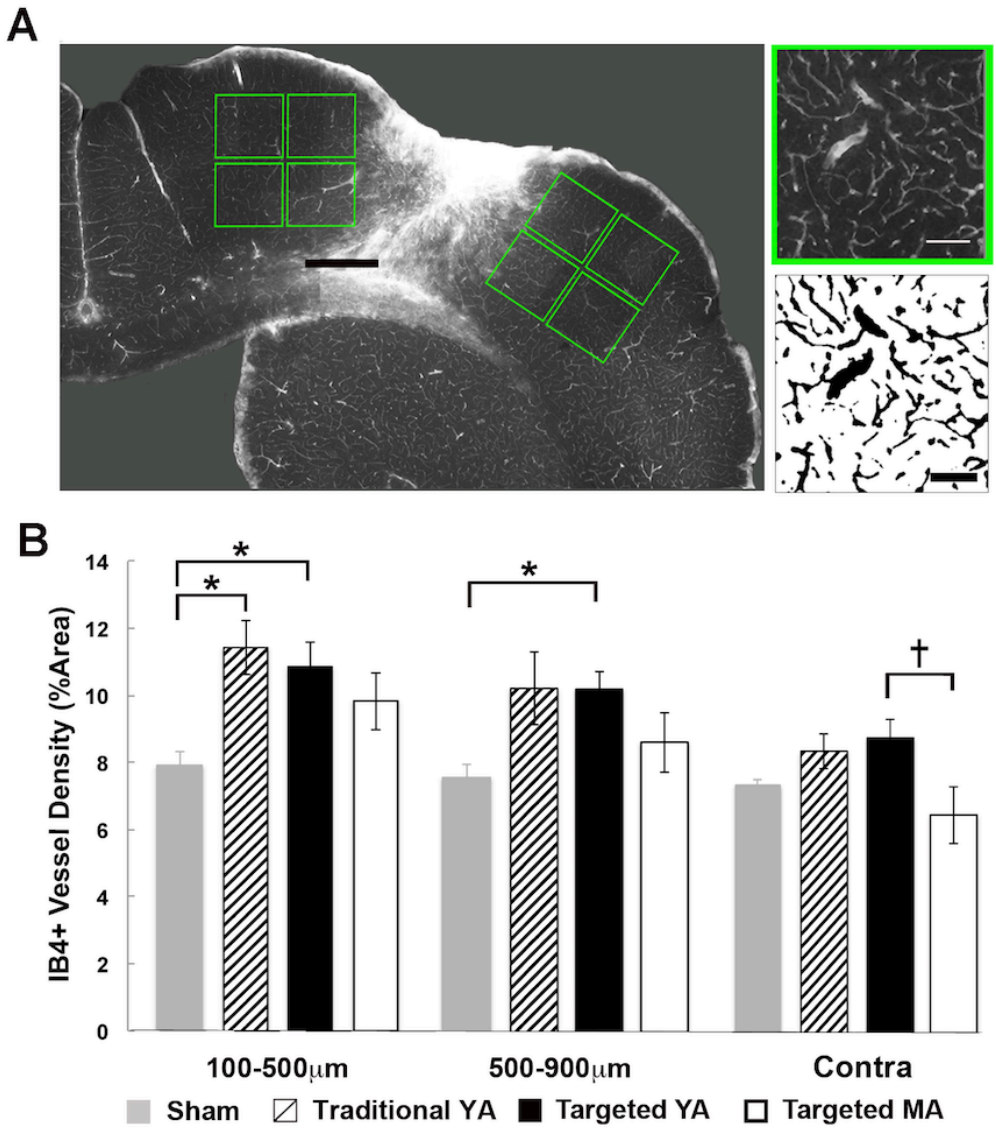

Figure 3.4 Artery-targeted and traditional photothrombosis instigated neovascularization. **(A)** Photomicrograph of IB4 labeling in the ipsilesional cortex at low magnification. Green insets correspond to sample sites shown at higher magnification on the right. To the right is a high magnification image of IB4 labeling (top right) and corresponding binarized image used for area fraction measurements (bottom left)**.** Scale bars = 500 μm (left) and 100 μm (right). **(B)** Vascular density represented as the % area of IB4-labeled blood vessels. Area fractions of vessels in the ipsilesional cortex were higher in both targeted young-adult and traditional young-adult groups compared to shams between 100-500 μm, but only in targeted young-adult animals between 500-900 μm**.** Area fractions in the contralateral cortex were also significantly reduced in targeted middle-aged animals compared to targeted young-adult animals. young-adult versus sham young-adult: *$p < 0.02$; Targeted middle-aged versus young-adult: †$p < 0.02$.

3.4.4 Lesion volume, but neither CBF deficits nor peri-infarct vascular densities, significantly varied with age after artery-targeted photothrombosis

The potential for age-dependencies in lesion volumes, post-occlusion CBF, and vascular structural patterns was assessed in a separate cohort of middle-aged mice that underwent artery-targeted photothrombosis. Lesion volumes were significantly larger in targeted middle-aged compared to young-adult animals ($t_{[12]} = 2.17$, $p = 0.014$ Fig. 3.3A) consistent with previous findings of increased infarct size with aging (Canese et al., 1998; Canese et al., 2004; Popa-Waggoner et al., 2007). Despite differences in histological lesion volume, post-ischemic CBF patterns were not significantly different between young-adult and middle-aged groups. ANOVAs revealed no significant effect of age group at any time point (6h: $F_{[1, 10]} = 0.27$, $p = 0.60$; 48h: $F_{[1, 13]} = 3.0$, $p = 0.10$; 120h: $F_{[1, 12]} = 1.18$, $p = 0.30$), nor a significant Group by Distance interaction (6h: $F_{[3, 30]} = 0.83$, $p = 0.44$; 48h: $F_{[3,39]} = 2.04$, $p = 0.15$; 120h: $F_{[3,36]} = 1.16$, $p = 0.45$). A tendency for CBF to be higher in middle-aged animals beyond 500μm from the ischemic core at the 120-hour time point was not significant (Fig. 3.2B). Thus, at least by middle age, there was not a significant effect of age on cortical CBF responses to artery-targeted photothrombosis.

Similarly, we found no effect of age on vascular density in peri-infarct cortex. The density of IB4+ vessels in peri-infarct cortex was not significantly different between young-adult and middle-aged groups at either distance (100-500 μm, $t_{[12]} = 2.18$, $p = 0.14$; 500-900 μm, $t_{[12]} = 2.18$, $p = 0.29$). However, area fractions of IB4+ vessels in the contralateral cortex were significantly smaller in the middle-aged compared to young-adult group ($t_{[12]} = 2.17$, $p = 0.02$; Fig. 4B) potentially reflecting age-related declines in vascular density. As with young adults, in the peri-infarct cortex of the middle-aged group, vascular density was significantly greater than

that of contralesional cortex at both distances (100-500 μm $t_{[5]} = 2.57$, $p = 0.0001$; 500-900 μm $t_{[5]} = 2.57$, $p = 0.001$) from the infarct border. Together these results are suggestive of vascular response to targeted photothrombosis in middle age that was generally similar in magnitude to that of young adults, at least proximal to the infarcts. Across age groups there was no significant correlation between lesion size and vascular density (100-500 μm: $r = 0.12$, $p = 0.67$; 500-900 μm: $r = -0.10$, $p = 0.97$), indicating that variation in lesion volumes was not strongly linked with variation in vascular structural responses.

3.4.5 Artery-targeted photothrombotic infarcts in motor cortex impaired forelimb function.

We examined the impact of artery-targeted photothrombosis to MC on skilled reaching, and found that targeted photothrombotic infarcts significantly impaired performance on a skilled reaching task compared to sham operates (Fig. 3.5C and Supplementary Fig. 3.6). Repeated measures ANOVA of post-operative reaching performance revealed a significant main effect of Group (Infarct vs. Sham, $F_{[1,23]}=145.50$, $p < 0.0001$), but no Group by Day interaction ($F_{[3,69]} = 2.77$, $p = 0.06$). However, by day 20 performance levels were similar between the infarct and sham group. These data support that targeted-artery photothrombosis is suitable for creating focal and reproducible lesions to motor cortex that can be used to model upper extremity impairments.

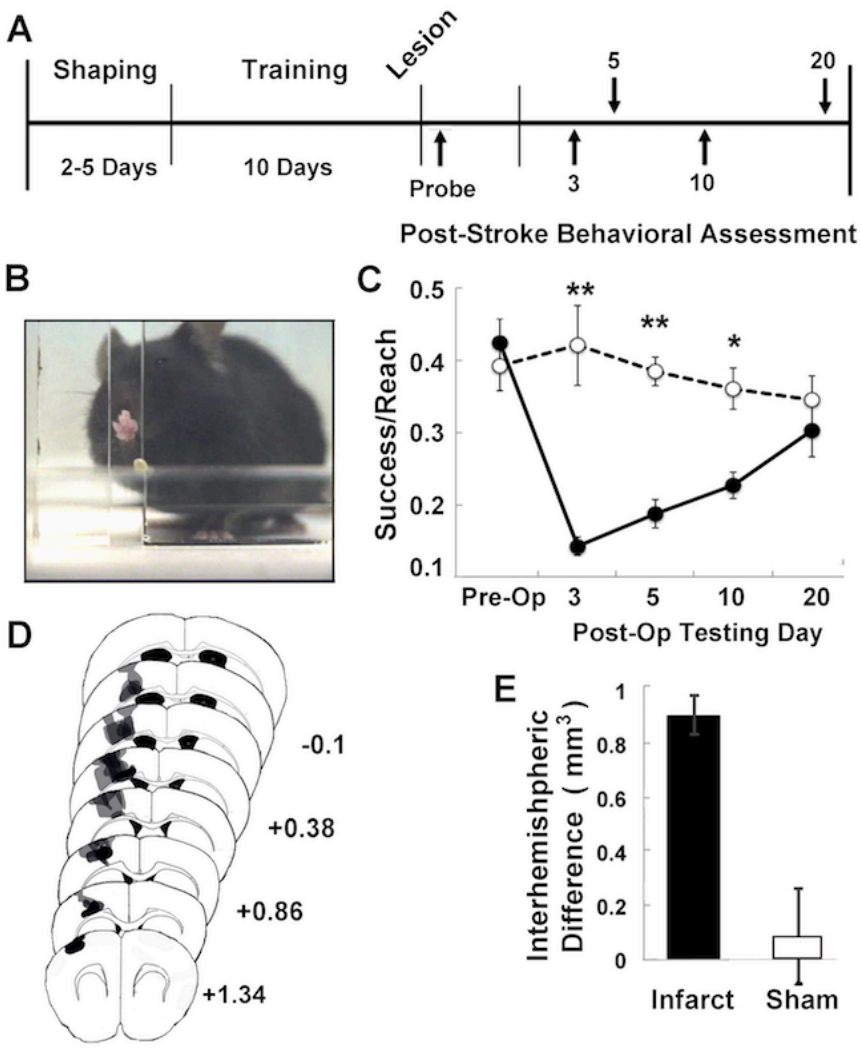

Figure 3.5 Artery-targeted photothrombosis to mouse motor cortex creates deficits in skilled forelimb reaching. (A) Experimental timeline for behavioral studies**. (B)** A mouse performing the single seed retrieval (SSR) task. (**C**) Pre and post-operative reaching performance measured by the number of fully retrieved seeds per reach attempt. Artery-targeted photothrombosis impaired performance on post stroke days 3, 5, and 10 (**$p < 0.001$, * $p < 0.02$) compared to shams. (**D)** Representative lesions reconstructions the infarct group overlayed on coronal templates. Numbers to the right represent anterior to posterior coordinates in mm relative to bregma.

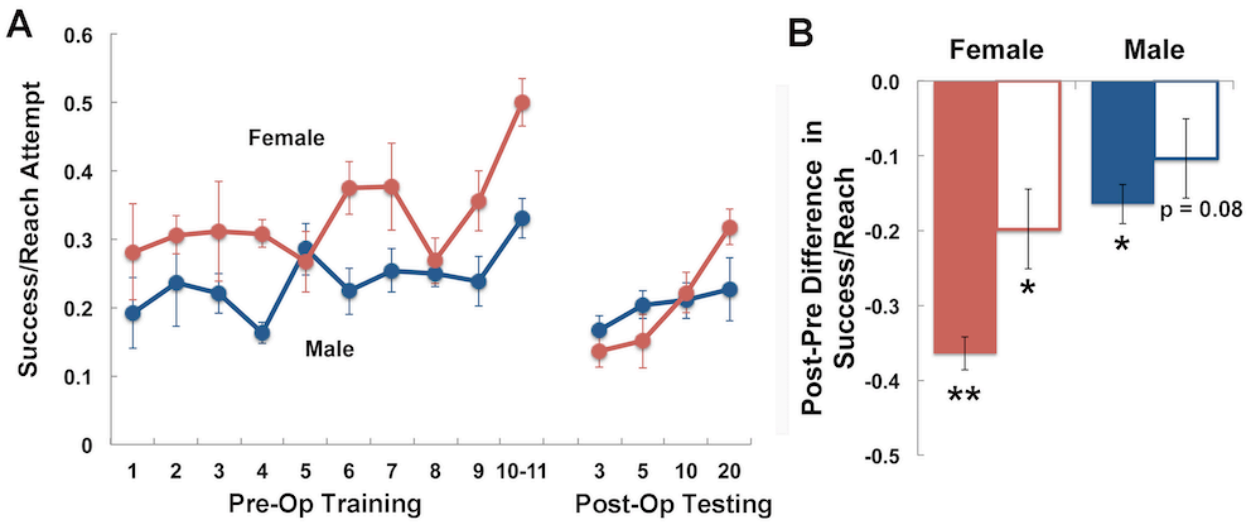

Supplementary Figure 3.6 Pre-operative and post-operative reaching performance separated by sex. (A) Pre-operative and post-operative reaching performance, measured as the % successes out of total reach attempts, compared in females and males in the infarct group. Females on average achieved greater performance levels pre-operatively. **(B)** Difference between baseline preoperative reaching performance (D10-11) and post-operative reaching performance on days 3 and 20 in females and males. Females tended to have a greater magnitude drop in performance on both days, but this was attributable to greater pre-operative performance levels in females. **$p < 0.0001$, *$p < 0.005$ post-operative versus pre-operative.

3.5 Discussion

The photothrombotic method is ideal for studying mechanisms of recovery following ischemia. However, it creates a relatively thin penumbra, making it challenging to understand how events within it impact cellular mechanisms of recovery (Sommer et al., 2017). In the present study, we demonstrated that confining laser illumination cortical surface arteries, increased the size of the penumbra, evident by the presence of graded CBF deficits encompassing a broader cortical area. At 48 h, the artery-targeted group had greater CBF deficits beyond 300 μm from the ischemic core that persisted until 120 h despite an increased likelihood of spontaneous reperfusion in the occluded artery, support that artery-targeted photothrombosis created a penumbra that more closely approximates human ischemic stroke. That there existed at least some degree of spontaneous reperfusion in occluded arteries after artery-targeted, but not traditional photothrombosis indicated that the artery-targeted approach can serve as an ischemia-reperfusion model, useful for studies examining how reperfusion impacts post-ischemic remodeling events and functional outcomes, a major focus of current therapeutic strategies (Sommer et al., 2017).

Several other variations of photothrombosis, including the photothrombotic ring-model (Gu et al., 1999) and single-point occlusion model (Nishimura et al., 2007; Siegler et al., 2008; Schaeffer et al., 2006) have been demonstrated to produce a larger vascular penumbra. In the photothrombotic-ring-model, the penumbral zone is contained within the ring-shaped core, and therefore, progressive vasogenic edema emanating from the ischemic ring results in inevitable deterioration of the penumbral region, limiting the examination of tissue recovery over longer periods.

In the single-point occlusion model, illumination through a two-photon microscope

generates spatially restricted photoactivation of vessels confined to a diameter smaller than the targeted artery (~20um), resulting in relatively small ischemic lesions, and making it challenging to apply to more than one vessel at a time. Here, we demonstrated that artery-targeted photothrombosis can be used to occlude multiple branches of the MCA, as well as limit collateral CBF by simultaneously occluding branches of the anterior cerebral artery (ACA), thus giving the experimenter better control over reperfusion.

Photothrombosis has also been adapted for distal MCA occlusion (MCAo). Following injection of Rose Bengal, the distal MCA is illuminated with a 532 nm laser through a craniotomy or intact skull (Sugimori et al.,2004; Qian et al., 2016) resulting in more reproducible infarcts in the extent of tissue damage compared to other MCAo models, while maintaining a vascular penumbra. Illumination with an infrared laser can be used to stimulate recanalization, such that this model can also serve as an ischemia-reperfusion model. However, infrared laser illumination triggers immediate restoration of CBF to baseline levels, whereas in clinical strokes spontaneous reperfusion can unfold very gradually and is often incomplete (Sommer et al., 2017; Khatri et al., 2014). Our finding that reperfusion of targeted arteries was quite delayed (120 h) supports that reperfusion in the present model unfolds slowly, making it well suited for studies of cellular responses to reperfusion.

Given the prominent effects of isoflurane on vasodilation (Hildebrandt et al., 2008) and evidence for its neuroprotective effects following ischemia (Kawaguchi et al., 2007; Wells et al., 1963) the use of isoflurane anesthesia in the present study during CBF measures and ischemia induction can be assumed to have impacted infarct evolution as well as the observed perfusion deficits across infarct conditions. In order to better characterize the impact of isoflurane

anesthesia and post-ischemic measures of CBF, future studies should be performed under differently acting anesthetics and/or in awake animals

In other focal rodent models, increased vascular density has been linked to the infiltration of macrophages to clear necrotic tissue around the lesion site (Manoonkitiwonsa et al., 2001; Wei et al., 2001) and to improved functional outcomes at longer time periods in other focal rodent models (Hayward et al., 2011; Martin et al., 2012; Lin et al., 2002; Lake et al., 2017; Ohab et al., 2006; Taguchi et al., 2009). In the present study, we found that both photothrombotic models, which indicated that both models instigate similar patterns of vascular structural remodeling despite differences in the development of the penumbra.

The role of neovascularization in cellular mechanisms of recovery over longer periods is unclear. New born neuroblasts in peri-infarct cortex have been shown to be associated with endothelial cells in new, unperfused vessels within weeks after focal ischemia (Taguchi et al., 2004; Thored et al., 2007) highlighting a role for neovascularization in cellular plasticity. That vascular density was increased in both models is consistent with the possibility that neovascularization during this time period could represent a remodeling phase of the vascular network that supports cellular repair.

Photothrombotic infarcts have been a popular choice for the purpose of modeling upper-extremity impairments (Cramer et al., 2011; Jones et al., 2011; Nudo et al., 2007). In the present study we demonstrated that artery-targeted photothrombosis maintained the ability to create focal infarcts to the forelimb containing region of MC, creating deficits in upper-limb function. However, these deficits were no longer evident at the last endpoint, a transience that is likely attributable to the fact that the infarcts were relatively small. Preliminary results from a

subsequent study indicate more persistent impairments in a skilled reaching task in mice after larger infarcts (Clark et al., SFN 2017).

Age is a prominent factor in stroke recovery (Herson & Traystman et al., 2014) and therefore an important consideration in experimental studies aimed at improving stroke outcomes. In rodents, aging is associated with increased lesion volumes (Canese et al., 1998; Canese et al., 2004) and worse functional outcomes (Anderson et al., 1999; Brown et al., 2003; Popa-Waggoner et al., 2017) but evidence for how aging impacts vascular responses to stroke was lacking. In the present study we found that targeted-artery photothrombosis instigated similar CBF and vascular structural responses in middle-aged animals compared with young-adults. We also found that the middle-aged group had significantly reduced vessel density in contralateral cortex compared to young-adult, but because a middle-aged sham group was not included, we cannot determine whether these results might reflect an age-associated decrease in vascular density, an age-dependency in remote vascular structural responses to ischemia, or a combination of the two. middle-aged animals did have significantly larger lesion volumes, but this was not related to the extent of neovascularization, indicating that larger lesion volumes in the middle-aged group did not impact group differences in vascular structural changes following infarcts. Together, these results suggest that, while middle-age is potentially associated with some decline in vascular density, the neovascularization response to ischemia remains robust.

In the present study we have shown that confining laser illumination to individual arteries on the cortical surface with a digital micromirror device expanded the ischemic penumbra, making it well-suited for studies examining the impact of remodeling events within the penumbra on mechanisms of recovery from ischemia. In addition, artery-targeted

photothrombosis maintained the strengths of the traditional model, in that it created focal and reproducible infarcts to motor cortex that impaired forelimb motor function, making it suitable for studies modeling post-stroke upper-extremity impairments.

Table 3.1 CBF disaggregated by sex at each imaging time point

Parenchymal CBF

6h	**< 500 μm**		**> 500 μm**	
Group	**Female (n)**	**Male (n)**	**Female (n)**	**Male (n)**
Sham	96.2 ± 1.4 (2)	96.3 ± 6.4 (2)	96.2 ± 1.9 (2)	1 00 ± 5.4 (2)
Traditional young-adult	31.3 ± 0.7 (3)	29.0 ± 5.5 (3)	32.0 ± 8.8 (3)	49.4 ± 5.9 (3)
Targeted young-adult	19.9 ± 9.1 (2)	26.3 ± 4.4 (2)	99.0 ± 1.4 (2)	39.0 ± 8.8 (2)
Targeted middle-aged	23.8 ± 5.0 (3)	21.7 ± 6.9 (2)	32.1 ± 13.3 (3)	42.1 ± 4.5 (2)

48h	**< 500 μm**		**> 500 μm**	
Group	**Female (n)**	**Male (n)**	**Female (n)**	**Male (n)**
Sham	100.± 7.1 (2)	101 ± 0.8 (2)	97.4 ± 0.5 (2)	1 05 ± 0.4 (2)
Traditional young-adult	49.0 ± 13.6 (3)	44.0 ± 8.0 (3)	85.7 ± 7.9 (3)	79.3 ± 3.5 (3)
Targeted young-adult	44.4 ± 4.8 (4)	45.4 ± 9.8 (4)	52.6 ± 6.6 (4)	61.8 ± 12.2 (4)
Targeted middle-aged	49.6 ± 8.4 (3)	44.5 ± 6.1 (2)	78.6 ± 13.3 (3)	9 0.1 ± 6.9 (2)

120h	**< 500 μm**		**> 500 μm**	
Group	**Female (n)**	**Male (n)**	**Female (n)**	**Male (n)**
Sham	92.9 ± 4.0 (2)	101 ± 1.1 (2)	96.8 ± 5.3 (2)	102 ± 1.7 (2)
Traditional young-adult	88.9 ± 14.5 (3)	81.1 ± 2.3 (2)	85.7 ± 7.9 (3)	89.3 ± 2.8 (2)
Targeted young-adult	61.4 ± 14.4 (4)	72.8 ± 15.6 (4)	52.6 ± 6.6 (4)	61.8 ± 13.2 (4)
Targeted middle-aged	77.6 ± 13.9 (3)	64.7 ± 12.6 (2)	78.6 ± 13.3 (3)	64.7 ± 12.5 (2)

Table 3.1 Cont.

Arterial CBF	*6h*		*48h*		*120h*	
Group	**Female**	**Male**	**Female**	**Male**	**Female**	**Male**
Sham	95.3 ± .1	101 ± .4	96.3 ± 3.1	97.8 ± 3.3	96.7 ± 1.6	97.8 ± 3.7
Traditional young-adult	18.8 ± 5.5	15.4 ± 2.3	27.7 ± 13.2	26.6 ± 3.5	59.3 ± 7.3	59.2 ± 30.8
Targeted young-adult	15.2 ± 2.0	18.6 ± 1.6	40.2 ± 10.6	49.8 ± 19.2	91.7 ± 18.4	89.3 ± 6.4
Targeted middle-aged	13.6 ± 6.4	22.2 ± 12	39.3 ± 18.0	41.3 ± 9.3	75.5 ± 37.9	94.7 ± 34.4

Note. CBF, cerebral blood flow. Group n's for arterial CBF are the same as those of the parenchymal CBF at the same time point. Values are *M* ± *SD*

Table 3.2 Cortical lesion volume disaggregated by sex.

CBF and Vascular Study

Group	**Male (n)**	**Female (n)**
Traditional young-adult	4.1 ± 0.4 (4)	2.5 ± 0.4 (4)
Targeted young-adult	3.0 ± 0.7 (5)	4.1 ± 0.8 (4)
Targeted middle-aged	5.1 ± 2.5 (2)	5.9 ± 0.8 (4)

Behavioral Study

Group	**Male (n)**	**Female (n)**
Infarct	3.0 ± 1.8 (7)	2.8 ± 1.5 (6)
Sham	0.6 ± 2.0 (6)	-0.1 ± 4.0 (4)

Note. Values are *M ± SD* contralesional-ipsilesional difference in cortical volume

Table 3.3 Area fractions of IB4-labeled blood vessels in ipsilesional and contralateral homotopic cortex disaggregated by sex

	Ipsi		***Contra***
Group (n)	*100-500µm*	*500-900µm*	
Trad young-adult			
Female (4)	12.0 ± 2.0	9.8 ± 2.0	8.3 ± 1.2
Male (4)	10.8 ± 2.6	10.9 ± 4.2	8.7 ± 1.8
Target young-adult			
Female (4)	10.5 ± 1.4	10.4 ± 1.0	8.8 ± 0.4
Male (4)	11.1 ± 2.4	10.7 ± 1.8	9.0 ± 2.2
Target middle-aged			
Female (4)	9.4 ± 2.0	8.1 ± 4.8	5.9 ± 2.0
Male (2)	10.9 ± 3.7	10.8 ± 1.8	7.9 ± 2.5
Sham young-adult			
Female (2)	8.4 ± 1.5	8.1 ± 1.2	7.8 ± 0.1
Male (2)	7.6 ± 0.1	6.8 ± 1.2	7.4 ± 0.3

Trad, traditional photothrombotic, Target, targeted photothromobotic, young-adult, young adult, middle-aged, middle aged. Values are *M* ± *SD*. Note that 100-500 and 500-900 μm distances were combined in contra cortices

Chapter 4: Rehabilitative training promotes the persistence of new spines formed in response to ischemia.

4.1 Abstract

Previous *in vivo* examinations of spine dynamics following photothrombotic infarcts have found that dendritic spine turnover in peri-infarct cortex remains elevated for up to 6 weeks in animals undergoing spontaneous recovery. We investigated the impact of behavioral experience, in the form of rehabilitative training, on both spine turnover and spine maintenance in peri-infarct cortex following artery-targeted photothrombosis. We found that spine turnover was increased for up to 5 weeks following post-insult in animals receiving rehabilitative training, and in animals undergoing spontaneous recovery relative to sham. The pattern of spine formation was similar between infarct groups, and new spines formed 1week after the infarct were more likely to remain by week 4, regardless of training condition, relative to sham.

Spine elimination returned to baseline levels by 4 weeks in animals receiving rehabilitative training, whereas it remained elevated in animals undergoing spontaneous recovery. This was linked with an increase in the persistence of new spines, formed during weeks 2 and 3, at week 4 in animals receiving rehabilitative training compared to animals spontaneously recovering. Furthermore, the percent of spines formed during weeks 2 and 3 that remained at week 4 was positively correlated with improvements in skilled reaching performance, indicating that preferential stabilization of this subset of newly formed spines may represent a structural mechanism for functional improvements in skilled forelimb function.

4.2 Introduction

Stroke is the leading cause of long-term disability in adults leaving nearly 80% of infarct survivors with long-term functional impairments, commonly affecting the upper-extremities, and limited recovery without treatment (Cramer & Riley 2008; Cramer & Dobkin 2011). Rehabilitative training (RT) approaches are the most common treatment for motor impairments after infarct, but these therapies are far from sufficient to normalize function. A better understanding of the neural mechanisms underlying infarct recovery and effective RT strategies is necessary for optimizing efforts to improve it.

Focal ischemia to cortex instigates a unique environment in the adjacent and surviving regions (peri-infacrt cortex) for heightened plasticity after stroke that is associated with improved functional outcomes (Cramer and Chopp, 2000; Carmichael, 2006). Many of these plastic events are activity dependent, and can be influenced by post-ischemic behavioral experience (Yu & Zuo, 2011). There are likely to be windows of opportunity for driving functionally useful brain remodeling, but this requires knowledge of the time course of neural remodeling events and their coordination with functional improvements. Therefore, monitoring changes in synaptic plasticity *in vivo* provides a unique opportunity to examine the coordination between structural remodeling events and functional outcomes. The main goal of the present study was to examine the impact of behavioral experience in the form of rehabilitative training (RT) on dendritic spine dynamics in peri-infarct motor cortex, and how this coincides with functional improvements forelimb use in mice trained on a skilled reaching task.

Furthermore, we sought to determine whether artery-targeted photothrombosis, which increases the size of the ischemic penumbra (Ch. 3), could also instigate more widespread

changes in spine dynamics following ischemia. Previous *in vivo* studies have shown that cortical ischemia induced by photothrombosis results in a loss of dendrites, spines and vasculature in remaining cortex (Brown et al., 2007, 2009) as well as time-dependent increases in dendritic branching and spine turnover that persist for weeks (Brown et al., 2007, 2009). However, these changes are restricted to the first 300 μm of cortex despite evidence of increased spine dynamics in more distant regions from the ischemic core in other cortical ischemia models (Mostany et al., 2010). Here we analyzed spine dynamics between 300 μm and up to 1mm from the occluded artery to determine whether spine turnover was increased even at more distant locations from the infarct.

A second goal was to determine the impact of rehabilitative training (RT), if any, on patterns of spine maintenance, and how this relates to functional recovery. Previous studies have found that new spines formed weeks after the initial infarct are preferentially stabilized for up to several months in mice spontaneously recovering after McAO (Mostany et al., 2010). Our lab and others (Xu et al., 2009; Yang & Gan, 2009) have found that motor skill training in intact mice is associated with preferential stabilization of spines formed early on during learning, the maintenance of which is correlated with performance gains. Several lines of evidence suggest that ischemia-induced structural remodeling mechanisms follow similar principles as experience-dependent plasticity in the intact brain (Zieler & Krakauer 2013; Bevelier et al., 2010) inciting the possibility that preferential spine stabilization after ischemic infarcts could represent a structural mechanism of functional recovery. However, the impact of post-ischemic behavioral experience on spine maintenance, and its relationship to functional recovery has never been

tested. Here we monitored the maintenance of new spines formed at weeks 1,2 and 3 post-infarct and their relationship to improvements in skilled reaching in mice.

A third goal of the present study was to determine the impact of RT on spine changes along the apical dendrites of layer V pyramidal neurons in deeper layers. Previous studies have shown that in peri-infarct cortex, spine density along the superficial apical dendrites imaged *in vivo* is decreased early on after infarcts, but recovers after weeks (Brown et al., 2007; Mostany et al., 2010) . Furthermore, spine density on this same population of dendrites in more distant regions from the infarct has been shown to surpass baseline levels several months after McAO (Mostany et al., 2010). Improvements in skilled reaching in intact animals are associated with changes in dendritic branching and complexity (Kleim, et al. 1997; Greenough and Withers 1985; Withers and Greenough 1989), and increases in spine density (Wang et al., 2012; Clark et al., 2014; Clark et al., 2018) on deeper dendrites of layer V pyramidal neurons in the trained MC. Therefore, spine changes on deeper dendrites in within peri-infarct cortex could represent a structural mechanism supporting functional improvements in skilled reaching after focal ischemia. This possibility was tested by examining spine density on the apical dendrites of layer V pyramidal neurons within layer II/III of the ipsilesional hemisphere eight weeks post-infarct.

A final goal of the present study was to examine the impact of RT on patterns of neovascularization after ischemia. The significance of neovascularization for chronic post-infarct outcomes, is unclear. In rodent models of focal ischemia (Arenillas et al., 2007; Hayward et al., 2011; Martin et al., 2012; Lin et al., 2002; Lake et al., 2017; Ohab et al., 2006; Taguchi et al., 2009) and after human infarct (Bogoslovsky et al., 2010; Krupinski et al., 1994; Sobrino et al.,

2007) increased vascular density in peri-infarct cortex has been linked to improved outcomes, but considerable variability in the magnitude and persistence of neovascularization has been reported across studies. Furthermore, little is known about how behavioral experience impacts neovascularization. Sufficient activity, such as voluntary running, can promote angiogenesis in intact motor cortex (MC) of rodents and primates (Adkins et al., 2006; Rhyu et al., 2010; Wallace et al., 2011). Learning a skilled reaching task normally does not promote angiogenesis in MC (Adkins et al., 2006) in intact mice, but whether neovascularization might be needed for functional improvements associated with RT remains unknown. Here, we used histological measures of lectin-labeled vessels to assess neovascularization patterns eight weeks after infarct and whether these patterns varied with RT.

4.3 Materials and Methods

4.3.1. Subjects

Twenty-four male (n=12) and female (n=14) C57/BL6 Green Fluorescent Protein (GFP)-M line (B6/Cg-Tg (thy-1 GFPM) 2Jrs/J) and 3 male C57/BL6 Yellow Fluorescent Protein (YFP)-H line (B6/Cg-Tg (thy-1 YFPH) 2Jrs/J; Jackson laboratories) mice were used ref. Both mouse lines express fluorescent proteins in a subset of layer 5 cortical pyramidal neurons. All animals were bred at the Animal Resource Center at the University of Texas at Austin (ARC) and were between 4 and 5 months old at the time of cranial window implantation. Mice were placed into one of four groups that underwent: (1) artery-targeted photothrombosis (infarct no RT, n=5 males, n=4 females), (2) artery-targeted photothrombosis and rehabilitative training, (infarct RT, n=2 males, n=3 females), (3) sham procedures and RT (n=3 males, n=2 females), or (4) sham procedures and no RT (n=2 males, n=3 females). The timeline of experimental procedures is

summarized in Figure 4.1. Three animals (n=1 female infarct No RT, n=1 female sham RT, n=1 male sham no RT) were included in behavioral analyses but not in spine dynamics analyses due to extremely dense of XFP labeling. 2 animals (1 female and 1 male infarct No RT) were included in spine dynamics analysis but not behavior because of failure to learn the task. Furthermore, behavioral data from 1 male (infarct No RT) was excluded due to failure to complete all 30 trials at several post-infarct testing probes, and 1 animal (female infarct No RT) had to be excluded from the study because lesion volume was much smaller that the group average, and 3 animals (1 male infarct no RT, 1 female sham no RT, and 1 female infarct RT) were excluded from the last imaging time point due to issues with window clarity.

Each cage had standardized supplementation including wooden toys, bedding and polyvinyl chloride pipes which were replaced weekly. During behavioral procedures, mice were placed on scheduled feeding (2.5-3g food once per day) to avoid satiation during behavioral training. Body weights were not permitted to fall below 90% of free feeding weights over the experimental time course ($M \pm SE$ weight, 28.3 ± 5g males and 21.3 ± 2g females). All animal use was in accordance with a protocol approved by the Animal Care and Use Committee of the University of Texas at Austin. In order to monitor estrous in females, vaginal smears were collected during baseline imaging sessions, and then again at each post-infarct imaging session (which also corresponded to behavioral probes) and placed onto glass slides. Slides were then stained with cresyl violet, coverslipped and visualized using a standard light microscope at a final magnification of 756X.

4.3.2 Cranial Window Creation

Cranial window implantation was performed as previously described. Briefly, mice were

anesthetized with ketamine (4 mg/kg, i.p.) and xylazine (3 mg/kg, i.p.). Dexamethasone (2 mg/kg s.c.) and carprofen (2.5 mg/kg s.c.) were administered pre-operatively to help minimize cortical swelling and inflammation during the procedures. Anesthetic plane was monitored via respiratory rate and toe pinch response throughout surgery. Booster injections of ketamine (4 mg/kg) were given as needed to maintain anesthesia. Following midline incision of the scalp, a 4 mm circular region of skull over frontoparietal cortex was thinned using a high-speed dental drill with a 0.5 mm diameter drill bit and removed, leaving dura intact. Saline was frequently applied to protect the brain from overheating. Skull was then replaced with a 4 mm diameter No. 1 coverglass and sealed with cyanoacrylate and dental cement. All windows were made over the forelimb area of the motor cortex contralateral to the preferred-for-reaching forelimb. Following surgery, animals were given buprenorphine (3 ml/kg, s.c.) for pain management and allowed to recover in their cage for 1 week, and were given daily injections of carprofen (2.5 mg/kg, i.p.) to help minimize inflammation that contributes to window clouding.

4.3.3 Artery-targeted Photothrombosis

Photothombotic infarcts were performed as previously described. Mice were anesthetized with isoflurane (4% induction, 1.5-2% maintenance) in O_2 and affixed to a stereotaxic frame. Arterial oxygen saturation and heart rate from pulse oximetry were recorded and temperature was maintained at 37° C with a feedback temperature control system. A green diode laser was coupled to the DMD to provide focused patterned illumination (20 mW) over 1-3 arterial branches ($M \pm SE$ target area was 0.13 ± 0.018 mm$^{2)}$ on the pial surface supplying the forelimb region of MC. Between 1 and 2 distal branches of the anterior cerebral artery (ACA) were also illuminated to control the level of collateral flow at the time of occlusion. Thirty seconds

following a retroorbital injection of Rose Bengal (50 μL, 15 mg/mL i.v., Sigma), target vessels were irradiated with the patterned laser. Sham animals were exposed to laser illumination after injections of sterile saline. In all animals, CBF was monitored in real time for up to 10 min following the occlusion using traditional laser speckle contrast imaging. Photothombosis or sham procedures were performed one day following the second baseline imaging session and final training day.

4.3.4 In Vivo Imaging of Dendrites

Animals were anesthetized with 1.5% isoflurane in O2 and inserted into a custom made stereotaxic apparatus fitted with a headbar to minimize breathing artifact. Prior to baseline imaging, penetrating arterioles over the caudal forelimb area (CFA) of the motor cortex (Tennant & Jones, 2011) were identified for photothrombosis from images taken at the time of cranial window implantation. Then, during the first baseline imaging session, five to six image stacks containing at least eight to ten dendrites with visible spines, were selected between 300 μm and 1 mm from the to-be-targeted arteriole. This distance range was selected based on results from Chapter 3, which indicated that the penumbra extended ~ 1mm from the infarct core. In several animals, image stacks within 300 μm from the ischemic core were gathered but were unable to be used in spine dynamics analysis due to inability to detect at least eight intact dendrites with distinguishable spines or gross changes in fluoresce stemming from dendritic damage. Images were acquired using a Prairie Ultima standard two-photon microscope with a Ti:Sapphire laser tuned to either 860nm (GFP) or 920 nm (YFP) at low laser power (~30 mW) to minimize phototoxicity. Laser power was adjusted through a Pockels cell in order to obtain near identical fluorescence at each imaging location and across imaging days. Image stacks were gathered

between 50 and 200 µm from the pial surface using a water immersion objective (20x, 1.0 NA, Olympus) and a digital zoom of 4X. Image stacks consisted of 150-200 optical sections spaced 1µm apart covering an area of 240 µm x 240 µm (512 x 512 pixels, 0.13 µm/pixel). Animals were imaged twice prior to photothrombosis, with the first imaging session occurring after the seventh day of behavioral training, and the second imaging session following the final training session. Animals were then imaged once a week for up to five weeks following ischemic insult (Fig. 4.1).

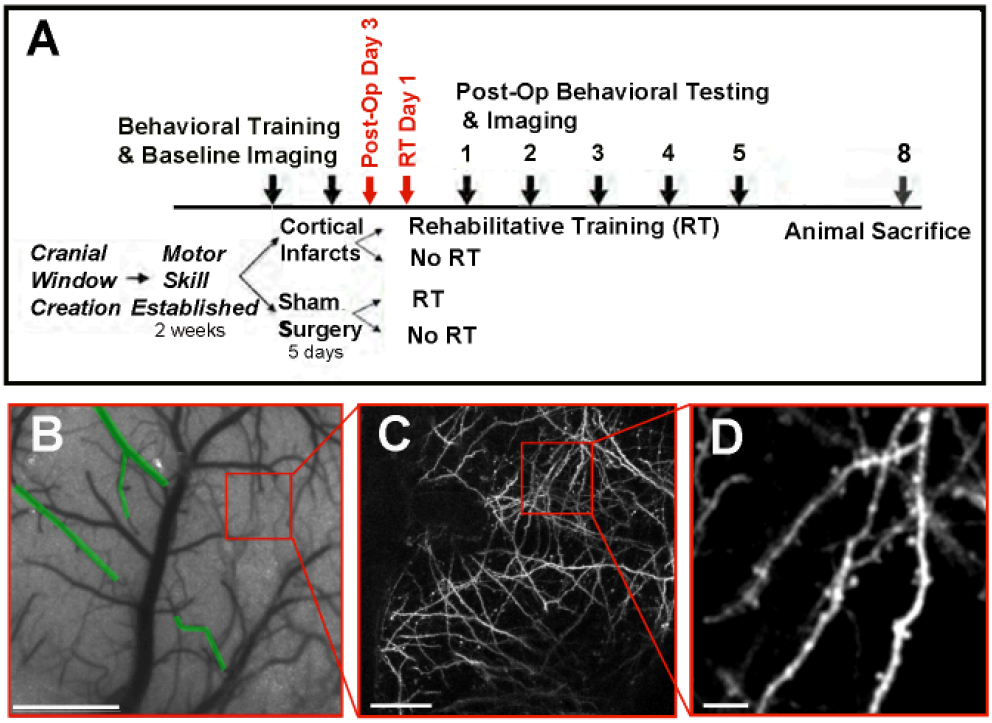

Figure 4.1. Experimental Design. (**A)** Experimental time course. Block arrows correspond to imaging sessions and behavioral probes **(B)** Speckle contrast image of cortical surface vasculature taken just before artery-targeted photothrombosis. Green overlays represent targeted arterioles. Red box indicates a sample imaging region**.** Scale bar 1mm. **(C).** Low-magnification image of GFP-labeled dendrites in the sample imaging location**.** Scale bar 100µm. **(D)** High magnification image of the sampling region. Scale bar 10µm.

4.3.5 Spine Dynamics Analyses

All analyses of dendritic spine turnover was performed blind to experimental condition. A total of 8-10 intact dendritic segments per image stack, each at least 20 μm in length, were analyzed (~100-200 spines per animal) using ImageJ software (Fig. 2). If more than half of an identified dendritic segment contained dendritic blebbing or beading from photothrombosis, it was excluded from analysis. Spines were considered to be the same between imaging sessions based on their relative position to adjacent dendrites and spines. Because of lower two-photon resolution in the axial plane, only dendritic spines projecting laterally were included in the analysis. For a spine to be considered new or lost, it had to clearly protrude out of the shaft by at least four pixels (0.55 m), and it could not be part of a dendritic segment that appeared to have significantly rotated or shifted, as judged by any gross changes in the appearance of neighboring spines or branches. Due to difficulty distinguishing dendritic filopodium, long-thin structures that turned into a shorter, more spine-like structures were omitted from analysis. Spine turnover was measured by comparing dendritic protrusions in the image being analyzed to those in the previous imaging session. A spine was counted as stable if it appeared in both the previous imaging session and the one being analyzed, as newly formed if it was only present in the image being analyzed, and as eliminated if it was visible in the previous imaging session but not the one being analyzed. The percentage of spine formation and elimination was calculated as the number of spines gained or lost divided by the total number of stable spines in the analyzed imaging session (Xu et al., 2009). Analyses were performed on raw unprocessed image stacks, but for presentation purposes, images are shown as median-filtered maximum intensity projections consisting of 5-10 optical sections with median and Gaussian filters applied.

The maintenance of newly spines formed between weeks 1 and 3 post-infarct was tracked up until the final imaging session (week 5). Per animal, if < 3 spines were counted as being formed within a given imaging session, spine data was not used in analysis of spine maintenance. This issue mainly involved animals in the sham group because spine turnover was quite low. However, occasionally in animals in the infarct group, imaging regions were either lost to ischemia (week1) or contained several dendrites previously used for analysis that were no longer visible (weeks 2 and 3). Therefore, sample sizes were adjusted as follows: Between weeks 1 and 5, 3 animals (n=1 sham, n=1 infarct no RT and n=1 infarct RT) were excluded from an insufficient spine sample, and there was attrition of 4 animals at week 5 (n=3 sham, n=1 infarct RT). Between weeks 2 and 5, data from 3 animals (n=2 sham, n=1 infarct No RT) was omitted, and there was attrition of 3 animals (n=2 sham, n=1 infarct RT). For weeks 3-5, data from 3 animals in the sham group was omitted, and there was attrition of 3 animals at week 5 (n=1 sham, n=1 infarct no RT, n=1 infarct RT).

4.3.6 Skilled Forelimb Training and Assessment

Prior to photothrombosis or sham procedures, all mice were trained to criterion on a manual skilled reaching task. The reaching task used was the single seed retrieval task (Chen et al., 2014; Farr & Wishaw 2002) in which mice were trained to reach for and obtain a millet seed placed on a platform outside of a custom-made clear Plexiglas training chamber (20 cm tall, 15 cm deep, and 8.5 cm wide, measured from outside; 0.5 cm thick Plexiglas). There were 4 mm wide vertical openings on the left and right sides of the chamber for mice to reach through with either the left or right paw, respectively. The platform (8.5 cm long, 4 cm wide, and 1.2 cm tall) contained 1 well at varying distances from each opening for positioning seeds. Relative to the

opening edge closest to the center of the chamber, the well was positioned 3 mm further from the center of the chamber opening and 2 mm ahead of the chamber opening. During shaping, the preferred limb for reaching was determined by allowing mice to reach for millet seeds with either limb placed just outside of both openings. The preferred-for-reaching forelimb was defined as the first limb used to make five consecutive reach attempts. For the remainder of the shaping phase (~ 2-3 days), mice were encouraged to reach for a single seed placed in the well outside of the chamber opening corresponding to their preferred-for-reaching forelimb. Training started once mice were able to successfully retrieve the pellet 10 times from the well. Mice then received 12-13 training sessions of 30 trials each, with two reach attempts per trial. Successful reach attempts were counted if the mouse obtained the seed and brought it inside of the chamber to its mouth. Unsuccessful reach attempts included those in which the seed was missed, displaced or dropped before eating. Data were analyzed as the percent of successful reaches per reach attempt, as well as the number of successes on the first reach attempt. Deficits in reaching performance were probed initially 3 days following photothrombotic infarcts and then once weekly for 5 weeks. RT consisted of the same procedures used for pre-operative training, and occurred five days a week for four weeks beginning five days after ischemia. In the infarct No RT group, one male was excluded from behavioral analyses due to failure to complete the 30 trials during several post-infarct probe sessions, and data from 1 female in the infarct RT group was omitted at post-infarct week 5 for the same reason.

4.3.7 Tissue Processing and Analysis of Lesion Volume

All animals were overdosed with sodium pentobarbital and transcardially perfused with 0.1 M phosphate buffer (PB) saline and 4% paraformaldehyde eight weeks after infarcts. Following

fixative perfusion, brains were extracted and stored in 4% paraformaldehyde for no more than 48 h before being sliced into 40 µm thick coronal sections using a Leica VT1000S vibratome.

Lesion volume was determined by first measuring the area of viable cortical tissue in a set of seven nissl stained coronal sections per animal with Neurolucida software (MBF Bioscience, Williston, VT). Sections encompassed the lesion and were from approximately 1.5 mm anterior to 0.7 mm posterior to bregma, spaced 240 µm apart. Sections were viewed at a final magnification of 17x. Cortical volume was estimated as the product of summed section areas and the distance between sections. Lesion volume was then calculated as the difference between cortical volumes of the contralesional and ipsilesional cortices.

4.3.8 Spine Density Analysis

One set of tissue was mounted on glass slides for visualization of spine density on YFP+ pyramidal neurons using confocal microscopy. Image stacks were acquired using the confocal mode on the two-photon microscope. The dichroic mirror was replaced with a lens tuned to 488nm (FITC) and image stacks containing apical dendritic branches within layer II/III (between 200-400um from the surface) of motor cortex were gathered using a water immersion objective (20x, 1.0NA; Olympus). All spine density analyses were performed using Image J software. A total of 8-10 apical dendrites measuring at least 50 µm in length were sampled between 300µm and 1mm from the edge of the core in the ipsilesional hemisphere. In sham animals, samples homotopic to the lesion site within the trained (ipsilesional) MC were gathered. Data from 2 animals (n=1 infarct RT, n=1 Infarct No RT) had to be omitted due to an inability to localize a sufficient sample of dendrites of this length. For all dendritic analyses, spines along the length of

measured dendrite were manually counted, and density was calculated as total spines per length of dendrite.

4.3.9 Vascular labeling with isolectin B4

To visualize vasculature, one set of free-floating sections was labeled with IB4 (Griffonia simplicifolia, 1:50, Sigma-aldrich cat no. L2140), using a protocol adapted from Walchli and colleagues, and previously described in Chapter 3 (Walchli et al., 2015). Briefly, sections were immersed in 50 mM NH_4Cl in 0.1 M phosphate-buffered saline (PBS) for 30 minutes. After several washes with PBS, sections were incubated in 50 mM glycine in 0.1 M Tris (pH 8.0) for 5 minutes at 80° C, washed in.1M PBS and then incubated in $CaCl_2$-containing buffer (0.1 mM $CaCl_2$, 0.1 mM $MgCl_2$ and 0.1 mM $MnCl_2$ diluted in 0.1 M PBS (pH 6.8), for 15 minutes at 65° C. Sections were then permeabilized in 0.1 M Tris-buffered saline and Triton X-100 (0.3% vol/vol) for 10 minutes, and incubated for 72 h with gentle shaking on an inclined table at 4° C in biotinylated IB4 diluted in $CaCl_2$-containing buffer and blocking solution (0.05% vol/vol Triton X-100 and 2% vol/vol normal goat serum in $CaCl_2$-containing buffer). Following lectin incubation and several PBS washes, sections were incubated overnight at 4° C in Cy3-conjugated strepdavidin (1:200, Jackson Laboratories, cat. no. 016-500-084) diluted in blocking solution. Sections were then thoroughly washed in PBS and mounted onto glass slides.

4.3.10 Analysis of Vascular Density

Images of IB4-labeled tissue sections were visualized using a standard light microscope with a reflected fluorescence system (Olympus America Inc; Melville, NY) and TRITC filter. Per each

of 3 coronal sections per animal containing a visible lesion, eight 400 µm by 400 µm images of peri-infarct cortex were collected at a final magnification of 756X. Per section, one set of four images was obtained from deeper and superficial cortex within 100 µm of the medial and lateral edges of cortical infarcts, and an additional set of four was taken immediately adjacent to the first (Fig. 4). Samples in the contralesional hemisphere and in sham animals were taken homotopic to those collected in the ipsilesional hemisphere. Vascular density measurements were made in ImageJ using a custom macro that calculated the area fraction of IB4-labeled vessels in thresholded and binarized images. Vessel densities are reported as a percentage of the contralateral hemisphere. Vascular densities in the contralesional hemisphere were similar, and therefore pooled, across sample positions. Data from two animals in the sham group (1 sham No RT and 1 sham RT), and 2 animals (1 male and 1 female) in the infarct No RT group was omitted due to poor lectin labeling.

4.3.11 Statistical Analyses

All statistical analyses were performed using the SPSS software package. The effect of RT on spine dynamics was examined using a repeated measures analyses of variance (ANOVA) with group (infarct RT v infarct No RT) as a between-subjects variable and time as a within-subjects variable. Each infarct group was additionally compared to the sham group in secondary analyses. The Shapiro-Wilks test was used to check for normality. When warranted by significant Group by Time interactions, post hoc group comparisons per time point were performed using Holm-Bonferroni corrected t-tests. Separate repeated measures ANOVAs between the groups outlined above were used to examine group differences in spine maintenance for new spines formed at weeks 1, 2 and 3 post-insult. The last imaging time point (week 5) was omitted from the spine

dynamics ANOVA because of animal attrition at this time point, but between-group comparisons at this time point were analyzed with t-tests, and this time point was counted as a comparison in the Bonferroni-Holm's correction when post-hoc tests per time point were warranted by ANOVA results.

Repeated measures ANOVAs were used to probe for differences in post-infarct reaching performance over time using the same group comparisons as above, and when warranted by ANOVAs, post-hoc Bonferroni-corrected t-tests were used to probe differences at individual time points between groups. Pearson correlations were used to probe for relationships between post-infarct reaching performance and new spine survival. Reaching data is presented as successful retrievals per attempt, but for correlations reaching performance is presented as the percent of baseline performance.

Using the same group comparisons as above, group differences in post-infarct reaching performance were examined using repeated measures ANOVA with group as a between-subjects factor, and time as a within-subjects factor. Differences in spine density and vascular density at 8 weeks post-infarct was assessed using independent samples t-tests. Data from males and females, as well as from both sham groups were combined for primary analyses of all measures listed above because there were no notable differences in the patterns of experimental results between them. Supplemental materials show individual group means for sham groups, as well as means disaggregated by sex. Group means for YFP and GFP males on spine measures, which did not significantly vary, can also be found in supplemental materials. Data are reported as $M \pm SE$.

4.4 Results

4.4.1 Artery-targeted photothrombosis increased spine turnover in peri-infarct cortex, the pattern of which differed with RT

Sustained increases in spine turnover have been reported over weeks following photothrombosis, but only within 300 μm from the ischemic core, which is about the size of the ischemic penumbra produced with photothrombosis. (Brown et al., 2007; 2009). In the present study, we examined the impact of RT on spine dynamics in peri-infarct regions of MC between 300 μm and 1 mm from the occluded arterioles. This was based on previous results indicating that artery-targeted photothrombosis increases the size of the vascular penumbra (see Ch. 3). In both infarct groups, spine formation was elevated during the 5 weeks following ischemia relative to sham animals. Repeated measures ANOVAs between each infarct group and sham revealed a significant main effect of Group on formation (No RT: $F_{(1,13)} = 76.58$, $p < 0.0001$; RT: $F_{(1,12)} = 26.9$, $p < 0.0001$) as well as a significant Group by Time interaction between infarct No RT and sham groups on spine formation (No RT: $F_{(3,39)} = 2.98$, $p = 0.59$; RT: $F_{(3,36)} = 0.79$, $p = 0.5$). Separate ANOVAs revealed significant Group by Time interactions between both infarct groups compared to sham on spine elimination (Infarct No RT: $F_{(3,33)} = 29.53$, $p < 0.0001$; Infarct RT: $_{(3,36)} = 28.26$, $p < 0.0001$) as well as a main effect of Group (Infarct No RT: $F_{(1,11)} = 84.78$, $p < 0.0001$; Infarct RT: $F_{(1,12)} = 23.79$, $p < 0.0001$) indicating that spine elimination in both infarct groups was also elevated relative to sham animals, the pattern of which varied over time. Bonferroni-corrected t-tests revealed that in both infarct groups, spine elimination was significantly higher compared to sham at weeks 1(No RT: $t_{(2,14)} = 2.15$, $p < 0.0001$, RT: $t_{(2,11)} = 2.20$, $p = 0.0009$) 2 (No RT: $t_{(2, 14)} = 2.15$, $p < 0.0001$, RT: $t_{(2, 11)} = 2.20$, $p < 0.0001$) and 3 (No

RT: $t_{(2,14)} = 2.15$, $p = 0.001$, RT: $t_{(2,11)} = 2.20$, $p = 0.02$), but only between the No RT group and sham at weeks 4 (No RT: $t_{(2,14)} = 2.15$, $p = 0.001$ RT: $t_{(2, 11)} = 2.20$, $p = 0.25$) and 5 (No RT: $t_{(2,12)} = 2.18$, $p = 0.001$)

In comparing spine turnover between infarct groups, ANOVA revealed that the pattern of spine formation was similar (Group by Time : $F_{(3,33)} = 1.03$, $p=0.39$; Main Effect: $F_{(1,11)} = 3.20$, $p = 0.1$). However, the pattern of spine elimination differed between groups and was greater in the no RT group relative to RT group at later time points (Group by Time : $F_{(3,27)} = 5.30$, $p = 0.009$; Main Effect $F_{(1,9)} = 3.00$, $p = 0.18$). Bonferroni-corrected t-tests revealed that at week 4, elimination was significantly higher in the infarct No RT compared to infarct RT group, an effect that just missed significance at week 5 (No RT: $t_{(2,9)} = 2.26$, $p = 0.051$, Fig. 4.2). These results indicate that artery-targeted photothrombosis instigates increases in spine turnover that persist for weeks. However, spine elimination returns to near baseline levels during RT, despite sustained elevations in spine formation. Reductions in spine elimination were associated with a near normalization of spine density to baseline levels by week 5 post-infarct in the RT group ($t_{(2,3)} = 3.18$, $p = 0.043$), but not in the No RT-group ($t_{(2,5)} = 2.57$, $p = 0.004$).

Across infarct groups, there was a tendency for males to have greater spine formation and elimination than females at weeks 1 and 2 post-infarct, but spine turnover was similar between sexes at all other time points (See Suppl. Table 4.2). Males also tended to have larger lesion volumes compared to females ($M \pm SE$ Females: 0.9 ± 0.1; Males : 1.1 ± 0.2; Suppl. Table 4.5), but there was no significant correlation between lesion size and spine turnover ($r = 0.51$, $t_{(9)} = 1.35$ $p= 0.23$).

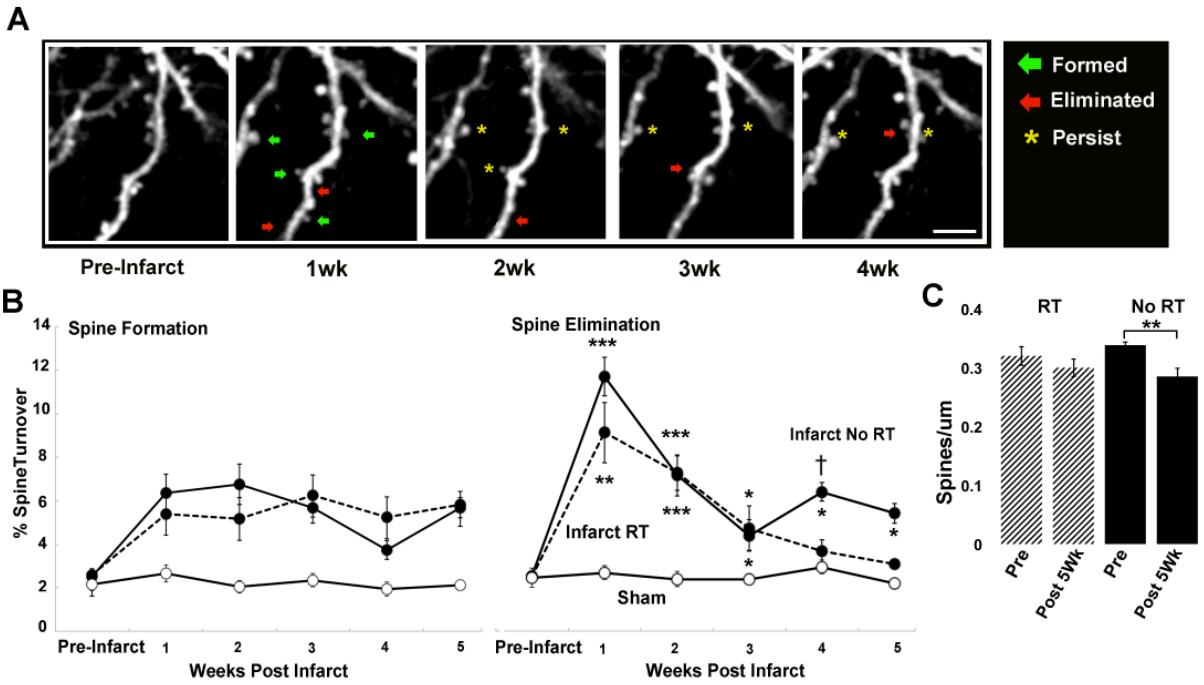

Figure 4.2. Patterns of spine turnover in peri-infarct cortex varied between groups. **(A)** Example of spine turnover in peri-infarct cortex over several weeks. Green arrows correspond to newly formed spines, and red arrows to disappeared spines. Yellow asterisks symbolize persisting spines. Scale bar 10µm. **(B)** The pattern of spine formation was similar between infarct no RT and infarct RT groups. Spine turnover in both infarct groups remained elevated over time compared to sham **(C)** The pattern of spine elimination differed between infarct No RT and RT groups. In both infarct groups, spine elimination was significantly elevated for up to 3 weeks post (***p's < 0.0001, ** p's < 0.001, *p's < 0.02). Spine elimination remained significantly elevated in the infarct no RT group at weeks 4 and 5 compared to both sham (*p < 0.02) and the RT group (week 4: †p < 0.02). **(D)** Spine Density returned to near baseline levels by 5 weeks post-infarct with RT (RT: *p < 0.04, No RT: **p = 0.001).

4.4.2 RT promoted New Spine Stabilization

Mostany and colleagues (2010) previously reported that, in mice spontaneously recovering from MCaO, spines formed during the first several weeks after the insult were more likely to persist relative to intact animals. We examined whether RT impacted the pattern of spine maintenance for new spines formed during weeks 1, 2 and 3 after artery-targeted photothrombosis (Fig. 4.3).

Between infarct groups, repeated measures ANOVA revealed neither a significant Group by Time interaction ($F_{(2,16)} = 2.92$, $p = 0.08$), nor a significant main effect of Group on the maintenance of spines formed during week 1 ($F_{(1,8)} = 0.12$, $p = 0.735$). In comparing each infarct group to sham, there were no significant Group by Time interactions (No RT: $F_{(2,18)} = 2.34$, $p = 0.13$; RT: $F_{(2,14)} = 2.27$, $p = 0.14$), but a significant main effect of Group for both (No RT: $F_{(1,9)} = 16.05$, $p = 0.003$; RT: $F_{(1,7)} = 22.4$, $p = 0.002$; Fig. 3A). These results indicate that spines formed in the first week after the infarct were more likely to remain until week 4 regardless of whether animals received RT, relative to sham. However, new spines formed in week 1 were more likely to persist to week 5 after the infarct in the RT group compared to No RT group ($t_{(2,7)} = 2.36$, $p = 0.02$). Maintenance of spines formed during week 1 was also no longer significantly different between the infarct No RT group and sham at this time point ($t_{(2,8)} = 2.30$, $p = 0.17$). These results indicate that RT promoted greater long-term persistence of new spines.

Between infarct groups, we found that RT was associated with a greater maintenance of new spines formed during the initial weeks after the infarct compared to no RT. Repeated measures ANOVA revealed a significant Group by Time interaction ($F_{(1,10)} = 63.7$, $p < 0.0001$), as well as significant main effect of Group ($F_{(1,10)} = 311.8$, $p < 0.0001$) for spines formed during the second week after the infarct. Post-hoc Bonferroni corrected t-tests revealed that spine maintenance was similar between groups during the second and third week ($t_{(2,10)} = 2.23$, $p = 0.2$; Fig. 3B). A tendency for spine maintenance to be greater in the RT compared to the No RT group at week 4 ($t_{(2,10)} = 2.23$, $p = 0.04$) did not reach significance after correcting for multiple comparisons. At week 5, elevated spine maintenance was significantly greater in the RT group relative to the no RT group at week 5 ($t_{(2,10)} = 2.26$, $p = 0.02$). Between infarct RT and sham

groups, there was no significant group by Time interaction ($F_{(1,9)} = 0.017$, $p = 0.89$), but a significant main effect of Group ($F_{(1,9)} = 9.54$, $p = 0.013$), reflecting that spine maintenance was greater on average in the RT group relative to sham at all time points. These and the above results support that RT is associated with increased stabilization of spines formed during week 2 after the infarct. Furthermore, between infarct No RT and sham groups, there was neither a main effect of Group ($F_{(1,11)} = 3.1$, $p = 0.11$) nor a Group by Time interaction ($F_{(1,11)} = 0.517$, $p = 0.28$), indicating that without RT, new spines formed during this time period were just as likely to disappear as in sham animals.

For spines formed 3 weeks post-infarct, independent-samples t-tests revealed that spine maintenance at week 5 was significantly greater in the infarct RT group compared to both the infarct No RT group and sham (RT v No RT: $t = 2.62$, $p= 0.04$; RT v sham: $t = 2.44$, $p = 0.04$), but not between the infarct No RT group and sham ($t = 2.62$, $p = 0.26$; Fig. 3C). Together, these results indicate that the maintenance of spines formed during weeks 1 and 3 after the infarct was greater in the RT group relative to both the No RT group and sham animals.

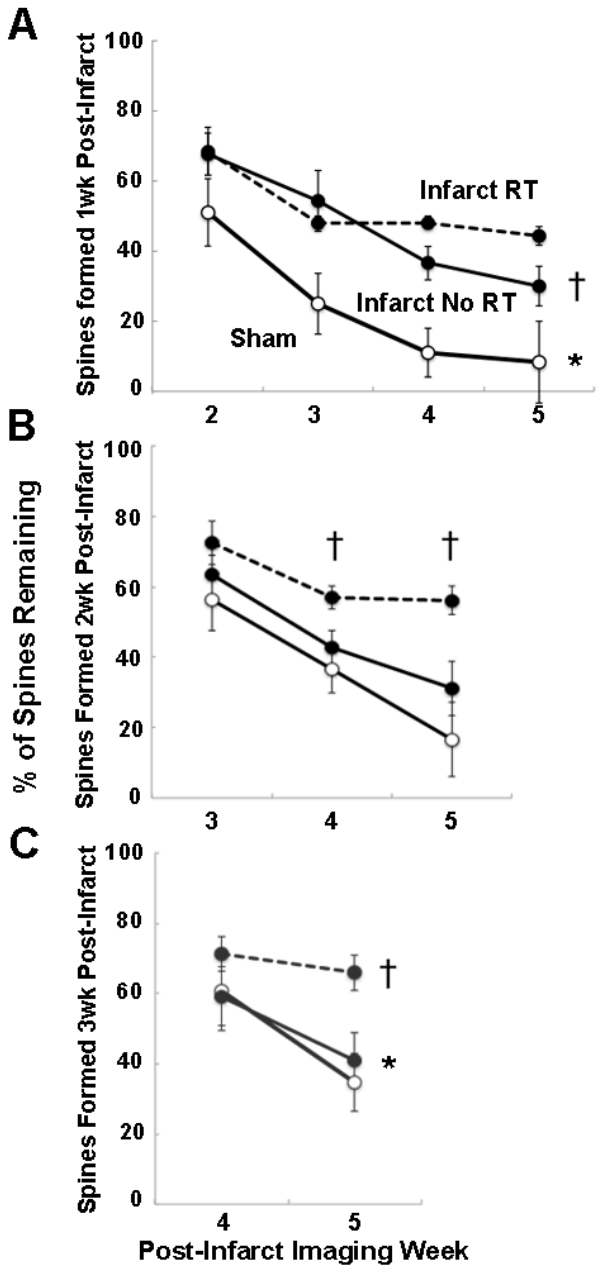

Figure 4.3. Stabilization of spines formed during weeks 1-3 post-infarct was greater with RT at later time points. **(A)** Percent of spines formed during the first week remaining at weeks 2 -5. At week 5, spines were more likely to persist in the infarct RT group compared to No RT group and compared to sham. **(B)** The percent of spines formed during week 2 remaining at weeks 3-5 was greater with RT compared to No RT at weeks 4 and 5. **(C)** The percent of spines formed during week 3 remaining at week 5 was greater with RT compared to No RT and sham. (†$p < 0.05$ No RT vs. RT; *$p < 0.05$ RT vs. sham). Independent samples t-tests were used for week 5, which was not included in the ANOVAs.

4.4.3 RT improved deficits in skilled reaching

Previously, we found that small motor cortical infarcts generated with artery-targeted photothrombosis instigated deficits in skilled reaching that recovered relatively quickly (See Ch. 3). In the present study we found that over the RT period animals in the RT group recovered reaching performance to near baseline levels while performance in the No RT group remained lowered. This was not reflected in a significant main effect of Group ($F_{(1,9)} = 3.61$, $p = 0.09$, Fig. 4) nor Group by Time interaction ($F_{(3,36)} = 1.91$, $p = 0.17$) on reaching performance. However, the pattern of performance improvements in skilled reaching varied between each infarct group relative to sham.

Repeated measures ANOVAs revealed no significant Group by Time interaction between the infarct No RT group and sham ($F_{(4,56)} = 1.37$, $p = 0.25$), but a significant main effect of Group ($F_{(1,14)} = 14.98$, $p = 0.002$), reflecting that reaching performance in the infarct No RT group was lower relative to sham and did not vary significantly with time. Between infarct RT and sham groups, there was both a significant Group by Time interaction ($F_{(4,52)} = 2.71$, $p = 0.035$), and a main effect of Group ($F_{(1,13)} = 5.61$, $p = 0.03$). Post-hoc Bonferroni t-tests revealed that the infarct RT group performed significantly worse at post-infarct day 3 compared to sham ($t_{(13)} = 2.16$, $p = 0.004$). However, performance was not significantly different between RT and sham groups at any other time point group (Fig. 4B). Lesion volumes were similar between infarct groups (Fig. 4C), and were neither correlated with initial deficits at post-infarct day 3 ($r = -0.31$, $t_{(10)} = 1.03$, $p = 0.32$), nor deficits assessed at week 5 ($r = -0.57$, $t_{(9)} = 2.09$, $p = 0.32$). These results indicated that RT improves recovery of reaching performance.

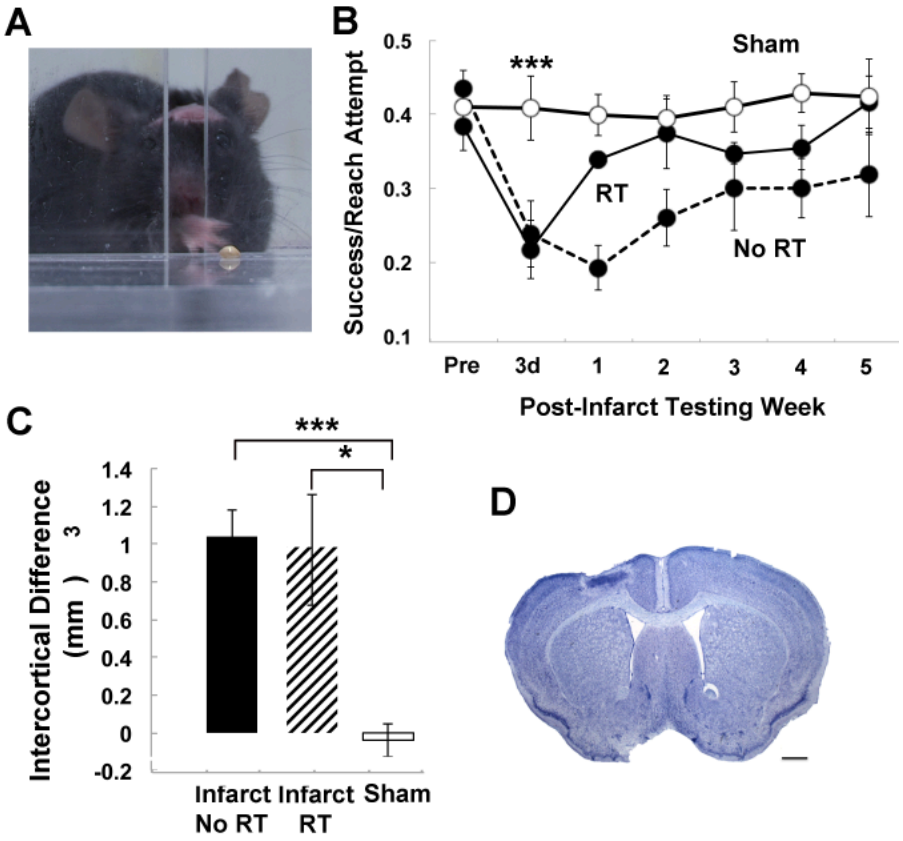

Figure 4.4. RT improved post-infarct skilled reaching performance. (A) Reaching performance on the single seed retrieval task. **(B)** Comparison of post-infarct reaching performance, measured as successful retrievals per reach attempt. Post-infarct performance declined in both infarct groups. In the No RT group, performance decrements relative to sham operates did not vary significantly with time post-infarct (***$p < 0.0001$ main effect of group). In contrast, the RT group performed significantly worse than sham at post-infarct day 3 (***$p < 0.0001$) but perform similar to sham at remaining testing weeks. Performance in the infarct No RT group is similar to the RT group at post-infarct day 3, but is lower, on average, compared to both infarct RT and Sham groups at remaining testing weeks. **(C).** Cortical lesion volume, measured as the difference in volumes between cortical hemispheres, was significantly greater compared to sham in both the infarct No RT group (***$p < 0.0001$) and in the infarct RT group (*$p < 0.01$). Lesion volumes are similar between infarct No RT and infarct RT groups. **(D).** Representative lesion reconstructions of the infarct group overlayed on coronal section templates. Numbers to the right represent anterior to posterior coordinates in mm relative to bregma.

While post-infarct reaching performance was not significantly different between males and females in either the RT group or No RT group. In both infarct groups, females tended to have smaller lesion sizes (Suppl. Table 4.5) but this was neither correlated with early performance deficits at post-infarct day 3 ($r = -0.42$, $t_{(8)} = 1.31$ $p = 0.22$) nor performance at the final testing week ($r = -0.17$, $t_{(8)} = 0.5$, $p = 0.62$). Female and male averages in post-infarct reaching performance can be found in Supplementary Table 4.4.

4.4.4 Post-infarct maintenance of new spines formed predicted reaching performance

We next examined whether the preferential stabilization of spines formed after the infarct related to skilled reaching performance at post-infarct week 4. While new spines formed during the first week after the infarct were more likely to remain in both infarct groups relative to sham, the maintenance of these spines was not correlated with reaching performance at week 4 ($r = 0.52$, $t_{(6)} = 1.75$, $p = 0.14$). However, the percent of spines formed during weeks 2 and 3 that remained at week 4 was significantly correlated with behavioral performance at this time point (2 weeks: $r = 0.74$, $t_{(8)} = 3.11$, $p = 0.02$, Fig. 5A; 3 weeks: $r = 0.77$, $t_{(5)} = 3.17$, $p = 0.03$, Fig. 5B). Since this population of spines was preferentially stabilized with RT relative to both no RT groups and sham, these data indicate that RT increased the maintenance of spines formed during weeks 2 and 3 that were associated with RT-mediated improvements in forelimb function.

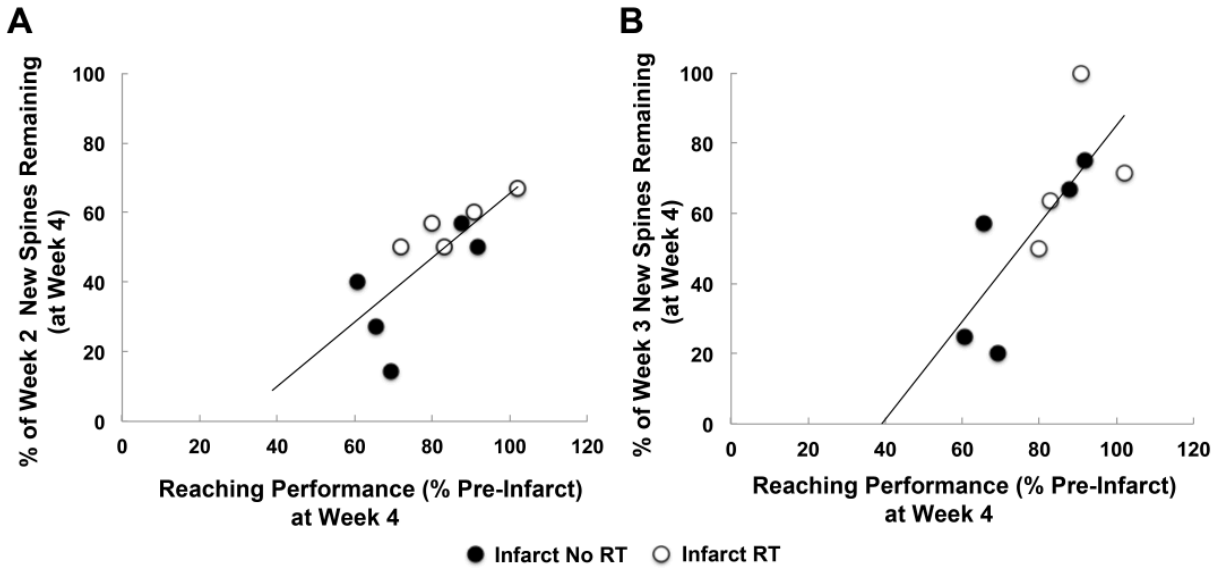

Figure 4.5. Maintenance of new spines formed during weeks 2 and 3 post-infarct were correlated with reaching performance. The percent of new spines formed during **(A)** week 2 and **(B)** week 3 remaining at week 4 positively correlate with and reaching performance, measured as a percent of baseline successful retrievals per reach attempt (*p = 0.02, *p =0.03).

4.4.5 RT increased spine density on apical dendrites in layer II/III of remaining MC.

Previously we found that in intact mice, training on a skilled reaching task increased spine density on the apical dendrites of layer V pyramidal neurons in layer II/III but not in layer 1 of trained MC (Clark et al., 2018). In rats, RT increases synaptic densities within layer V of peri-infarct motor cortex relative to both animals undergoing spontaneous recovery and no-infarct controls (Kim et al., 2018). Here, we examined the impact of RT on spine density along the apical dendrites of the same neuronal population imaged *in vivo* within layer II/III of peri-infarct MC at 8 weeks post-infarct and found that spine density in the infarct RT group was greater compared to both the no RT group ($t_{(9)} = 2.26$, $p = 0.03$) and sham ($t_{(10)} = 2.22$, $p = 0.0001$; Fig. 6B). Spine density was also increased in the No RT group relative to sham ($t_{(13)} =$

2.16, p = 0.007). Across groups, the magnitude of the increase, however, was not correlated with behavioral improvements at the final testing week (r = 0.23, $t_{(8)} = 0.68$, p = 0.51). These results indicate that while artery-targeted photothrombosis increased spine density along the deeper apical dendrites of layer V pyramidal neurons irrespective of training condition, this effect was enhanced with RT and could also support functional improvements in skilled reaching performance in mice.

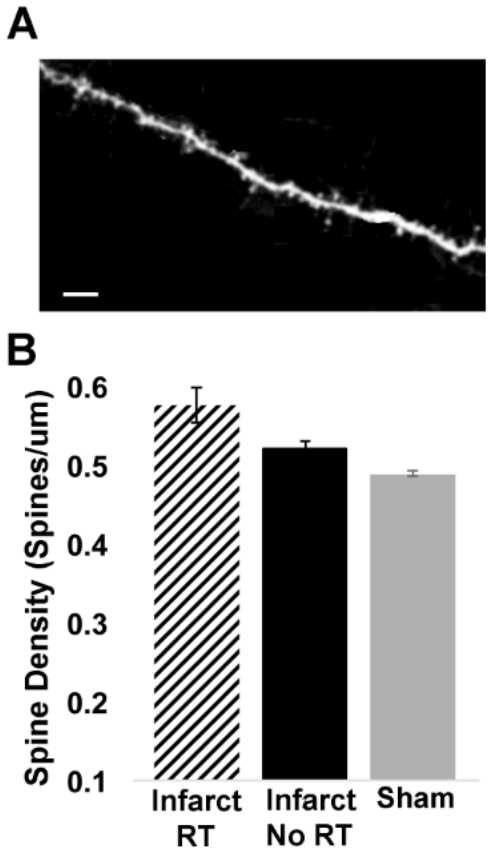

Figure 4.6. RT increased spine density on apical dendrites of layer V pyramidal neurons in layer II/III of peri-infarct MC. (A) Confocal image of apical dendrite sampled in layer II/III. Scale bar 10µm. Spine density, measured as spines/µm, is increased with RT at 8 weeks post-op relative to both No RT (†p < 0.05) and sham (***p < 0.0001). Spine density is also increased in the No RT group compared with sham (**p < 0.01).

4.4.6 Neovascularization was not evident at 8 weeks following artery-targeted photothrombosis

Plenty of evidence from rodent models suggests that ischemia instigates neovascularization early on and well into the chronic post-infarct phase (Arenillas et al., 2007; Hayward et al., 2011; Martin et al., 2012; Lin et al., 2002; Lake et al., 2017; Ohab et al., 2006; Taguchi et al., 2009). However, whether initial increases in vascular density persist and for how long, and the impact of RT on the pattern of results remains unclear. Previously, using immunohistochemical analyses of IB4+ labeled vessels, we found that vascular density was increased up to 2 weeks following artery-targeted photothrombosis (Ch. 3). In the present study we used the same labeling method to examine vascular density 8 weeks following artery-targeted photothrombosis. Independent samples- t-tests revealed that vascular density in the ipsilesional cortex was similar between each infarct group and sham between 100-400 μm from the lesion edge (infarct No RT v sham: $t_{(13)} = 2.16$, $p = 0.66$; infarct RT v sham: $t_{(11)} = 2.20$, $p = 0.72$), and between 500-900 μm (infarct No RT v sham: $t_{(13)} = 2.16$, $p = 0.66$; infarct RT v sham : $t_{(11)} = 2.20$, $p = 0.97$; Fig. 6). There were also no differences in vascular density between infarct No RT and RT groups at either distance (100-500 μm: $t_{(10)} = 2.23$, $p = 0.78$; 500-900 μm: $t_{(10)} = 2.23$, $p = 0.36$). Furthermore, combined vascular density (average of both distances) in the ipsilesional cortex was not correlated with infarct size ($r = 0.42$, $t_{(10)} = 1.42$, $p = 0.23$). These results indicated that there was neither an increase in vascular density at 8 weeks nor a significant impact of RT on vascular density during this time frame.

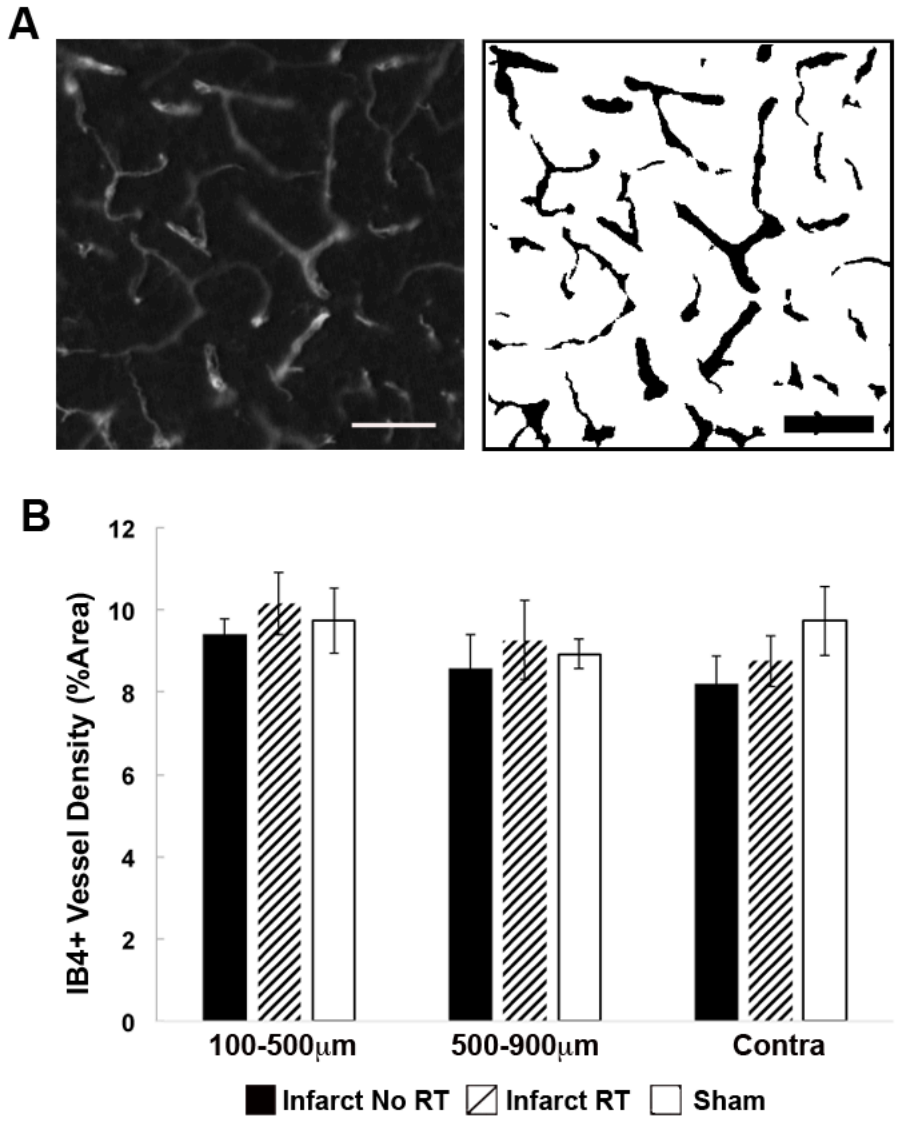

Figure 4.7. Vascular density was stable 8 weeks following artery-targeted photothrombosis. **(A)** Photomicrograph of IB4 labeling in the ipsilesional cortex at the magnification used for analysis. To the right is a corresponding binarized image used for area fraction measurements. Scale bars = 100 μm. **(B)** Vascular density, represented as the % area of IB4-labeled blood vessels, in the ipsilesional cortex was similar between infarct No RT and RT groups, and between both infarct groups and sham.

4.5 Discussion

Rehabilitative training (RT) approaches are the most common treatment for motor impairments, an especially prevalent consequence of infarct. In rodents, RT is associated with increased synaptic densities in peri-infarct cortex, as well as the reorganization of motor maps, both of which are linked to positive behavioral outcomes (Biernaskie et al., 2001; Dancause et al., 2005; Frost et al., 2003; Jones et al., 1999; Nudo et al., 1996; Murphy & Corbett 2009; Ward et al., 2004). However, previously lacking was a detailed understanding of how structural remodeling events unfold over time, and how they interact with RT to drive functionally beneficial outcomes. An understanding of the temporal sequence of remodeling events is crucial for optimizing the timing of therapeutic strategies aimed at improving functional outcomes. By monitoring synaptic structural plasticity at the level of individual dendritic spines *in vivo* we have shown that focal ischemia to the MC induced by artery-targeted photothrombosis increased spine turnover for up to 5 weeks following ischemia. Unlike previous studies, which found that spine turnover is restricted to the first several hundred μm of the ischemic core following traditional photothrombosis (Brown et al., 2008), we found that artery-targeted photothrombosis instigates widespread increases in spine turnover that extend at least 1mm from the occluded artery. Due to malfunctioning of equipment, we were only able to image CBF using MESI in half of the animals in the present study, and therefore CBF data was omitted from analyses. We did find however, that in the subset of animals imaged at 48 hours post-stroke at least some degree of reperfusion was evident in the targeted arteries. Furthermore, across animals CBF was found to be > 65% of baseline CBF in peri-infarct imaging locations at 48 hours post-infarct indicating

that increases in spine turnover persisted despite the reestablishment of CBF to peri-infarct cortex.

In both infarct groups, the extent of spine elimination was greater than spine formation during the first 2 weeks following ischemia, similar to previous reports (Brown et al., 2009). However, at weeks 4 and 5, spine elimination returned to near baseline levels in the infarct RT group, but remained elevated in the No RT group despite sustained increases in spine formation in both groups. These results indicated that RT was associated with improved spine stability at later time points. In comparing the maintenance of new spines formed between post-infarct weeks 1 and 3, we found that RT was associated with greater stability of this population of new spines at weeks 4 and 5 relative to both the infarct No RT group and sham. These and the above results suggested that the decrease in spine elimination with RT at weeks 4 and 5 is reflective of the increased maintenance of new spines formed after the infarct, which could be related to improvements in performance.

When we examined the relationship between new spine maintenance and behavioral performance at week 4, we found that the percent of new spines, formed during weeks 2 and 3, remaining at week 4 was positively correlated with reaching performance at week4, which was greater in RT animals. These results are suggestive of the possibility that the maintenance of this population of spines could represent a structural mechanism supporting improvements in behavioral performance, and support the notion that the structural mechanisms underlying experience-dependent plasticity in the MC of intact mice learning a skilled reaching task (Xu et al., 2009, Yang & Gan, 2009), are similar with RT after ischemia. Furthermore, these data are in

agreement with previous results, which found that RT promotes increased synapse efficacy, as gauged by increased perforated synapse densities. (Kim et al., 2018).

In rats, RT after focal ischemia increases synaptic densities within layer V of the peri-infarct MC indicating that structural spine changes on dendrites in deeper layers are also associated with improvements in functional recovery with RT. Likewise, in the present study we found that RT also increases spine density on apical dendritic branches of layer V pyramidal neurons in layer II/III peri-infarct MC up to 8 weeks following artery-targeted photothrombosis. This is not surprising, given that in intact animals skilled reach training has been shown to increase dendritic branching and complexity of layer V pyramidal neurons (Greenough & Withers, 1985; Greenough 1989) as well as increase dendritic spines density on apical branches of these same cells in deeper cortical layers (Wang et al., 2012; Clark et al., 2018). These data support the notion that, similar to learning-induced structural plasticity in intact animals, RT-driven functional improvements in skilled reaching performance are likely the product of coordinated changes in synaptic connectivity across various neuronal and dendritic populations both within and beyond peri-infarct MC. Furthermore, these results highlight that monitoring spine dynamics on the superficial apical branches of cortical pyramidal neurons provide only a small window for understanding the structural mechanisms underlying functional improvements with RT.

Previously, we found that small motor cortical infarcts to MC (Ch. 3) created impairments in skilled reaching, but that recovered quickly, which is not ideal for examining the interaction between RT and recovery mechanisms associated with functional recovery over longer periods. In the present study, we demonstrated that artery-targeted photothrombosis can

be used to generate larger infarcts to MC that create lasting impairments in skilled reaching in mice. In both infarct groups, reaching performance remained lower, on average, over the 5 weeks, relative to sham. While significant improvements in skilled reaching were observed during week 1 in animals receiving RT, reaching performance never reached pre-operative or sham levels. These results indicated that artery-targeted photothrombosis is a useful model for studies examining the relationship between structural remodeling events and functional outcomes over the chronic post-infarct phase.

Although plenty of evidence from rodent studies suggests that ischemia instigates neovascularization, there is a considerable amount of variability in the magnitude and persistence reported across studies (Arenillas et al., 2007; Hayward et al., 2011; Martin et al., 2012; Lin et al., 2002; Lake et al., 2017; Ohab et al., 2006; Taguchi et al., 2009), and debate on whether early neovascularization yields lasting increases in vascular density. In the present study, we probed for neovascularization, using endothelial cell marker IB4, at 8 weeks post-infarct and found that vascular density in the ipsilesional cortex of animals that received artery-targeted photothrombosis was similar to sham. This was irrespective of distance from the lesion border. Previously, using the same detection method, we found that vascular density was increased at 2 weeks after photothrombotic infarcts. These results highlighted that while photothrombotic infarcts instigated neovascularization into the chronic post-infarct phase, there was no ongoing neovascularization by 8 weeks post-infarct. Likewise, *in vivo* studies of perfused vasculature report no evidence of neovascularization following McAO at later time points. (Mostany et al., 2010). Since vessel densities were not tracked over time, the present data are insufficient to rule

out the possibility that the lack of neovascularization at later time points is reflective of maturation of new vessels.

Previous studies have found that new born neuroblasts in peri-infarct cortex associate with endothelial cells in new, unperfused vessels several weeks after focal ischemia (Ohab et al., 2006; Taguchi et al., 2004; Thored et al., 2007) indicating that neovascularization could play a role in supporting cellular plasticity. Other studies have also reported that increases in vascular density 1 week after focal ischemia are correlated with increases in CBF (Lake et al., 2017), indicating that neovascularization could also be supporting the restoration of CBF to peri-infarct cortex. That we observed no increase in vascular density 8 weeks after focal ischemia suggested that while neovascularization may support improvements in CBF perfusion as well as cellular recovery in peri-infarct cortex early on after infarct, it is not needed to support mechanisms of recovery at later time points.

Very little is known about whether, or the extent to which, RT impacts neovascularization after ischemia. While activities such as voluntary running have been shown to instigate angiogenesis in intact MC (Adkins et al., 2006; Rhyu et al., 2010; Wallace et al., 2011), learning a skilled reaching task does not (Adkins et al., 2006). In the present study we found that vascular density in the ipsilesional cortex was similar between animals receiving RT compared to animals undergoing spontaneous recovery. These results indicated that improvements skilled reaching performance with RT are not associated with increased neovascularization at later time points. However, because vascular density was only assessed at 8 weeks post-infarct, these results cannot rule out the possibility that RT may alter the pattern of neovascularization early

after ischemia, nor the possibility that neovascularization at earlier time points could support early improvements in reaching performance.

The most effective treatments for motor impairments after infarct are rehabilitative training (RT) approaches, which are far from sufficient to improve functional outcomes. In rodents, RT has the capacity to increases synaptic densities and movement representations within peri-infarct MC that are associated with improved functional outcomes, but the time course over which this occurred was unknown. A better understanding of how RT drives coincidental changes in structural plasticity that are associated with improved outcomes is essential for uncovering time-dependencies in RT that could guide optimization of current therapeutic strategies. Here we present evidence that RT is associated with a greater persistence of new spines formed between post-infarct weeks 2 and 3, the extent of which correlates with recovery of skilled reaching performance. These data support the notion that ischemia-induced synaptic structural plasticity follows similar mechanisms as experience-dependent plasticity in the intact brain, and incite the possibility that the increased maintenance of this population of spines could be a structural substrate for functional improvements in skilled reaching behavior following ischemia.

Table 4.1 Sham Group Averages for all Reported Measures

Spine Turnover

Formation	***Baseline***	***1wk***	***2wk***	***3wk***	***4wk***	***5wk***
Group (n)						
Sham No RT (4)	2.3 ± 0.4	2.9 ± 0.7	2.4 ± 0.3	2.4 ± 0.4	2.1 ± 0.2	2.0 ± 0.1(3)
Sham RT (4)	1.9 ± 0.3	2.0 ± 0.3	1.8 ± 0.1	2.2 ± 0.3	1.8 ± 0.2	2.2 ± 0.3
Elimination						
Group						
Sham No RT (4)	2.6 ± 0.5	2.7 ± 0.2	2.3 ± 0.3	2.4 ± 0.3	3.0 ± 0.2	2.2 ± 0.1(3)
Sham RT (4)	2.2 ± 0.1	2.4 ± 0.4	1.9 ± 0.2	2.2 ± 0.4	2.2 ± 0.1	2.2 ± .4

Spine Maintenance

	1-2wk	**1-3wk**	**1-4wk**	**1-5wk**
Group(n)				
Sham No RT (3)	52.5 ± 7.3	25.0 ± 4.0	16.7 ± 16.7	16.7 ± 16.7 (2)
Sham RT (4)	58.4 ± 8.4	25.0 ± 8.3	16.7 ± 16.7 (3)	33.3 ± n/a (3)

	2-3wk	**2-4wk**	**2-5wk**
Group(n)			
Sham No RT (4)	52.5 ± 7.3	25.0 ± 4.0	16.7 ± 16.7 (3)
Sham RT (3)	75.0 ± 25.0	58.5 ± 8.5	33.3 ± n/a

	3-4wk	**4-5wk**
Group(n)		
Sham No RT (3)	47.2 ± 12.0	37.5 ± 12.5 (2)
Sham RT (2)	66.7 ± 33.3	16.6 ± 16.6

Table 4.1 Cont.

Post-infarct Reaching Performance

	3D	***1wk***	***2wk***	***3wk***	***4wk***	***5wk***
Sham No RT	.40 ± .04	.44 ± .03	.44 ± .02	.44 ± .04	.40 ± .03	.50 ± .07
Sham RT	.49 ± .07	.41 ± .03	.46 ± .05	.43 ± .05	.47 ± .04	.46 ± .05

Cortical Lesion Volume

group	**Male (n)**	**Female (n)**
Infarct RT	4.1 ± 0.2 (4)	2.5 ± 0.2 (4)
Infarct No RT	3.0 ± 0.3 (5)	4.1 ± 0.4 (4)
Sham	5.1 ± 1.8 (2)	5.9 ± 0.4 (4)

Density of IB4 Labeled Vessels

Group (n)	*100-500µm*	*500-900µm*	*Combined*	*100-500µm*	*500-900µm*
Sham RT	10.1 ± 1.0	8.9 ± 0.4	9.9 ± 1.0	9.8 ± 1.0	9.5 ± .7
Sham No RT	8.8 ± 0.5	8.9 ± 0.6	8.8 ± 0.6	9.5 ± 0.7	9.8 ± 1.1

Values are *M* ± *SE*

Table 4.2 Spine Turnover Disaggregated by Sex

	Baseline	***1wk***	***2wk***	***3wk***	***4wk***	***5wk***
Group (n)	**Formation**					
Infarct RT	**2.6 ± 0.3**	**5.4 ± 0.9**	**5.1 ± 0.9**	**5.5 ± 0.6**	**4.3 ± 0.7**	**3.0 ± 0.3**
Female (3)	2.3 ± .4	4.3 ± 1.2	4.0 ± 1.0	4.9 ± .8	4.1 ± 0.6	2.7 ± 0.1
Male (2)	3.1 ± .3	7.0 ± 0.2	7.0 ± 0.9	6.5 ± 0.2	4.7 ± 0.2	2.7 ± 3.2
Infarct No RT	**2.5 ± 0.9**	**6.3 ± 0.9**	**6.8 ± 0.9**	**5.9 ± 0.7**	**3.7 ± 0.4**	**5.7 ± 0.5**
Female (3)	2.6 ± 0.1	4.1 ± 0.6	6.2 ± 1.5	6.0 ± 1.3	4.2 ± 1.0	5.3 ± 1.2
Male (5)	2.4 ± 0.3	8.0 ± 0.6	7.1 ± 1.3	5.8 ± 1.0	3.5 ± 0.4	5.6 ± 0.2
Sham	**2.2 ± 0.3**	**2.7 ± 0.4**	**2.0 ± 0.3**	**2.4 ± 0.3**	**1.9 ± 0.3**	**2.1 ± 0.2**
Female (4)	2.2 ± 0.4	2.9 ± 0.7	1.9 ± 0.5	2.5 ± 0.6	2.1 ± 0.6	2.2 ± 0.4
Male (4)	2.2 ± 0.1	2.1 ± 0.3	2.2 ± 0.4	2.0 ± 0.4	1.6 ± 0.1	1.8 ± 0.1
Group (n)	**Elimination**					
Infarct RT	**2.5 ± 0.2**	**8.0 ± 1.5**	**7.2 ± 0.8**	**4.7 ± 0.4**	**3.6 ± 0.5**	**5.4 ± 0.8**
female	2.3 ± 0.4	6.8 ± 1.5	6.6 ± 1.2	3.7 ± 1.1	2.8 ± 0.1	3.0 ± 0.2
male	2.7 ± 0.1	10.0 ± 3.0	8.1± 0.4	6.2 ± 1.9	4.9 ± 0.2	2.9 ± 0.3
Infarct No RT	**2.5 ± 0.3**	**11.6 ± 0.9**	**7.1 ± 0.8**	**4.3 ± 0.4**	**6.3 ± 0.7**	**3.6 ± 0.5**
Female	2.6 ± 0.5	11.0 ± 2.3	7.1 ± 1.5	4.8 ± 0.7	4.8 ± 0.6	7.4 ± 0.2
male	2.4 ± 0.3	12.1 ± 0.5	7.1 ± 1.2	4.0 ± 0.6	7.3 ± 0.8	3.8 ± 0.6
Sham	**2.4 ± 0.4**	**2.7 ± 0.3**	**2.3 ± 0.4**	**2.3 ± 0.3**	**2.9 ± 0.3**	**2.1 ± 0.2**
Female	2.8 ± 0.8	2.6 ± 0.7	2.7 ± 0.7	2.2 ± 0.4	3.4 ± 0.4	1.9 ± 0.3
Male	2.0 ± 0.2	2.8 ± 0.1	2.0 ± 0.1	2.6 ± 0.3	2.3 ± 0.1	2.3 ± 0.3

Group Ns are the same for all time points unless denoted otherwise. Group Ns for elimination are the same as for formation. Values are *M* ± *SE*

Table 4.3 Spine Maintenance Disaggregated by Sex

Group(n)	1-2wk	1-3wk	1-4wk	1-5wk
Infarct RT	**68.5 ± 6.7**	**48.6 ± 1.9**	**48.6 ± 1.9**	**48.1 ± 1.9**
Female	58.5 ± 8.5 (2)	47.2 ± 2.8 (2)	47.2 ± 2.8 (2)	44.4 ±n/a (2)
Male	78.5 ± 1.5 (2)	50.0 ± 0 (2)	50.0 ± 0 (2)	50.0 ± 0 (2)
Infarct No RT	**67.7 ± 6.0**	**54.4 ± 8.7**	**36.7 ± 4.8**	**30.0 ± 5.6**
Female	70.5 ± 12.8 (2)	61.6 ± 21.7 (2)	45.0 ± 5.0 (2)	35.0 ± 15.0 (2)
Male	66.3 ± 6.9 (4)	50.8 ± 6.3 (4)	32.5 ± 4.3 (4)	28.3 ± 6.0 (4)
Sham	**51.2 ± 9.7**	**25.0 ± 8.7**	**11.1 ± 7.0**	**8.3 ± 11.7**
Female	58.4 ± 8.4 (2)	25.0 ± 8.3 (2)	16.7 ± 16.7 (2)	33.3 ± n/a (1)
Male	35.4 ± 5.3 (4)	14.6 ± 8.6 (4)	0 ± 0 (2)	0 ± 0 (2)

	2-3wk	2-4wk	2-5wk
Infarct RT	**72.4 ± 6.1**	**56.8 ± 3.2**	**56.0 ± 4.0**
Female	68.3 ± 9.3 (3)	53.3 ± 3.3 (3)	50.0 ± 0 (2)
Male	78.5 ± 7.1 (2)	62.0 ± 5.0 (2)	62.0 ± 5.0 (2)
Infarct No RT	**63.3 ± 3.4**	**42.6 ± 4.8**	**31.2 ±7.8**
Female	62.6 ± 6.4 (3)	49.0 ± 4.9 (3)	34.0 ± 11.6 (3)
Male	62.8 ± 8.6 (4)	31.9 ± 4.0 (4)	20.5 ± 3.8 (4)
Sham	**57.2 ± 10.0**	**34.3 ± 7.5**	**16.7 ± 10.4**
Female	70.0 ± 15.3 (3)	46.7 ± 3.3 (3)	25 ± 25 (3)
Male	44.4 ± 11.0 (3)	22.1 ± 11.1 (3)	0 ± 0 (3)

	3-4wk	*3-5wk*
Infarct RT	**71.2 ± 10.6**	**65.9 ± 11.8**
Female	81.8 ± 0 (2)	81.8 ± 0 (2)
Male	60.7 ± 10.6 (2)	50.0 ± 0 (2)
Infarct No RT	**59.2 ± 8.4**	**39.8 ± 6.6**
Female	66.8 ± 0.2 (2)	38.0 ± 4.7 (2)

Table 4.3 Cont.

Male	56.2 ± 9.9 (5)	40.5 ± 7.9 (5)
Sham	**56.2 ± 13.3**	**27.7 ± 10.4**
Female	37.5 ± 12.5 (2)	25.0 ± n/a (1)
Male	66.6 ± 19.3 (3)	27.6 ± 20.7 (3)

Values are *M* ± *SE*

Table 4.4 Post-infarct Behavioral Performance Disaggregated by Sex

	3D	*1wk*	*2wk*	*3wk*	*4wk*	*5wk*
Infarct RT	**.21 ± .04**	**.33 ± .01**	**.37 ± .05**	**.34 ± .01**	**.35 ± .03**	**.41 ± .03**
Female (3)	.25 ± .02	.33 ± .01	.34 ± .04	.33 ± .01	.35 ± .01	.40 ± .07
Male (2)	.17 ± .05	.34 ± .02	.40 ± .07	.36 ± .03	.36 ± .09	.42 ± .04
Infarct No RT	**.21 ± .04**	**.33 ± .01**	**.37 ± .05**	**.34 ± .01**	**.35 ± .03**	**.41 ± .03**
Female (3)	.25 ± .09	.23 ± .06	.31 ± .06	.39 ± .07	.43 ± .04	.45 ± .03
Male (3)	.23 ± .05	.15 ± .02	.20 ± .04	.23 ± .06	.25 ± .03	.42 ± .04
Sham	**.40 ± .04**	**.40 ± .03**	**.40 ± .03**	**.40 ± .03**	**.42 ± .03**	**.42 ± .05**
Female (5)	.38 ± .06	.45 ± .03	.39 ± .04	.44 ± .04	.45 ± .02	.43 ± .09
Male (5)	.38 ± .04	.33 ± .03	.36 ± .04	.38 ± .05	.40 ± .04	.36 ± .06

Values are *M* ± *SE*

Table 4.5 Cortical lesion volume disaggregated by sex.

group	**Male (n)**	**Female (n)**
Infarct RT	1.13 ± 0.61 (2)	0.84 ± 0.12 (3)
Infarct No RT	1.1 ± 0.18 (5)	0.95 ± 0.24 (4)
Sham	0.07 ± .14 (5)	-0.14 ± 0.1 (4)

Values are *M* ± *SE.*

Table 4.6 Area fractions of IB4-labeled blood vessels in ipsilesional and contralateral homotopic cortices disaggregated by sex

	Ipsi			***Contra***	
Group (n)	*100-500µm*	*500-900µm*	*Combined*	*100-500µm*	*500-900µm*
Infarct RT	**10.1 ± 0.8**	**10.4 ± 0.9**	**9.3 ± 0.9**	**9.8 ± .8**	**9.0 ± 0.5**
Female (3)	9.5 ± 0.2	8.3 ± 0.4	8.3 ± 0.1	9.2 ± 0.3	9.0 ± 0.8
Male (2)	11.2 ± 2.0	10.9 ± 2.1	10.7 ± 2.0	10.7 ± 2.0	8.9 ± 1.1
Infarct No RT	**9.4 ± 0.4**	**8.6 ± 0.8**	**8.5 ± 0.4**	**8.7 ± 0.8**	**8.3 ± 0.7**
Female (3)	9.5 ± 0.4	10.1 ± 0.3	8.2 ± 0.3	9.2 ± 0.3	9.0 ± 0.8
Male (4)	9.3 ± 0.6	8.0 ± 0.9	8.7 ± 0.6	10.7 ± 2.0	8.9 ± 1.1
Sham	**9.7 ± 0.8**	**8.9 ± 0.4**	**9.7 ± 0.8**	**9.5 ± 0.7**	**9.7 ± 0.7**
Female (4)	9.2 ± 0.3	9.3 ± 0.3	9.2 ± 0.3	9.2 ± 0.3	9.2 ± 0.6
Male (4)	10.1 ± 1.4	8.6 ± 0.6	9.9 ± 1.4	9.7 ± 1.1	9.8 ± 1.2

Values are *M* ± *SE*

Table 4.7 YFP and GFP averages for spine measures

Spine Turnover

Formation	***Baseline***	***1wk***	***2wk***	***3wk***	***4wk***	***5wk***
Group (n)						
GFP (3)	2.7 ± 0.6	8.9 ± 2.1	7.8 ± 0.6	6.1 ± 0.6	7.4 ± 0.6	4.1 ± 0.8
YFP (4)	2.7 ± 0.3	11.1 ± 0.6	7.0 ± 1.4	3.7 ± 0.1	6.5 ± 1.2	3.6 ± 1.3
Elimination						
Group						
GFP (3)	2.5 ± 0.3	12.0 ± 0.7	7.9 ± 0.7	6.8 ± 1.4	6.8 ± 0.7	3.8 ± 0.7
YFP (4)	2.6± 0.1	11.1 ± 1.4	7.0 ± 1.4	3.7 ± 0.3	6.4 ± 1.2	3.3 ± 0.2

Chapter 5: Discussion

Stroke remains one of the leading causes of long-term disability in adults leaving nearly 80% of stroke survivors with long-term functional impairments, and limited recovery without treatment (Kwakkel et al., 2003; Lai et al., 2002; Mozaffarian et al., 2016). Impairments in the upper-extremities are a particularly prevalent consequence of stroke. Rehabilitative training (RT) approaches are the main tools used for improving function in the impaired limb, but are far from sufficient to normalize function. Optimization of current therapeutic strategies could benefit from a more detailed understanding of the time course over which RT therapies drive coincidental brain plasticity.

From rodent models of ischemia-induced chronic upper-limb impairments, we know that RT of the impaired limb increases that limb's representation in remaining motor cortex (MC), indicating that it is sufficient to drive large scale structural and functional reorganization of peri-infarct MC (Butler et al., 2007; Nudo et al., 2007; Ward et al., 2003; Wittenberg et al., 2010). However, until now, the time course over which RT instigated functionally beneficial structural remodeling events was unclear. A main goal of these dissertation studies was to advance our basic understanding of structural synaptic responses to RT as a first step in understanding the itme course of RT-mediated structural remodeling events in order to identify sensitive periods when RT may be maximally beneficial for driving structural remodeling events associated with positive functional outcomes. Here we showed that in intact adult mice, skilled forelimb training increases spine formation and is followed by an equal and opposite increase in spine elimination, but newly formed spines are preferentially stabilized and correlated with improvements in performance of the task. These results suggested the possibility that maintenance of this

population of spines could represent a structural substrate for refinements in skill learning that are related to improved performance (Ch. 2).

Previous studies found that focal ischemia instigates profound and sustained increases in spine turnover (Brown et al., 2007; Brown et al. 2009; Mostany et al., 2010). Furthermore, in areas more devastated by the infarct, newly formed spines are preferentially stabilized compared to new spines formed in more distant regions (Mostany et al., 2010), indicating that new spine stabilization may be more beneficial for recovery in adjacent tissue regions that suffered more extensive damage (Mostany et al., 2010). However, whether behavioral experience could impact spine maintenance in more distant cortical regions was unknown. We found that RT on a skilled reaching task after motor-cortical infarcts increases the maintenance of new spines formed during weeks 2 and 3 post-infarct relative to animals undergoing spontaneous recovery, and that spine maintenance was associated with improvements in performance, assessed 4 weeks post-op (Ch. 4). These results indicate that RT improves function of skilled reaching performance after ischemia through similar structural mechanisms as skilled motor training in intact mice *in vivo*. Lastly, previous studies using photothrombosis have found increases in dendritic spine turnover are restricted to within a short range surrounding the infarct, likely a consequence of the small penumbra. Here we have shown that a modified version of photothrombosis that restricts laser illumination within arteries on the cortical surface increases the vascular penumbra, and is sufficient to drive increases in spine turnover over greater distances.

5.1 Experience-dependent structural synaptic plasticity in the intact brain

In the first study we sought to clarify the time course and extent of training-induced structural synaptic plasticityin the MC of adult mice, and its relevance to skill retention. Previous studies in young adult animals (Xu et al., 2009; Yang & Gan, 2009) found that skilled reach training drastically increased spine turnover within the trained MC starting as early as 1 day (Xu et al., 2009) after the onset of training. Furthermore, new spines formed early on during training were preferentially stabilized and more likely to persist, relative to spines in control animals, up to several months after training was terminated (Xu et. al., 2009). These results raised the possibility that this population of new spines represents a structural mechanism for the long-term retention of the newly acquired skill.

There is a wealth of evidence to suggest that while spine turnover in cortex is remarkably stable in adults, a subset of spines remains plastic and are sensitive to manipulations of experience (Grutzendler et al., 2002; Majewaska et al., 2006; Trachtenberg et al., 2002). Furthermore, the mechanisms that underlie experience-dependent plasticity in adolescence are similar, albeit to a lesser extent, as the mechanisms underlying experience-dependent plasticity observed in adolescence (Bavelier et al., 2010; Holtmaat & Svoboda, 2009; Zito & Svoboda, 2002). We found that, in adults, skilled reach training increases spine turnover in the trained MC similar to young adults; however, the time course over which these changes occur is delayed, as well as the extent of spine turnover. Notably, just as with training in adolescents, new spines formed early after the onset of training (Day 3) are preferentially stabilized, and more likely to persist until the final training session.

By comparing spine dynamics in animals that received 15 days of training with animals that stopped training after 3 days, when spine formation is highest, we were able to investigate the relationship between new spine maintenance and long-term retention of the task. Interestingly, we found spine turnover follows a similar pattern in animals that stop training after 3 days, but that new spines formed early on during training are no longer preferentially stabilized. These results indicated that continued training is necessary for the preferential stabilization of this population of new spines. However, animals that stopped training early were still able to perform the task just as well as they did on day 3 when tested again on day 15, indicating that the maintenance of new spines was not necessary for the maintenance of the skill. Instead, we found that new spine stabilization is a better predictor of performance gains, rather than skill maintenance, indicating that training-induced spine stabilization might be more strongly related to skill refinement instead of memory endurance.

Importantly, we also found that while training did not impact spine density on the population of dendrites in layer 1 imaged *in vivo*, it was associated with an increase in spine density on deeper apical dendrites within layer II/III of trained MC. These results indicate that there is variation in structural plasticity induced with skill learning on nearby dendritic subpopulations of the same neuronal population. These results highlight that while *in vivo* imaging is an invaluable approach for examining the structural basis of experience-dependent plasticity, spine alterations occurring on the superficial apical branches of cortical pyramidal neurons provide only a small window into training-induced structural plasticity, which was taken into consideration in Ch. 4, when examining the effects of ischemia on dendritic spine dynamics on this same population of dendrites *in vivo.*

5.2 A Photothrombotic Model that Better Approximates the Vascular Penumbra

The photothrombotic stroke model is particularly well-suited in rodent models of ischemia-induced upper-limb impairments because it creates focal infarcts that can be placed, with anatomical precision, over the MC to instigate impairments in skilled forelimb function (Carmichael et al., 2005; Kleim et al., 2007; Krakauer et al., 2006; Nudo et al., 1999). It can also easily be combined with *in vivo* imaging techniques, since ischemia can be induced through cranial windows (Carmichael et al., 2005). For these reasons, photothrombosis was the most appropriate choice for the studies outlined in Ch. 3 and 4. However, one main drawback of the model is that it creates relatively little ischemic penumbra (Carmichael et al., 2005), which makes it challenging to examine how vascular events within the penumbra contribute to structural remodeling events over longer periods. This was particularly concerning given that a main goal of the current dissertation studies was to understand the impact of the vascular penumbra on structural remodeling events. Therefore, in collaboration with a graduate student in Dr. Andrew Dunn's lab, we tested whether of a variation of the standard photothrombotic approach that confines laser illumination to a set of arterioles on the cortical surface, could better mimic the vascular penumbra in humans. To do this, we coupled a digital micromirror device (DMD) to the standard photothrombotic setup in order to produce patterned illumination on the surface of the cortex that could be shaped to match any expanse of identified surface arteries and/or arterioles.

By monitoring cerebral blood flow (CBF) during the acute phase after artery-targeted and traditional photothrombosis, we found that artery-targeted photothrombosis instigates more widespread and sustained increases in CBF relative to the traditional model. We took this as

evidence that artery-targeted photothrombosis better articulates the vascular penumbra compared to the standard model and is thus better suited for studies examining the impact of remodeling events within it on mechanisms of recovery over longer periods.

This model is not the first variation of photothrombosis that has been proposed. Other models include the photothrombotic-ring model (Gu et al., 1999), the single-point occlusion model (Schaffer et al., 2006; Sigler et al., 2008) and modified McAO through photothrombosis (Sugimori et al.,2004). The photothrombotic-ring model creates ring-shaped lesions of variable sizes, wherein the ischemic penumbra is fully contained within the core region, giving the experimenter better control over its size. However, progressive vasogenic edema quickly propagates inward from the ring towards the penumbra, limiting the ability to examine events in this tissue over longer periods, and therefore understand how events in the penumbra might impact mechanisms of recovery during the chronic post-stroke phase. In the single-point occlusion model, illumination through a two-photon microscope creates precise infarcts that are contained within individual arteries. An advantage of this model is that it can be used to occlude penetrating arterioles at a point just under the cortical surface, where they begin to dive into deeper cortical layers, to ensure downstream effects in connecting microvasculature. However, because illumination occurs at a single point, lesions can be relatively small and subject to the effects of collateral circulation from nearby arteries. In Ch. 3, we showed that artery-targeted photothrombosis could be used to simultaneously occlude branches of the middle-cerebral artery (MCA) draining into MC as well as branches of the anterior cerebral artery (ACA) in order to better control the effects of reperfusion at the time of ischemia.

The main advantage of the modified McAO model for photothrombosis, is that it gives the experimenter better control over infarct size, which is the main disadvantage of the model. McAO can also be used as an ischemia-reperfusion model, an advantage given the recent interest in therapeutic strategies to improve reperfusion after stroke (Fisher et al., 1997; Gravanis et al., 2008). However, reperfusion must be instigated by the experimenter, which is quite different than what is seen in humans where reperfusion unfolds gradually over time (Khatri et al., 2014; Sommer et al., 2017). We found that artery-targeted photothrombosis instigates delayed and spontaneous reperfusion, better approximating human stroke.

The results obtained in Ch. 3 indicated that artery-targeted photothrombosis creates a wider, more dispersed penumbra relative to the traditional model, and can be used as an ischemia-reperfusion model, while maintaining the ability to create focal infarcts do discrete regions of cortex. We took this as evidence that artery-targeted photothrombosis is better suited to model important aspects in human stroke, therefore improving its translational relevance as a pre-clinical stroke model.

5.3 The Impact of Artery-Targeted Photothrombosis on Vascular Remodeling

Vascular remodeling in peri-infarct cortex is multifaceted. In the more acute phases, surface arteries and arterioles may expand in diameter in order to increase collateral flow to the damaged tissue, and microvasculature has been shown to redirect blood flow towards the lesion site (Schaffer et al., 2006). Significant neovascularization has also been reported as early as 24 hours following ischemia (Lin et al., 2002). However, evidence for neovascularization in the chronic post-stroke phase is murky, and early increases in neovascularization do not necessarily lead to

lasting increases in vascular density (Wei et al., 2001). In the following dissertation studies, we chose to focus on understanding the impact of photothrombosis on neovascularization given that there is considerable debate over its extent, time course, and relevance to structural remodeling events in the chronic-post stroke phase (Arenillas et al., 2007; Brown et al., 2007; Hayashi et al., 2003; Hayward et al., 2011; Lake et al., 2017;Lin et al., 2008; Martin et al., 2012; Marti et al., 2000; Manoonkitiwongsa et al., 2001; Mostany et al. 2010; Prakash et al., 2013' Taguchi et al., 2004; Thored et al., 2007; Wei et al., 2001; Zhang et al., 2000).

Previous studies have found that increases in vascular density are correlated with increases in CBF 7 days after ischemia (Martin et al., 2012), indicating that neovascularization in the subacute phase following stroke could support improvements in regional CBF. In Ch. 3, we found that photothrombosis increases vascular density, assessed using endothelial cell label IB4, up to 2 weeks following ischemic infarcts. However, because we did not monitor CBF at this time point, the impact (if any) neovascularization had on CBF is unclear.

Results from several studies suggest that angiogenesis is transient, and only necessary for the removal of necrotic debris around the lesion site (Manoonkitiwongsta et al., 2001; Wei et al., 2001). While we were unable to determine the precise time course of neovascularization with just three time points (1,2 weeks and 8 weeks), in Ch. 4 we found that ongoing neovascularization needed to maintain increased vessel densities is no longer evident at 8 weeks following photothrombosis. These results could reflect retraction or pruning of vessels, as well as maturation of vessels from earlier time points.

Previous *in vivo* studies reported no evidence for neovascularization after photothrombosis (Brown et al., 2007; Mostany et al., 2010; Schrandt et al., 2014; Tennant et al.,

2013). One question that remained was whether the lack of neovascularization could be attributed to differences in the model, in detection methods, or both. All of these studies used intravascular labeling techniques with fluorescent dextran dyes that label blood plasma, and therefore cannot detect new unperfused vessels. By examining neovascularization using histological techniques similar to studies that reported neovascularization in other focal ischemia models (Hayward et al., 2011; Hayashi et al., 2003; Lin et al., 2002; Lin et al., 2008; Lake et al., 2017; Martin et al., 2012; Marti et al., 2000; Ohab et al., 2006; Taguchi et al., 2009;), we verified that photothrombosis does instigate neovascularization early on after ischemia that dissipates several months after stroke. Therefore, these data are in line with both previous studies using histological techniques, and within *vivo* studies reporting a lack of neovascularization at later time points. (Mostany et al., 2010).

5.4 The Impact of Artery-Targeted Photothrombosis on Neuronal Structural Plasticity

Very few studies have monitored the impact of focal ischemia on structural plasticity over time during the chronic post-stroke phase (Brown et al., 2007; Brown et al., 2009; Brown et al., 2010; Mostany et al., 2010). Brown and colleagues found that photothrombosis instigated robust increases in dendritic spine turnover that persist for up to 6 weeks after the infarct. However, increases in spine turnover were restricted to within the first 300 μm of cortex which is about the size of the ischemic penumbra (See Ch. 3). These results were quite different compared to Mostany and colleagues, who reported widespread increases in spine turnover even in more distant regions several mm from the infarct after McAO. In Ch. 4 we examined whether artery-targeted photothrombosis, which better approximates the ischemic penumbra in humans, could

increase the range with which increases in spine turnover were observed. We monitored spine changes on dendritic segments between 300 µm and 1mm from the occluded artery and found that artery-targeted photothrombosis instigates robust and widespread changes in dendritic spine turnover even at distant regions from the infarct. Similar to Brown and colleagues, we found that elevated spine turnover persists for up to 5 weeks (the final imaging time point) following ischemic infarcts. Although I was unable to accurately quantify CBF at 48 h post-infarct in the majoorty of animals utilized in Ch. 4 do to equipment malfunction, in the subset of animals I did collect data for, some degree of spontaneous reperfusion was evident in the occluded arteries at 48 h. These results are in line with results from Ch. 3 where I found that delayed spontaneous reperfusion of the occluded arteries occurred by 120 h post-infarct and indicated that enhanced spine turnover is maintained well after the re-establishment of CBF to the damaged region.

5.5 RT shapes ischemia-induced structural plasticity that supports functional outcomes

To our knowledge, these dissertation studies provide the first evidence of how rehabilitative training (RT) impacts structural brain plasticity over time in the living animal. Previous end-point studies have found that RT increases synaptic densities in peri-infarct MC (Jones et al., 1996), and increases the impaired limb's representation in spared MC, as assessed using intracortical microstimulation (Butler et al., 2007; Nudo et al., 2007; Ward et al., 2003; Wittenberg et al., 2010). However, previously lacking was an account of how structural plasticity unfolds over time, and in relation to functional improvements in forelimb function. In Ch. 4, we found that the pattern of spine turnover over the first several weeks is similar in animals receiving RT compared to animals undergoing spontaneously recovery. However, at

later time points (weeks 4 and 5), RT is associated with a return of spine elimination to near baseline levels. We found that this decrease in spine elimination is associated with an increase in the maintenance of new spines formed between weeks 1 and 3 during these same time points. Furthermore, the percent of new spines, formed during weeks 2 and 3, remaining until week 4 is positively correlated with improvements in skilled reaching performance. These results are suggestive of the possibility that preferential stabilization of this population of spines could represent a structural mechanism for functional improvements in skilled reaching.

5.6 Similarities and differences between ischemia-induced structural remodeling events and experience-dependent plasticity in the intact brain

It is thought that ischemia-induced structural plasticity follows similar principles as experience-dependent plasticity in the intact brain (Bavelier et al., 2010). By monitoring structural synaptic plasticity during skilled reach training in the intact MC of adult mice, and then again during RT after focal ischemia to MC, we were able to compare differences in structural plasticity mechanisms under normal circumstances and following brain damage. We found that following ischemia there are robust increases in spine turnover even without RT. These results support the idea that after ischemic damage, there is a capacity for heightened plasticity within peri-infarct cortex, and that the environment for experience-dependent plasticity might be more similar to what is observed in adolescence (Bavelier et al., 2010; Grutzendler et al. 2002; Holtmaat & Svoboda, 2009; Zito & Svoboda, 2002). Furthermore, the time period over which increases in spine turnover are observed is much greater in mice following ischemia compared with intact mice, which suggests that ischemia expands the time window over which structural plasticity unfolds.

Previous studies reported that ischemia instigates preferential stabilization of spines formed in the weeks following the infarct for up to several months in animals undergoing spontaneous recovery (Mostany et al., 2010). Our finding that RT is associated with greater maintenance of new spines formed between weeks 2 and 3 after infarcts, the extent to which is positively correlated with improvements in skilled reaching, parallels our previous finding in intact mice, that preferential stabilization of spines formed in response to training is associated with performance gains. Both animals receiving RT and animals undergoing spontaneous recovery show some degree of improvement in skilled reaching performance. However, the degree of improvement is greater with RT, and is associated with a greater maintenance of new spines formed after the infarct. These results iincite the possibility of an ongoing role for new spine maintenance in refinement strategies that underlie improvements in skilled forelimb use after ischemia. It is important to note that the use of the term functional recovery in the present dissertation studies should not be mistaken for true functional recovery (Murphy & Corbett, 2009) because we did compare the quality of forelimb movements made in mice after ischemia. Within the scope of these studies functional recovery refers to improved performance in skilled reaching behavior, which undoubtedly involves some form of compensation (Murphy & Corbett, 2009).

In Chapter 2, we found that despite differences in the stabilization of new spines, formed in response to training, on dendrites in layer 1 of superficial cortex with continued versus brief training, spine densities on apical dendrites of layer V pyramidal neurons increased under both conditions. These results indicated that there are dramatically different structural responses to skill learning on dendrites slightly deeper in cortex, and spine changes even on the same

dendritic population can vary greatly with dendritic location. Evidence from previous studies has shown that skilled training both before (Adkins et al., 2009; Greenough & Withers 1985 Kleim et al., 2002; Kleim et al., 2005; Wang et al., 2012; Withers & Greenough 1989) and after motor cortical infarcts (Brown et al., 2008; Jones et al., 1998; Kim et al., 2018; Kleim et al., 2003) can instigate changes in spine density and dendritic branching. Furthermore, recent *in vivo* evidence highlights that difference pyramidal cell populations within MC have different structural responses to skill training (Ma et al., 2016; Tija et al., 2017).

In rats, RT is sufficient to promote increases in synaptic densities within layer V of the spared MC. Furthermore, I found that spine density on the apical branches of layer V pyramidal neurons in layers II/III of spared MC is increased with RT up to 8 weeks post-infarct. Whether this increase in spine density persists over longer periods, and its relationship to functional recovery cannot be determined from the present studies. However, at the very least these results highlight that neuronal structural responses to skilled training both before and after brain damage are complex, and that this complex learning process undoubtedly requires the coordination of structural remodeling events on various dendritic and neuronal populations both between and beyond MC. Therefore, the suggestion that newly formed stabilized spines at weeks 2 and 3 post-infarct could signify a structural substrate underlying functional improvements in skilled reaching, represents just one small piece in our understanding of ischemia-induced structural plasticity.

5.7 Sex differences in ischemia-induced structural plasticity and functional outcomes

In clinical populations, stroke in women is associated with poorer functional outcomes compared to men. In rodents, previous studies have found that estrogen levels have a profound impact on stroke severity as well as functional recovery and are compounded by risk factors associated with aging (Appelros et al., 2009; Hall et al., 1991; Ikayed et al., 2008; Liu & McCullough, 2012; McCullough et al., 2003). Here, we did not find any notable sex differences in the pattern of results outlined in Chapters 3 or 4. However, it is important to note that the studies performed in Chapters 3 and 4 were underpowered for rigorously determining whether sex differences in neuronal and vascular structural remodeling, or functional outcomes exist after ischemia.

Recently, our lab has shown there are substantial reductions in the cortical territory devoted to forelimb movements beginning around middle age in female rats, which corresponds to the time when stroke incidence rises dramatically in women. These results indicate that there may be alterations in motor cortical plasticity in older females that could affect structural and functional responses to RT in the chronic post-stroke period, and could explain why no observable sex differences were seen in young adults. While we detected no obvious differences in post-ischemic CBF or neovascularization following ischemia in middle-aged animals, we cannot rule out the possibility that middle-age impacts other post-ischemic remodeling mechanisms. We chose to examine middle-aged animals because this is around the time when stroke incidence begins to rise dramatically, and when differences in post-stroke outcomes arise between men and women (Mozaffarian et al., 2016; Sommer et al., 2017). However, future studies should incorporate older *aged* animals.

5.8 Concluding Remarks and Future Directions

In the present dissertation studies, I provide a general framework for the impact of motor-cortical ischemia on neuronal and vascular structural remodeling events, and the impact of RT on these events. I present data on how structural remodeling events unfold over time following ischemia using a modified model of photothrombosis that is more sensitive to the impact of the ischemic penumbra on remodeling events during the chronic post-stroke phase, and we provide an account of how ischemia-induced remodeling events relate experience-dependent structural synaptic remodeling events. These data could be useful in beginning to understand how to optimize current clinical therapeutic strategies so that rehabilitative training can coincide with more dynamic stages of remodeling in the peri-infarct cortex.

Tied to optimizing current therapeutic strategies for improving functional outcomes after stroke, is the general consensus that RT therapies should be tailored to the individual. In order to expand on the results obtained from these dissertation studies, future studies should begin to examine the impact of risk factors affecting stroke outcomes, particularly sex and age, on patterns of structural plasticity and functional recovery. While we did not find any notable sex differences on patterns of CBF recovery, neovascularization, spine dynamics, or recovery of skilled reaching in the present studies, plenty of evidence suggests that sex and age interact in a way that inhibits functional recovery from stroke (Appelros et al., 2009; Hall et al., 1991; Ikayed et al., 2008; Liu & McCullough, 2012; McCullough et al., 2003).

Recent reports from the AHA have reported that nearly half of all stroke survivors are women, who suffer from worse functional outcomes compared to men. Furthermore, stroke

incidence rises dramatically after the age of 55, and prognosis declines steeply with increasing age (Mozaffarian et al., 2016). Despite this knowledge, the majority of stroke studies have been performed in young adult males. These studies provide a basic framework for which future studies can then incorporate the impact of important risk factors in stroke, in order to improve the translational relevance of these results.

References

Adkins, D. L., Boychuk, J., Remple, M. S., & Kleim, J. A. (2006). Motor training induces experience-specific patterns of plasticity across motor cortex and spinal cord. *Journal of Applied Physiology (Bethesda, Md.: 1985)*, *101*(6), 1776–1782. https://doi.org/10.1152/japplphysiol.00515.2006

Adkins, D. L., Bury, S. D., & Jones, T. A. (2002). Laminar-dependent dendritic spine alterations in the motor cortex of adult rats following callosal transection and forced forelimb use. *Neurobiology of Learning and Memory*, *78*(1), 35–52. https://doi.org/10.1006/nlme.2001.4045

Alaverdashvili, M., Moon, S.-K., Beckman, C. D., Virag, A., & Whishaw, I. Q. (2008). Acute but not chronic differences in skilled reaching for food following motor cortex devascularization vs. photothrombotic stroke in the rat. *Neuroscience*, *157*(2), 297–308. https://doi.org/10.1016/j.neuroscience.2008.09.015

Alkayed, N. J., Harukuni, I., Kimes, A. S., London, E. D., Traystman, R. J., & Hurn, P. D. (1998). Gender-linked brain injury in experimental stroke. *Stroke*, *29*(1), 159–165; discussion 166.

Anderson, R. E., Tan, W. K., & Meyer, F. B. (1999). Brain acidosis, cerebral blood flow, capillary bed density, and mitochondrial function in the ischemic penumbra. *Journal of Stroke and Cerebrovascular Diseases*, *8*(6), 368–379. https://doi.org/10.1016/S1052-3057(99)80044-5

Appelros, P., Stegmayr, B., & Terént, A. (2009). Sex differences in stroke epidemiology: a systematic review. *Stroke*, *40*(4), 1082–1090. https://doi.org/10.1161/STROKEAHA.108.540781

Arai, K., Jin, G., Navaratna, D., & Lo, E. H. (2009). Brain angiogenesis in developmental and pathological processes: neurovascular injury and angiogenic recovery after stroke. *The FEBS Journal*, *276*(17), 4644–4652. https://doi.org/10.1111/j.1742-4658.2009.07176.x

Arenillas, J. F., Sobrino, T., Castillo, J., & Dávalos, A. (2007). The role of angiogenesis in damage and recovery from ischemic stroke. *Current Treatment Options in Cardiovascular Medicine*, *9*(3), 205–212.

Astrup, J., Siesjö, B. K., & Symon, L. (1981). Thresholds in cerebral ischemia - the ischemic penumbra. *Stroke*, *12*(6), 723–725.

Ballermann, M., Metz, G. A., McKenna, J. E., Klassen, F., & Whishaw, I. Q. (2001). The pasta matrix reaching task: a simple test for measuring skilled reaching distance, direction, and dexterity in rats. *Journal of Neuroscience Methods*, *106*(1), 39–45.

Barber, P. A., Davis, S. M., Infeld, B., Baird, A. E., Donnan, G. A., Jolley, D., & Lichtenstein, M. (1998). Spontaneous Reperfusion After Ischemic Stroke Is Associated With Improved Outcome. *Stroke*, *29*(12), 2522–2528. https://doi.org/10.1161/01.STR.29.12.2522

Bavelier, D., Levi, D. M., Li, R. W., Dan, Y., & Hensch, T. K. (2010). Removing brakes on adult brain plasticity: from molecular to behavioral interventions. *The Journal of Neuroscience: The Official Journal of the Society for Neuroscience*, *30*(45), 14964–14971. https://doi.org/10.1523/JNEUROSCI.4812-10.2010

Beck, H., & Plate, K. H. (2009). Angiogenesis after cerebral ischemia. *Acta Neuropathologica*, *117*(5), 481–496. https://doi.org/10.1007/s00401-009-0483-6

Benjamin, E. J., Blaha, M. J., Chiuve, S. E., Cushman, M., Das, S. R., Deo, R., … Subcommittee, O. behalf of the A. H. A. S. C. and S. S. (2017). Heart Disease and Stroke Statistics—2017 Update:

A Report From the American Heart Association. *Circulation*, CIR.0000000000000485. https://doi.org/10.1161/CIR.0000000000000485

Biane, J. S., Scanziani, M., Tuszynski, M. H., & Conner, J. M. (2015). Motor cortex maturation is associated with reductions in recurrent connectivity among functional subpopulations and increases in intrinsic excitability. *The Journal of Neuroscience: The Official Journal of the Society for Neuroscience*, *35*(11), 4719–4728. https://doi.org/10.1523/JNEUROSCI.2792-14.2015

Biernaskie, J., & Corbett, D. (2001). Enriched rehabilitative training promotes improved forelimb motor function and enhanced dendritic growth after focal ischemic injury. *The Journal of Neuroscience: The Official Journal of the Society for Neuroscience*, *21*(14), 5272–5280.

Biernaskie, J., Corbett, D., Peeling, J., Wells, J., & Lei, H. (2001). A serial MR study of cerebral blood flow changes and lesion development following endothelin-1-induced ischemia in rats. *Magnetic Resonance in Medicine*, *46*(4), 827–830.

Bloss, E. B., Cembrowski, M. S., Karsh, B., Colonell, J., Fetter, R. D., & Spruston, N. (2018). Single excitatory axons form clustered synapses onto CA1 pyramidal cell dendrites. *Nature Neuroscience*, *21*(3), 353–363. https://doi.org/10.1038/s41593-018-0084-6

Bosch, M., & Hayashi, Y. (2012). Structural plasticity of dendritic spines. *Current Opinion in Neurobiology*, *22*(3), 383–388. https://doi.org/10.1016/j.conb.2011.09.002

Bourne, J. N., & Harris, K. M. (2008). Balancing structure and function at hippocampal dendritic spines. *Annual Review of Neuroscience*, *31*, 47–67. https://doi.org/10.1146/annurev.neuro.31.060407.125646

Braeuninger, S., & Kleinschnitz, C. (2009). Rodent models of focal cerebral ischemia: procedural pitfalls and translational problems. *Experimental & Translational Stroke Medicine*, *1*, 8. https://doi.org/10.1186/2040-7378-1-8

Brann, D., Raz, L., Wang, R., Vadlamudi, R., & Zhang, Q. (2012). Oestrogen signalling and neuroprotection in cerebral ischaemia. *Journal of Neuroendocrinology*, *24*(1), 34–47. https://doi.org/10.1111/j.1365-2826.2011.02185.x

Branston, N. M., Symon, L., Crockard, H. A., & Pasztor, E. (1974). Relationship between the cortical evoked potential and local cortical blood flow following acute middle cerebral artery occlusion in the baboon. *Experimental Neurology*, *45*(2), 195–208.

Brown, A. W., Marlowe, K. J., & Bjelke, B. (2003). Age effect on motor recovery in a post-acute animal stroke model. *Neurobiology of Aging*, *24*(4), 607–614.

Brown, C. E., Boyd, J. D., & Murphy, T. H. (2010). Longitudinal in vivo imaging reveals balanced and branch-specific remodeling of mature cortical pyramidal dendritic arbors after stroke. *Journal of Cerebral Blood Flow and Metabolism: Official Journal of the International Society of Cerebral Blood Flow and Metabolism*, *30*(4), 783–791. https://doi.org/10.1038/jcbfm.2009.241

Brown, C. E., Li, P., Boyd, J. D., Delaney, K. R., & Murphy, T. H. (2007). Extensive turnover of dendritic spines and vascular remodeling in cortical tissues recovering from stroke. *The Journal of Neuroscience: The Official Journal of the Society for Neuroscience*, *27*(15), 4101–4109. https://doi.org/10.1523/JNEUROSCI.4295-06.2007

Brown, C. E., Wong, C., & Murphy, T. H. (2008). Rapid morphologic plasticity of peri-infarct dendritic spines after focal ischemic stroke. *Stroke*, *39*(4), 1286–1291. https://doi.org/10.1161/STROKEAHA.107.498238

Brown, C. M., Suzuki, S., Jelks, K. A. B., & Wise, P. M. (2009). Estradiol is a potent protective, restorative, and trophic factor after brain injury. *Seminars in Reproductive Medicine*, *27*(3), 240–249. https://doi.org/10.1055/s-0029-1216277

Butler, A. J., & Wolf, S. L. (2007). Putting the brain on the map: use of transcranial magnetic stimulation to assess and induce cortical plasticity of upper-extremity movement. *Physical Therapy*, *87*(6), 719–736. https://doi.org/10.2522/ptj.20060274

Canese, R., Fortuna, S., Lorenzini, P., Podo, F., & Michalek, H. (1998). Transient global brain ischemia in young and aged rats: differences in severity and progression, but not localisation, of lesions evaluated by magnetic resonance imaging. *Magma (New York, N.Y.)*, *7*(1), 28–34.

Canese, R., Lorenzini, P., Fortuna, S., Volpe, M. T., Giannini, M., Podo, F., & Michalek, H. (2004). Age-dependent MRI-detected lesions at early stages of transient global ischemia in rat brain. *Magma (New York, N.Y.)*, *17*(3–6), 109–116. https://doi.org/10.1007/s10334-004-0072-6

Carmichael, S. T. (2005). Rodent models of focal stroke: size, mechanism, and purpose. *NeuroRx: The Journal of the American Society for Experimental NeuroTherapeutics*, *2*(3), 396–409. https://doi.org/10.1602/neurorx.2.3.396

Carmichael, S. T. (2006). Cellular and molecular mechanisms of neural repair after stroke: making waves. *Annals of Neurology*, *59*(5), 735–742. https://doi.org/10.1002/ana.20845

Carmichael, S. T., Archibeque, I., Luke, L., Nolan, T., Momiy, J., & Li, S. (2005). Growth-associated gene expression after stroke: evidence for a growth-promoting region in peri-infarct cortex. *Experimental Neurology*, *193*(2), 291–311. https://doi.org/10.1016/j.expneurol.2005.01.004

Caroni, P., Donato, F., & Muller, D. (2012). Structural plasticity upon learning: regulation and functions. *Nature Reviews. Neuroscience*, *13*(7), 478–490. https://doi.org/10.1038/nrn3258

Castro-Alamancos, M. A., & Borrel, J. (1995). Functional recovery of forelimb response capacity after forelimb primary motor cortex damage in the rat is due to the reorganization of adjacent areas of cortex. *Neuroscience*, *68*(3), 793–805.

Chen, C., Parsons, M. W., Clapham, M., Oldmeadow, C., Levi, C. R., Lin, L., … Bivard, A. (2017). Influence of Penumbral Reperfusion on Clinical Outcome Depends on Baseline Ischemic Core Volume. *Stroke*, *48*(10), 2739–2745. https://doi.org/10.1161/STROKEAHA.117.018587

Chen, C.-C., Lu, J., & Zuo, Y. (2014). Spatiotemporal dynamics of dendritic spines in the living brain. *Frontiers in Neuroanatomy*, *8*. https://doi.org/10.3389/fnana.2014.00028

Chen, J. L., & Nedivi, E. (2010). Neuronal structural remodeling: is it all about access? *Current Opinion in Neurobiology*, *20*(5), 557–562. https://doi.org/10.1016/j.conb.2010.06.002

Chen, S. X., Kim, A. N., Peters, A. J., & Komiyama, T. (2015). Subtype-specific plasticity of inhibitory circuits in motor cortex during motor learning. *Nature Neuroscience*, *18*(8), 1109–1115. https://doi.org/10.1038/nn.4049

Cichon, J., & Gan, W.-B. (2015). Branch-specific dendritic Ca(2+) spikes cause persistent synaptic plasticity. *Nature*, *520*(7546), 180–185. https://doi.org/10.1038/nature14251

Clarkson, A. N., López-Valdés, H. E., Overman, J. J., Charles, A. C., Brennan, K. C., & Thomas Carmichael, S. (2013). Multimodal examination of structural and functional remapping in the mouse photothrombotic stroke model. *Journal of Cerebral Blood Flow and Metabolism: Official Journal of the International Society of Cerebral Blood Flow and Metabolism*, *33*(5), 716–723. https://doi.org/10.1038/jcbfm.2013.7

Conner, J. M., Chiba, A. A., & Tuszynski, M. H. (2005). The basal forebrain cholinergic system is essential for cortical plasticity and functional recovery following brain injury. *Neuron*, *46*(2), 173–179. https://doi.org/10.1016/j.neuron.2005.03.003

Cramer, S. C., Sur, M., Dobkin, B. H., O'Brien, C., Sanger, T. D., Trojanowski, J. Q., … Vinogradov, S. (2011). Harnessing neuroplasticity for clinical applications. *Brain: A Journal of Neurology*, *134*(Pt 6), 1591–1609. https://doi.org/10.1093/brain/awr039

Dancause, N., Barbay, S., Frost, S. B., Plautz, E. J., Chen, D., Zoubina, E. V., … Nudo, R. J. (2005). Extensive cortical rewiring after brain injury. *The Journal of Neuroscience: The Official Journal of the Society for Neuroscience*, *25*(44), 10167–10179. https://doi.org/10.1523/JNEUROSCI.3256-05.2005

Davis, M. A., Gagnon, L., Boas, D. A., & Dunn, A. K. (2016). Sensitivity of laser speckle contrast imaging to flow perturbations in the cortex. *Biomedical Optics Express*, *7*(3), 759–775. https://doi.org/10.1364/BOE.7.000759

Davis, M., Mendelow, A. D., Perry, R. H., Chambers, I. R., & James, O. F. (1995). Experimental stroke and neuroprotection in the aging rat brain. *Stroke*, *26*(6), 1072–1078.

Davis, S., & Donnan, G. A. (2014). Time Is Penumbra: Imaging, Selection and Outcome. *Cerebrovascular Diseases*, *38*(1), 59–72. https://doi.org/10.1159/000365503

De Roo, M., Klauser, P., Garcia, P. M., Poglia, L., & Muller, D. (2008). Spine dynamics and synapse remodeling during LTP and memory processes. *Progress in Brain Research*, *169*, 199–207. https://doi.org/10.1016/S0079-6123(07)00011-8

del Zoppo, G. J., & Mabuchi, T. (2003). Cerebral microvessel responses to focal ischemia. *Journal of Cerebral Blood Flow and Metabolism: Official Journal of the International Society of Cerebral Blood Flow and Metabolism*, *23*(8), 879–894. https://doi.org/10.1097/01.WCB.0000078322.96027.78

Diedrichsen, J., & Kornysheva, K. (2015). Motor skill learning between selection and execution. *Trends in Cognitive Sciences*, *19*(4), 227–233. https://doi.org/10.1016/j.tics.2015.02.003

Dietrich, W. D., Ginsberg, M. D., Busto, R., & Watson, B. D. (1986). Photochemically induced cortical infarction in the rat. 2. Acute and subacute alterations in local glucose utilization. *Journal of Cerebral Blood Flow and Metabolism: Official Journal of the International Society of Cerebral Blood Flow and Metabolism*, *6*(2), 195–202. https://doi.org/10.1038/jcbfm.1986.32

Dong, Y., Winstein, C. J., Albistegui-DuBois, R., & Dobkin, B. H. (2007). Evolution of FMRI activation in the perilesional primary motor cortex and cerebellum with rehabilitation training-related motor gains after stroke: a pilot study. *Neurorehabilitation and Neural Repair*, *21*(5), 412–428. https://doi.org/10.1177/1545968306298598

Donnan, G. A., & Davis, S. M. (2002). Neuroimaging, the ischaemic penumbra, and selection of patients for acute stroke therapy. *The Lancet. Neurology*, *1*(7), 417–425.

Dunn, A. K. (2012). Laser speckle contrast imaging of cerebral blood flow. *Annals of Biomedical Engineering*, *40*(2), 367–377. https://doi.org/10.1007/s10439-011-0469-0

Eilaghi, A., Brooks, J., d'Esterre, C., Zhang, L., Swartz, R. H., Lee, T.-Y., & Aviv, R. I. (2013). Reperfusion Is a Stronger Predictor of Good Clinical Outcome than Recanalization in Ischemic Stroke. *Radiology*, *269*(1), 240–248. https://doi.org/10.1148/radiol.13122327

Endres, M., Engelhardt, B., Koistinaho, J., Lindvall, O., Meairs, S., Mohr, J. P., … Dirnagl, U. (2008). Improving outcome after stroke: overcoming the translational roadblock.

Cerebrovascular Diseases (Basel, Switzerland), *25*(3), 268–278. https://doi.org/10.1159/000118039

Enright, L. E., Zhang, S., & Murphy, T. H. (2007). Fine mapping of the spatial relationship between acute ischemia and dendritic structure indicates selective vulnerability of layer V neuron dendritic tufts within single neurons in vivo. *Journal of Cerebral Blood Flow and Metabolism: Official Journal of the International Society of Cerebral Blood Flow and Metabolism*, *27*(6), 1185–1200. https://doi.org/10.1038/sj.jcbfm.9600428

Fan, Y., Shen, F., Frenzel, T., Zhu, W., Ye, J., Liu, J., … Yang, G.-Y. (2010). Endothelial progenitor cell transplantation improves long-term stroke outcome in mice. *Annals of Neurology*, *67*(4), 488–497. https://doi.org/10.1002/ana.21919

Feldman, D. E. (2009). Synaptic mechanisms for plasticity in neocortex. *Annual Review of Neuroscience*, *32*, 33–55. https://doi.org/10.1146/annurev.neuro.051508.135516

Ferrer, I., & Planas, A. M. (2003). Signaling of cell death and cell survival following focal cerebral ischemia: life and death struggle in the penumbra. *Journal of Neuropathology and Experimental Neurology*, *62*(4), 329–339.

Fisher, M. (2004). The ischemic penumbra: identification, evolution and treatment concepts. *Cerebrovascular Diseases (Basel, Switzerland)*, *17 Suppl 1*, 1–6. https://doi.org/10.1159/000074790

Font, M. A., Arboix, A., & Krupinski, J. (2010). Angiogenesis, Neurogenesis and Neuroplasticity in Ischemic Stroke. *Current Cardiology Reviews*, *6*(3), 238–244. https://doi.org/10.2174/157340310791658802

Frauenknecht, K., Diederich, K., Leukel, P., Bauer, H., Schäbitz, W.-R., Sommer, C. J., & Minnerup, J. (2016). Functional Improvement after Photothrombotic Stroke in Rats Is Associated with Different Patterns of Dendritic Plasticity after G-CSF Treatment and G-CSF Treatment Combined with Concomitant or Sequential Constraint-Induced Movement Therapy. *PloS One*, *11*(1), e0146679. https://doi.org/10.1371/journal.pone.0146679

Frost, S. B., Barbay, S., Friel, K. M., Plautz, E. J., & Nudo, R. J. (2003). Reorganization of remote cortical regions after ischemic brain injury: a potential substrate for stroke recovery. *Journal of Neurophysiology*, *89*(6), 3205–3214. https://doi.org/10.1152/jn.01143.2002

Fu, M., Yu, X., Lu, J., & Zuo, Y. (2012). Repetitive motor learning induces coordinated formation of clustered dendritic spines in vivo. *Nature*, *483*(7387), 92–95. https://doi.org/10.1038/nature10844

Fu, M., & Zuo, Y. (2011). Experience-dependent Structural Plasticity in the Cortex. *Trends in Neurosciences*, *34*(4), 177–187. https://doi.org/10.1016/j.tins.2011.02.001

Gertz, K., Priller, J., Kronenberg, G., Fink, K. B., Winter, B., Schröck, H., … Endres, M. (2006). Physical activity improves long-term stroke outcome via endothelial nitric oxide synthase-dependent augmentation of neovascularization and cerebral blood flow. *Circulation Research*, *99*(10), 1132–1140. https://doi.org/10.1161/01.RES.0000250175.14861.77

Gibb, R. L., Gonzalez, C. L. R., Wegenast, W., & Kolb, B. E. (2010). Tactile stimulation promotes motor recovery following cortical injury in adult rats. *Behavioural Brain Research*, *214*(1), 102–107. https://doi.org/10.1016/j.bbr.2010.04.008

Gipson, C. D., & Olive, M. F. (2017). Structural and functional plasticity of dendritic spines - root or result of behavior? *Genes, Brain, and Behavior*, *16*(1), 101–117. https://doi.org/10.1111/gbb.12324

Gloor, C., Luft, A. R., & Hosp, J. A. (2015). Biphasic plasticity of dendritic fields in layer V motor neurons in response to motor learning. *Neurobiology of Learning and Memory*, *125*, 189–194. https://doi.org/10.1016/j.nlm.2015.08.009

Go, A. S., Mozaffarian, D., Roger, V. L., Benjamin, E. J., Berry, J. D., Borden, W. B., … Subcommittee, on behalf of the A. H. A. S. C. and S. S. (2012). Heart Disease and Stroke Statistics—2013 Update A Report From the American Heart Association. *Circulation*, CIR.0b013e31828124ad. https://doi.org/10.1161/CIR.0b013e31828124ad

Greenough, W. T., Hwang, H. M., & Gorman, C. (1985). Evidence for active synapse formation or altered postsynaptic metabolism in visual cortex of rats reared in complex environments. *Proceedings of the National Academy of Sciences of the United States of America*, *82*(13), 4549–4552.

Greenough, W. T., Larson, J. R., & Withers, G. S. (1985). Effects of unilateral and bilateral training in a reaching task on dendritic branching of neurons in the rat motor-sensory forelimb cortex. *Behavioral and Neural Biology*, *44*(2), 301–314.

Grutzendler, J., Kasthuri, N., & Gan, W.-B. (2002). Long-term dendritic spine stability in the adult cortex. *Nature*, *420*(6917), 812–816. https://doi.org/10.1038/nature01276

Gu, W. G., Brännström, T., Jiang, W., & Wester, P. (1999). A photothrombotic ring stroke model in rats with remarkable morphological tissue recovery in the region at risk. *Experimental Brain Research*, *125*(2), 171–183.

Hall, E. D., Pazara, K. E., & Linseman, K. L. (1991). Sex differences in postischemic neuronal necrosis in gerbils. *Journal of Cerebral Blood Flow and Metabolism: Official Journal of the International Society of Cerebral Blood Flow and Metabolism*, *11*(2), 292–298. https://doi.org/10.1038/jcbfm.1991.61

Harms, K. J., & Dunaevsky, A. (2007). Dendritic spine plasticity: looking beyond development. *Brain Research*, *1184*, 65–71. https://doi.org/10.1016/j.brainres.2006.02.094

Harms, K. J., Rioult-Pedotti, M. S., Carter, D. R., & Dunaevsky, A. (2008). Transient spine expansion and learning-induced plasticity in layer 1 primary motor cortex. *The Journal of Neuroscience: The Official Journal of the Society for Neuroscience*, *28*(22), 5686–5690. https://doi.org/10.1523/JNEUROSCI.0584-08.2008

Hayashi, T., Noshita, N., Sugawara, T., & Chan, P. H. (2003). Temporal profile of angiogenesis and expression of related genes in the brain after ischemia. *Journal of Cerebral Blood Flow and Metabolism: Official Journal of the International Society of Cerebral Blood Flow and Metabolism*, *23*(2), 166–180. https://doi.org/10.1097/01.WCB.0000041283.53351.CB

Hayashi-Takagi, A., Yagishita, S., Nakamura, M., Shirai, F., Wu, Y. I., Loshbaugh, A. L., … Kasai, H. (2015). Labelling and optical erasure of synaptic memory traces in the motor cortex. *Nature*, *525*(7569), 333–338. https://doi.org/10.1038/nature15257

Heiss, W. D., & Rosner, G. (1983). Functional recovery of cortical neurons as related to degree and duration of ischemia. *Annals of Neurology*, *14*(3), 294–301. https://doi.org/10.1002/ana.410140307

Heiss, W.-D. (2011). The Ischemic Penumbra: Correlates in Imaging and Implications for Treatment of Ischemic Stroke. *Cerebrovascular Diseases*, *32*(4), 307–320. https://doi.org/10.1159/000330462

Henery, C. C., & Mayhew, T. M. (1989). The cerebrum and cerebellum of the fixed human brain: efficient and unbiased estimates of volumes and cortical surface areas. *Journal of Anatomy*, *167*, 167–180.
Herson, P. S., & Traystman, R. J. (2014). Animal models of stroke: translational potential at present and in 2050. *Future Neurology*, *9*(5), 541–551. https://doi.org/10.2217/fnl.14.44
Hildebrandt, I. J., Su, H., & Weber, W. A. (2008). Anesthesia and Other Considerations for in Vivo Imaging of Small Animals. *ILAR Journal*, *49*(1), 17–26. https://doi.org/10.1093/ilar.49.1.17
Hofer, S. B., Mrsic-Flogel, T. D., Bonhoeffer, T., & Hübener, M. (2009). Experience leaves a lasting structural trace in cortical circuits. *Nature*, *457*(7227), 313–317. https://doi.org/10.1038/nature07487
Holtmaat, A., De Paola, V., Wilbrecht, L., & Knott, G. W. (2008). Imaging of experience-dependent structural plasticity in the mouse neocortex in vivo. *Behavioural Brain Research*, *192*(1), 20–25. https://doi.org/10.1016/j.bbr.2008.04.005
Holtmaat, A. J. G. D., Trachtenberg, J. T., Wilbrecht, L., Shepherd, G. M., Zhang, X., Knott, G. W., & Svoboda, K. (2005). Transient and persistent dendritic spines in the neocortex in vivo. *Neuron*, *45*(2), 279–291. https://doi.org/10.1016/j.neuron.2005.01.003
Holtmaat, Anthony, & Svoboda, K. (2009). Experience-dependent structural synaptic plasticity in the mammalian brain. *Nature Reviews. Neuroscience*, *10*(9), 647–658. https://doi.org/10.1038/nrn2699
Holtmaat, Anthony, Wilbrecht, L., Knott, G. W., Welker, E., & Svoboda, K. (2006). Experience-dependent and cell-type-specific spine growth in the neocortex. *Nature*, *441*(7096), 979–983. https://doi.org/10.1038/nature04783
Hubel, D. H., & Wiesel, T. N. (n.d.). The period of susceptibility to the physiological effects of unilateral eye closure in kittens. *The Journal of Physiology*, *206*(2), 419–436. https://doi.org/10.1113/jphysiol.1970.sp009022
Hubel, D. H., Wiesel, T. N., & LeVay, S. (1977). Plasticity of ocular dominance columns in monkey striate cortex. *Philosophical Transactions of the Royal Society of London. Series B, Biological Sciences*, *278*(961), 377–409.
Hubel, David H, & Wiesel, T. N. (1998). Early Exploration of the Visual Cortex. *Neuron*, *20*(3), 401–412. https://doi.org/10.1016/S0896-6273(00)80984-8
Ito, U., Kuroiwa, T., Nagasao, J., Kawakami, E., & Oyanagi, K. (2006). Temporal profiles of axon terminals, synapses and spines in the ischemic penumbra of the cerebral cortex: ultrastructure of neuronal remodeling. *Stroke*, *37*(8), 2134–2139. https://doi.org/10.1161/01.STR.0000231875.96714.b1
Jones, T. A., Chu, C. J., Grande, L. A., & Gregory, A. D. (1999). Motor skills training enhances lesion-induced structural plasticity in the motor cortex of adult rats. *The Journal of Neuroscience: The Official Journal of the Society for Neuroscience*, *19*(22), 10153–10163.
Jones, T. H., Morawetz, R. B., Crowell, R. M., Marcoux, F. W., FitzGibbon, S. J., DeGirolami, U., & Ojemann, R. G. (1981). Thresholds of focal cerebral ischemia in awake monkeys. *Journal of Neurosurgery*, *54*(6), 773–782. https://doi.org/10.3171/jns.1981.54.6.0773
Jones, Theresa A, Klintsova, A. Y., Kilman, V. L., Sirevaag, A. M., & Greenough, W. T. (1997). Induction of Multiple Synapses by Experience in the Visual Cortex of Adult Rats. *Neurobiology of Learning and Memory*, *68*(1), 13–20. https://doi.org/10.1006/nlme.1997.3774

Jørgensen, H. S., Sperling, B., Nakayama, H., Raaschou, H. O., & Olsen, T. S. (1994). Spontaneous Reperfusion of Cerebral Infarcts in Patients With Acute Stroke: Incidence, Time Course, and Clinical Outcome in the Copenhagen Stroke Study. *Archives of Neurology*, *51*(9), 865–873. https://doi.org/10.1001/archneur.1994.00540210037011

Jørgensen H, Sperling B, Nakayama H, Raaschou H, & Olsen T. (1994). Spontaneous reperfusion of cerebral infarcts in patients with acute stroke: Incidence, time course, and clinical outcome in the copenhagen stroke study. *Archives of Neurology*, *51*(9), 865–873. https://doi.org/10.1001/archneur.1994.00540210037011

Kapinya, K. J., Löwl, D., Fütterer, C., Maurer, M., Waschke, K. F., Isaev, N. K., & Dirnagl, U. (2002). Tolerance against ischemic neuronal injury can be induced by volatile anesthetics and is inducible NO synthase dependent. *Stroke*, *33*(7), 1889–1898.

Kasai, H., Hayama, T., Ishikawa, M., Watanabe, S., Yagishita, S., & Noguchi, J. (2010). Learning rules and persistence of dendritic spines. *The European Journal of Neuroscience*, *32*(2), 241–249. https://doi.org/10.1111/j.1460-9568.2010.07344.x

Kawaguchi, M., Drummond, J. C., Cole, D. J., Kelly, P. J., Spurlock, M. P., & Patel, P. M. (2004). Effect of isoflurane on neuronal apoptosis in rats subjected to focal cerebral ischemia. *Anesthesia and Analgesia*, *98*(3), 798–805, table of contents.

Kazmi, S. M. S., Parthasarthy, A. B., Song, N. E., Jones, T. A., & Dunn, A. K. (2013). Chronic imaging of cortical blood flow using Multi-Exposure Speckle Imaging. *Journal of Cerebral Blood Flow & Metabolism*, *33*(6), 798–808. https://doi.org/10.1038/jcbfm.2013.57

Kazmi, S. S., Richards, L. M., Schrandt, C. J., Davis, M. A., & Dunn, A. K. (2015). Expanding Applications, Accuracy, and Interpretation of Laser Speckle Contrast Imaging of Cerebral Blood Flow. *Journal of Cerebral Blood Flow & Metabolism*, *35*(7), 1076–1084. https://doi.org/10.1038/jcbfm.2015.84

Khatri, P., Yeatts, S. D., Mazighi, M., Broderick, J. P., Liebeskind, D. S., Demchuk, A. M., … IMS III Trialists. (2014). Time to angiographic reperfusion and clinical outcome after acute ischaemic stroke: an analysis of data from the Interventional Management of Stroke (IMS III) phase 3 trial. *The Lancet. Neurology*, *13*(6), 567–574. https://doi.org/10.1016/S1474-4422(14)70066-3

Kleim, J. A., Lussnig, E., Schwarz, E. R., Comery, T. A., & Greenough, W. T. (1996). Synaptogenesis and Fos expression in the motor cortex of the adult rat after motor skill learning. *The Journal of Neuroscience: The Official Journal of the Society for Neuroscience*, *16*(14), 4529–4535.

Kleim, Jeffrey A., Barbay, S., Cooper, N. R., Hogg, T. M., Reidel, C. N., Remple, M. S., & Nudo, R. J. (2002). Motor learning-dependent synaptogenesis is localized to functionally reorganized motor cortex. *Neurobiology of Learning and Memory*, *77*(1), 63–77. https://doi.org/10.1006/nlme.2000.4004

Kleim, Jeffrey A., Jones, T. A., & Schallert, T. (2003). Motor enrichment and the induction of plasticity before or after brain injury. *Neurochemical Research*, *28*(11), 1757–1769.

Knott, G., & Holtmaat, A. (2008). Dendritic spine plasticity--current understanding from in vivo studies. *Brain Research Reviews*, *58*(2), 282–289. https://doi.org/10.1016/j.brainresrev.2008.01.002

Knott, G. W., Holtmaat, A., Wilbrecht, L., Welker, E., & Svoboda, K. (2006). Spine growth precedes synapse formation in the adult neocortex in vivo. *Nature Neuroscience*, *9*(9), 1117–1124. https://doi.org/10.1038/nn1747

Koellhoffer, E. C., & McCullough, L. D. (2013). The Effects of Estrogen in Ischemic Stroke. *Translational Stroke Research*, *4*(4), 390–401. https://doi.org/10.1007/s12975-012-0230-5
Kolb, B., Cioe, J., & Comeau, W. (2008). Contrasting effects of motor and visual spatial learning tasks on dendritic arborization and spine density in rats. *Neurobiology of Learning and Memory*, *90*(2), 295–300. https://doi.org/10.1016/j.nlm.2008.04.012
Krakauer, J. W., Carmichael, S. T., Corbett, D., & Wittenberg, G. F. (2012). Getting neurorehabilitation right: what can be learned from animal models? *Neurorehabilitation and Neural Repair*, *26*(8), 923–931. https://doi.org/10.1177/1545968312440745
Kwakkel, G., Kollen, B. J., van der Grond, J., & Prevo, A. J. H. (2003). Probability of regaining dexterity in the flaccid upper limb: impact of severity of paresis and time since onset in acute stroke. *Stroke*, *34*(9), 2181–2186. https://doi.org/10.1161/01.STR.0000087172.16305.CD
Lai, S.-M., Studenski, S., Duncan, P. W., & Perera, S. (2002). Persisting consequences of stroke measured by the Stroke Impact Scale. *Stroke*, *33*(7), 1840–1844.
Lamprecht, R., & LeDoux, J. (2004). Structural plasticity and memory. *Nature Reviews. Neuroscience*, *5*(1), 45–54. https://doi.org/10.1038/nrn1301
Lenz, C., Rebel, A., van Ackern, K., Kuschinsky, W., & Waschke, K. F. (1998). Local cerebral blood flow, local cerebral glucose utilization, and flow-metabolism coupling during sevoflurane versus isoflurane anesthesia in rats. *Anesthesiology*, *89*(6), 1480–1488.
Liebeskind, D. S. (2003). Collateral circulation. *Stroke*, *34*(9), 2279–2284. https://doi.org/10.1161/01.STR.0000086465.41263.06
Liepert, J., Bauder, H., Wolfgang, H. R., Miltner, W. H., Taub, E., & Weiller, C. (2000). Treatment-induced cortical reorganization after stroke in humans. *Stroke*, *31*(6), 1210–1216.
Lin, C.-Y., Chang, C., Cheung, W.-M., Lin, M.-H., Chen, J.-J., Hsu, C. Y., … Lin, T.-N. (2008). Dynamic changes in vascular permeability, cerebral blood volume, vascular density, and size after transient focal cerebral ischemia in rats: evaluation with contrast-enhanced magnetic resonance imaging. *Journal of Cerebral Blood Flow and Metabolism: Official Journal of the International Society of Cerebral Blood Flow and Metabolism*, *28*(8), 1491–1501. https://doi.org/10.1038/jcbfm.2008.42
Lin, T. N., Wang, C. K., Cheung, W. M., & Hsu, C. Y. (2000). Induction of angiopoietin and Tie receptor mRNA expression after cerebral ischemia-reperfusion. *Journal of Cerebral Blood Flow and Metabolism: Official Journal of the International Society of Cerebral Blood Flow and Metabolism*, *20*(2), 387–395. https://doi.org/10.1097/00004647-200002000-00021
Lin, T.-N., Sun, S.-W., Cheung, W.-M., Li, F., & Chang, C. (2002). Dynamic changes in cerebral blood flow and angiogenesis after transient focal cerebral ischemia in rats. Evaluation with serial magnetic resonance imaging. *Stroke*, *33*(12), 2985–2991.
Lippman, J., & Dunaevsky, A. (2005). Dendritic spine morphogenesis and plasticity. *Journal of Neurobiology*, *64*(1), 47–57. https://doi.org/10.1002/neu.20149
Liu, F., & McCullough, L. D. (2012). Interactions between age, sex, and hormones in experimental ischemic stroke. *Neurochemistry International*, *61*(8), 1255–1265. https://doi.org/10.1016/j.neuint.2012.10.003
Liu, J., Wang, Y., Akamatsu, Y., Lee, C. C., Stetler, R. A., Lawton, M. T., & Yang, G.-Y. (2014). Vascular remodeling after ischemic stroke: mechanisms and therapeutic potentials. *Progress in Neurobiology*, *115*, 138–156. https://doi.org/10.1016/j.pneurobio.2013.11.004

Ma, L., Qiao, Q., Tsai, J.-W., Yang, G., Li, W., & Gan, W.-B. (2016). Experience-dependent plasticity of dendritic spines of layer 2/3 pyramidal neurons in the mouse cortex. *Developmental Neurobiology*, *76*(3), 277–286. https://doi.org/10.1002/dneu.22313

Magariños, A. M., McEwen, B. S., Flügge, G., & Fuchs, E. (1996). Chronic psychosocial stress causes apical dendritic atrophy of hippocampal CA3 pyramidal neurons in subordinate tree shrews. *The Journal of Neuroscience: The Official Journal of the Society for Neuroscience*, *16*(10), 3534–3540.

Majewska, A. K., Newton, J. R., & Sur, M. (2006). Remodeling of synaptic structure in sensory cortical areas in vivo. *The Journal of Neuroscience: The Official Journal of the Society for Neuroscience*, *26*(11), 3021–3029. https://doi.org/10.1523/JNEUROSCI.4454-05.2006

Majewska, A., & Sur, M. (2003). Motility of dendritic spines in visual cortex in vivo: changes during the critical period and effects of visual deprivation. *Proceedings of the National Academy of Sciences of the United States of America*, *100*(26), 16024–16029. https://doi.org/10.1073/pnas.2636949100

Makino, H., Hwang, E. J., Hedrick, N. G., & Komiyama, T. (2016). Circuit Mechanisms of Sensorimotor Learning. *Neuron*, *92*(4), 705–721. https://doi.org/10.1016/j.neuron.2016.10.029

Malonek, D., & Grinvald, A. (1996). Interactions between electrical activity and cortical microcirculation revealed by imaging spectroscopy: implications for functional brain mapping. *Science (New York, N.Y.)*, *272*(5261), 551–554.

Marchal, G., Furlan, M., Beaudouin, V., Rioux, P., Hauttement, J. L., Serrati, C., … Baron, J. C. (1996). Early spontaneous hyperperfusion after stroke. A marker of favourable tissue outcome? *Brain: A Journal of Neurology*, *119 (Pt 2)*, 409–419.

Marchal, G., Serrati, C., Rioux, P., Petit-Taboué, M. C., Viader, F., de la Sayette, V., … Orgogozo, J. M. (1993). PET imaging of cerebral perfusion and oxygen consumption in acute ischaemic stroke: relation to outcome. *Lancet (London, England)*, *341*(8850), 925–927.

Marcoux, F. W., Morawetz, R. B., Crowell, R. M., DeGirolami, U., & Halsey, J. H. (1982). Differential regional vulnerability in transient focal cerebral ischemia. *Stroke*, *13*(3), 339–346.

Masamizu, Y., Tanaka, Y. R., Tanaka, Y. H., Hira, R., Ohkubo, F., Kitamura, K., … Matsuzaki, M. (2014). Two distinct layer-specific dynamics of cortical ensembles during learning of a motor task. *Nature Neuroscience*, *17*(7), 987–994. https://doi.org/10.1038/nn.3739

Matsuzaki, M., Honkura, N., Ellis-Davies, G. C. R., & Kasai, H. (2004). Structural basis of long-term potentiation in single dendritic spines. *Nature*, *429*(6993), 761–766. https://doi.org/10.1038/nature02617

McCullough, L. D., & Hurn, P. D. (2003). Estrogen and ischemic neuroprotection: an integrated view. *Trends in Endocrinology and Metabolism: TEM*, *14*(5), 228–235.

Memezawa, H., Minamisawa, H., Smith, M. L., & Siesjö, B. K. (1992). Ischemic penumbra in a model of reversible middle cerebral artery occlusion in the rat. *Experimental Brain Research*, *89*(1), 67–78.

Mergenthaler, P., Dirnagl, U., & Meisel, A. (2004). Pathophysiology of Stroke: Lessons from Animal Models. *Metabolic Brain Disease*, *19*(3–4), 151–167. https://doi.org/10.1023/B:MEBR.0000043966.46964.e6

Monfils, M.-H., Plautz, E. J., & Kleim, J. A. (2005). In search of the motor engram: motor map plasticity as a mechanism for encoding motor experience. *The Neuroscientist: A Review Journal*

Bringing Neurobiology, Neurology and Psychiatry, *11*(5), 471–483. https://doi.org/10.1177/1073858405278015

Moon, S.-K., Alaverdashvili, M., Cross, A. R., & Whishaw, I. Q. (2009). Both compensation and recovery of skilled reaching following small photothrombotic stroke to motor cortex in the rat. *Experimental Neurology*, *218*(1), 145–153. https://doi.org/10.1016/j.expneurol.2009.04.021

Morrison, J. H., Brinton, R. D., Schmidt, P. J., & Gore, A. C. (2006). Estrogen, menopause, and the aging brain: how basic neuroscience can inform hormone therapy in women. *The Journal of Neuroscience: The Official Journal of the Society for Neuroscience*, *26*(41), 10332–10348. https://doi.org/10.1523/JNEUROSCI.3369-06.2006

Moser, M. B., Trommald, M., & Andersen, P. (1994). An increase in dendritic spine density on hippocampal CA1 pyramidal cells following spatial learning in adult rats suggests the formation of new synapses. *Proceedings of the National Academy of Sciences of the United States of America*, *91*(26), 12673–12675.

Mostany, R., Chowdhury, T. G., Johnston, D. G., Portonovo, S. A., Carmichael, S. T., & Portera-Cailliau, C. (2010). Local hemodynamics dictate long-term dendritic plasticity in peri-infarct cortex. *The Journal of Neuroscience: The Official Journal of the Society for Neuroscience*, *30*(42), 14116–14126. https://doi.org/10.1523/JNEUROSCI.3908-10.2010

Mostany, R., & Portera-Cailliau, C. (2011). Absence of large-scale dendritic plasticity of layer 5 pyramidal neurons in peri-infarct cortex. *The Journal of Neuroscience: The Official Journal of the Society for Neuroscience*, *31*(5), 1734–1738. https://doi.org/10.1523/JNEUROSCI.4386-10.2011

Mozaffarian, D., Benjamin, E. J., Go, A. S., Arnett, D. K., Blaha, M. J., Cushman, M., … Subcommittee, on behalf of the A. H. A. S. C. and S. S. (2016). Heart disease and stroke statistics-2016 update a report from the American Heart Association. *Circulation*, *133*(4), e38–e48. https://doi.org/10.1161/CIR.0000000000000350

Murphy, T. H., & Corbett, D. (2009). Plasticity during stroke recovery: from synapse to behaviour. *Nature Reviews. Neuroscience*, *10*(12), 861–872. https://doi.org/10.1038/nrn2735

Nedergaard, M., Vorstrup, S., & Astrup, J. (1986). Cell density in the border zone around old small human brain infarcts. *Stroke*, *17*(6), 1129–1137.

Nishimura, N., Schaffer, C. B., Friedman, B., Lyden, P. D., & Kleinfeld, D. (2007). Penetrating arterioles are a bottleneck in the perfusion of neocortex. *Proceedings of the National Academy of Sciences of the United States of America*, *104*(1), 365–370. https://doi.org/10.1073/pnas.0609551104

Nishimura, N., Schaffer, C. B., Friedman, B., Tsai, P. S., Lyden, P. D., & Kleinfeld, D. (2006). Targeted insult to subsurface cortical blood vessels using ultrashort laser pulses: three models of stroke. *Nature Methods*, *3*(2), 99–108. https://doi.org/10.1038/nmeth844

Nudo, R. J., & Milliken, G. W. (1996). Reorganization of movement representations in primary motor cortex following focal ischemic infarcts in adult squirrel monkeys. *Journal of Neurophysiology*, *75*(5), 2144–2149. https://doi.org/10.1152/jn.1996.75.5.2144

Nudo, R. J., Wise, B. M., SiFuentes, F., & Milliken, G. W. (1996). Neural substrates for the effects of rehabilitative training on motor recovery after ischemic infarct. *Science (New York, N.Y.)*, *272*(5269), 1791–1794.

Nudo, Randolph J. (2007). Postinfarct cortical plasticity and behavioral recovery. *Stroke*, *38*(2 Suppl), 840–845. https://doi.org/10.1161/01.STR.0000247943.12887.d2

Ohab, J. J., Fleming, S., Blesch, A., & Carmichael, S. T. (2006). A neurovascular niche for neurogenesis after stroke. *The Journal of Neuroscience: The Official Journal of the Society for Neuroscience*, *26*(50), 13007–13016. https://doi.org/10.1523/JNEUROSCI.4323-06.2006

Padmashri, R., Reiner, B. C., Suresh, A., Spartz, E., & Dunaevsky, A. (2013). Altered structural and functional synaptic plasticity with motor skill learning in a mouse model of fragile X syndrome. *The Journal of Neuroscience: The Official Journal of the Society for Neuroscience*, *33*(50), 19715–19723. https://doi.org/10.1523/JNEUROSCI.2514-13.2013

Parthasarathy, A. B., Kazmi, S. M. S., & Dunn, A. K. (2010). Quantitative imaging of ischemic stroke through thinned skull in mice with Multi Exposure Speckle Imaging. *Biomedical Optics Express*, *1*(1), 246–259. https://doi.org/10.1364/BOE.1.000246

Picard, N., Matsuzaka, Y., & Strick, P. L. (2013). Extended practice of a motor skill is associated with reduced metabolic activity in M1. *Nature Neuroscience*, *16*(9), 1340–1347. https://doi.org/10.1038/nn.3477

Platholi, J., Herold, K. F., Jr, H. C. H., & Halpain, S. (2014). Isoflurane Reversibly Destabilizes Hippocampal Dendritic Spines by an Actin-Dependent Mechanism. *PLOS ONE*, *9*(7), e102978. https://doi.org/10.1371/journal.pone.0102978

Popa-Wagner, A., Glavan, D.-G., Olaru, A., Olaru, D.-G., Margaritescu, O., Tica, O., … Sandu, R. E. (2018). Present Status and Future Challenges of New Therapeutic Targets in Preclinical Models of Stroke in Aged Animals with/without Comorbidities. *International Journal of Molecular Sciences*, *19*(2). https://doi.org/10.3390/ijms19020356

Qian, C., Li, P.-C., Jiao, Y., Yao, H.-H., Chen, Y.-C., Yang, J., … Teng, G.-J. (2016). Precise Characterization of the Penumbra Revealed by MRI: A Modified Photothrombotic Stroke Model Study. *PloS One*, *11*(4), e0153756. https://doi.org/10.1371/journal.pone.0153756

Ramanathan, D., Conner, J. M., & Tuszynski, M. H. (2006). A form of motor cortical plasticity that correlates with recovery of function after brain injury. *Proceedings of the National Academy of Sciences of the United States of America*, *103*(30), 11370–11375. https://doi.org/10.1073/pnas.0601065103

Ramaswamy, S., & Markram, H. (2015). Anatomy and physiology of the thick-tufted layer 5 pyramidal neuron. *Frontiers in Cellular Neuroscience*, *9*. https://doi.org/10.3389/fncel.2015.00233

Reiner, B. C., & Dunaevsky, A. (2015). Deficit in Motor Training-Induced Clustering, but Not Stabilization, of New Dendritic Spines in fmr1 Knock-Out Mice. *PLoS ONE*, *10*(5). https://doi.org/10.1371/journal.pone.0126572

Rhyu, I. J., Bytheway, J. A., Kohler, S. J., Lange, H., Lee, K. J., Boklewski, J., … Cameron, J. L. (2010). Effects of aerobic exercise training on cognitive function and cortical vascularity in monkeys. *Neuroscience*, *167*(4), 1239–1248. https://doi.org/10.1016/j.neuroscience.2010.03.003

Richard Green, A., Odergren, T., & Ashwood, T. (2003). Animal models of stroke: do they have value for discovering neuroprotective agents? *Trends in Pharmacological Sciences*, *24*(8), 402–408. https://doi.org/10.1016/S0165-6147(03)00192-5

Roberts, T. F., Tschida, K. A., Klein, M. E., & Mooney, R. (2010). Rapid spine stabilization and synaptic enhancement at the onset of behavioural learning. *Nature*, *463*(7283), 948–952. https://doi.org/10.1038/nature08759

Robinson, T. E., & Kolb, B. (1999). Alterations in the morphology of dendrites and dendritic spines in the nucleus accumbens and prefrontal cortex following repeated treatment with amphetamine or cocaine. *The European Journal of Neuroscience*, *11*(5), 1598–1604.

Rossouw, J. E., Anderson, G. L., Prentice, R. L., LaCroix, A. Z., Kooperberg, C., Stefanick, M. L., … Writing Group for the Women's Health Initiative Investigators. (2002). Risks and benefits of estrogen plus progestin in healthy postmenopausal women: principal results From the Women's Health Initiative randomized controlled trial. *JAMA*, *288*(3), 321–333.

Schaffer, C. B., Friedman, B., Nishimura, N., Schroeder, L. F., Tsai, P. S., Ebner, F. F., … Kleinfeld, D. (2006). Two-Photon Imaging of Cortical Surface Microvessels Reveals a Robust Redistribution in Blood Flow after Vascular Occlusion. *PLOS Biology*, *4*(2), e22. https://doi.org/10.1371/journal.pbio.0040022

Schlaug, G., Benfield, A., Baird, A. E., Siewert, B., Lövblad, K. O., Parker, R. A., … Warach, S. (1999). The ischemic penumbra: operationally defined by diffusion and perfusion MRI. *Neurology*, *53*(7), 1528–1537.

Schrandt, C. J., Kazmi, S. M. S., Jones, T. A., & Dunn, A. K. (2015). Chronic monitoring of vascular progression after ischemic stroke using multiexposure speckle imaging and two-photon fluorescence microscopy. *Journal of Cerebral Blood Flow & Metabolism*, *35*(6), 933–942. https://doi.org/10.1038/jcbfm.2015.26

Shen, F., Su, H., Fan, Y., Chen, Y., Zhu, Y., Liu, W., … Yang, G.-Y. (2006). Adeno-associated viral-vector-mediated hypoxia-inducible vascular endothelial growth factor gene expression attenuates ischemic brain injury after focal cerebral ischemia in mice. *Stroke*, *37*(10), 2601–2606. https://doi.org/10.1161/01.STR.0000240407.14765.e8

Sigler, A., Goroshkov, A., & Murphy, T. H. (2008). Hardware and methodology for targeting single brain arterioles for photothrombotic stroke on an upright microscope. *Journal of Neuroscience Methods*, *170*(1), 35–44. https://doi.org/10.1016/j.jneumeth.2007.12.015

Soares, B. P., Tong, E., Hom, J., Cheng, S.-C., Bredno, J., Boussel, L., … Wintermark, M. (2010). Reperfusion Is a More Accurate Predictor of Follow-Up Infarct Volume Than Recanalization: A Proof of Concept Using CT in Acute Ischemic Stroke Patients. *Stroke*, *41*(1), e34–e40. https://doi.org/10.1161/STROKEAHA.109.568766

Sommer, C. J. (2017). Ischemic stroke: experimental models and reality. *Acta Neuropathologica*, *133*(2), 245–261. https://doi.org/10.1007/s00401-017-1667-0

Stoll, G., Kleinschnitz, C., Meuth, S. G., Braeuninger, S., Ip, C. W., Wessig, C., … Bendszus, M. (2009). Transient widespread blood-brain barrier alterations after cerebral photothrombosis as revealed by gadofluorine M-enhanced magnetic resonance imaging. *Journal of Cerebral Blood Flow and Metabolism: Official Journal of the International Society of Cerebral Blood Flow and Metabolism*, *29*(2), 331–341. https://doi.org/10.1038/jcbfm.2008.129

Strong, A. J., Venables, G. S., & Gibson, G. (1983). The cortical ischaemic penumbra associated with occlusion of the middle cerebral artery in the cat: 1. Topography of changes in blood flow, potassium ion activity, and EEG. *Journal of Cerebral Blood Flow and Metabolism: Official Journal of the International Society of Cerebral Blood Flow and Metabolism*, *3*(1), 86–96. https://doi.org/10.1038/jcbfm.1983.11

Sun, Y., Jin, K., Xie, L., Childs, J., Mao, X. O., Logvinova, A., & Greenberg, D. A. (2003). VEGF-induced neuroprotection, neurogenesis, and angiogenesis after focal cerebral ischemia. *The Journal of Clinical Investigation*, *111*(12), 1843–1851. https://doi.org/10.1172/JCI17977

Symon, L. (1980). The relationship between CBF, evoked potentials and the clinical features in cerebral ischaemia. *Acta Neurologica Scandinavica. Supplementum*, *78*, 175–190.
Szpak, G. M., Lechowicz, W., Lewandowska, E., Bertrand, E., Wierzba-Bobrowicz, T., & Dymecki, J. (1999). Border zone neovascularization in cerebral ischemic infarct. *Folia Neuropathologica*, *37*(4), 264–268.
Taguchi, A., Soma, T., Tanaka, H., Kanda, T., Nishimura, H., Yoshikawa, H., … Matsuyama, T. (2004). Administration of CD34+ cells after stroke enhances neurogenesis via angiogenesisin a mouse model. *Journal of Clinical Investigation*, *114*(3), 330–338. https://doi.org/10.1172/JCI200420622
Tennant, K. A., Adkins, D. L., Donlan, N. A., Asay, A. L., Thomas, N., Kleim, J. A., & Jones, T. A. (2011). The organization of the forelimb representation of the C57BL/6 mouse motor cortex as defined by intracortical microstimulation and cytoarchitecture. *Cerebral Cortex (New York, N.Y.: 1991)*, *21*(4), 865–876. https://doi.org/10.1093/cercor/bhq159
Tennant, K. A., Adkins, D. L., Scalco, M. D., Donlan, N. A., Asay, A. L., Thomas, N., … Jones, T. A. (2012). Skill learning induced plasticity of motor cortical representations is time and age-dependent. *Neurobiology of Learning and Memory*, *98*(3), 291–302. https://doi.org/10.1016/j.nlm.2012.09.004
Tennant, K. A., Kerr, A. L., Adkins, D. L., Donlan, N., Thomas, N., Kleim, J. A., & Jones, T. A. (2015). Age-dependent reorganization of peri-infarct "premotor" cortex with task-specific rehabilitative training in mice. *Neurorehabilitation and Neural Repair*, *29*(2), 193–202. https://doi.org/10.1177/1545968314541329
Thored, P., Wood, J., Arvidsson, A., Cammenga, J., Kokaia, Z., & Lindvall, O. (2007). Long-Term Neuroblast Migration Along Blood Vessels in an Area With Transient Angiogenesis and Increased Vascularization After Stroke. *Stroke*, *38*(11), 3032–3039. https://doi.org/10.1161/STROKEAHA.107.488445
Tjia, M., Yu, X., Jammu, L. S., Lu, J., & Zuo, Y. (2017). Pyramidal Neurons in Different Cortical Layers Exhibit Distinct Dynamics and Plasticity of Apical Dendritic Spines. *Frontiers in Neural Circuits*, *11*. https://doi.org/10.3389/fncir.2017.00043
Trachtenberg, J. T., Chen, B. E., Knott, G. W., Feng, G., Sanes, J. R., Welker, E., & Svoboda, K. (2002). Long-term in vivo imaging of experience-dependent synaptic plasticity in adult cortex. *Nature*, *420*(6917), 788–794. https://doi.org/10.1038/nature01273
Turner, A. M., & Greenough, W. T. (1985). Differential rearing effects on rat visual cortex synapses. I. Synaptic and neuronal density and synapses per neuron. *Brain Research*, *329*(1–2), 195–203.
Uylings, H. B., Kuypers, K., Diamond, M. C., & Veltman, W. A. (1978). Effects of differential environments on plasticity of dendrites of cortical pyramidal neurons in adult rats. *Experimental Neurology*, *62*(3), 658–677.
Volkmar, F. R., & Greenough, W. T. (1972). Rearing complexity affects branching of dendrites in the visual cortex of the rat. *Science (New York, N.Y.)*, *176*(4042), 1445–1447.
Wälchli, T., Mateos, J. M., Weinman, O., Babic, D., Regli, L., Hoerstrup, S. P., … Vogel, J. (2015). Quantitative assessment of angiogenesis, perfused blood vessels and endothelial tip cells in the postnatal mouse brain. *Nature Protocols*, *10*(1), 53–74. https://doi.org/10.1038/nprot.2015.002
Wallace, C. S., Withers, G. S., Farnand, A., Lobingier, B. T., & McCleery, E. J. (2011). Evidence that angiogenesis lags behind neuron and astrocyte growth in experience-dependent plasticity. *Developmental Psychobiology*, *53*(5), 435–442. https://doi.org/10.1002/dev.20559

Wang, L., Conner, J. M., Rickert, J., & Tuszynski, M. H. (2011). Structural plasticity within highly specific neuronal populations identifies a unique parcellation of motor learning in the adult brain. *Proceedings of the National Academy of Sciences of the United States of America*, *108*(6), 2545–2550. https://doi.org/10.1073/pnas.1014335108

Wang, R.-Y., Wang, P. S.-G., & Yang, Y.-R. (2003). Effect of age in rats following middle cerebral artery occlusion. *Gerontology*, *49*(1), 27–32. https://doi.org/10.1159/000066505

Ward, N. S. (2005). Mechanisms underlying recovery of motor function after stroke. *Postgraduate Medical Journal*, *81*(958), 510–514. https://doi.org/10.1136/pgmj.2004.030809

Watson, B. D., Dietrich, W. D., Busto, R., Wachtel, M. S., & Ginsberg, M. D. (1985). Induction of reproducible brain infarction by photochemically initiated thrombosis. *Annals of Neurology*, *17*(5), 497–504. https://doi.org/10.1002/ana.410170513

Wei, L., Erinjeri, J. P., Rovainen, C. M., & Woolsey, T. A. (2001). Collateral growth and angiogenesis around cortical stroke. *Stroke*, *32*(9), 2179–2184.

Wells, B. A., Keats, A. S., & Cooley, D. A. (1963). Increased tolerance to cerebral ischemia produced by general anesthesia during temporary carotid occlusion. *Surgery*, *54*, 216–223.

Wilbrecht, L., Holtmaat, A., Wright, N., Fox, K., & Svoboda, K. (2010). Structural plasticity underlies experience-dependent functional plasticity of cortical circuits. *The Journal of Neuroscience: The Official Journal of the Society for Neuroscience*, *30*(14), 4927–4932. https://doi.org/10.1523/JNEUROSCI.6403-09.2010

Wilson, C. A., & Hatchell, D. L. (1991). Photodynamic retinal vascular thrombosis. Rate and duration of vascular occlusion. *Investigative Ophthalmology & Visual Science*, *32*(8), 2357–2365.

Withers, G. S., & Greenough, W. T. (1989). Reach training selectively alters dendritic branching in subpopulations of layer II-III pyramids in rat motor-somatosensory forelimb cortex. *Neuropsychologia*, *27*(1), 61–69.

Wittenberg, G. F. (2010). Experience, cortical remapping, and recovery in brain disease. *Neurobiology of Disease*, *37*(2), 252–258. https://doi.org/10.1016/j.nbd.2009.09.007

Xu, H.-T., Pan, F., Yang, G., & Gan, W.-B. (2007). Choice of cranial window type for in vivo imaging affects dendritic spine turnover in the cortex. *Nature Neuroscience*, *10*(5), 549–551. https://doi.org/10.1038/nn1883

Xu-Friedman, M. A., & Regehr, W. G. (2004). Structural contributions to short-term synaptic plasticity. *Physiological Reviews*, *84*(1), 69–85. https://doi.org/10.1152/physrev.00016.2003

Yang, G., Chang, P. C., Bekker, A., Blanck, T., & Gan, W.-B. (2011). Transient effects of anesthetics on dendritic spines and filopodia in the living mouse cortex. *Anesthesiology*, *115*(4). https://doi.org/10.1097/ALN.0b013e318229a660

Yang, G., Pan, F., & Gan, W.-B. (2009). Stably maintained dendritic spines are associated with lifelong memories. *Nature*, *462*(7275), 920–924. https://doi.org/10.1038/nature08577

Yasumatsu, N., Matsuzaki, M., Miyazaki, T., Noguchi, J., & Kasai, H. (2008). Principles of long-term dynamics of dendritic spines. *The Journal of Neuroscience: The Official Journal of the Society for Neuroscience*, *28*(50), 13592–13608. https://doi.org/10.1523/JNEUROSCI.0603-08.2008

Yu, X., & Zuo, Y. (2011). Spine Plasticity in the Motor Cortex. *Current Opinion in Neurobiology*, *21*(1), 169–174. https://doi.org/10.1016/j.conb.2010.07.010

Yuste, R. (2011). Dendritic spines and distributed circuits. *Neuron*, *71*(5), 772–781. https://doi.org/10.1016/j.neuron.2011.07.024

Zhang, S., & Murphy, T. H. (2007). Imaging the impact of cortical microcirculation on synaptic structure and sensory-evoked hemodynamic responses in vivo. *PLoS Biology*, *5*(5), e119. https://doi.org/10.1371/journal.pbio.0050119

Zito, K., Scheuss, V., Knott, G., Hill, T., & Svoboda, K. (2009). Rapid functional maturation of nascent dendritic spines. *Neuron*, *61*(2), 247–258. https://doi.org/10.1016/j.neuron.2008.10.054

Zito, K., & Svoboda, K. (2002). Activity-dependent synaptogenesis in the adult Mammalian cortex. *Neuron*, *35*(6), 1015–1017.

Zuo, Y., Lin, A., Chang, P., & Gan, W.-B. (2005). Development of long-term dendritic spine stability in diverse regions of cerebral cortex. *Neuron*, *46*(2), 181–189. https://doi.org/10.1016/j.neuron.2005.04.001